

In Vitro and In Vivo Analysis of Insulin-Induced Oxidative Stress and DNA Damage

In vitro und in vivo Untersuchungen von
Insulin-induzierten
oxidativen Stress und DNA-Schäden

**Dissertation for Submission to a Doctoral Degree
at the Graduate School of Life Sciences,
Julius-Maximilians-University Würzburg,
Section: Biomedicine**

Submitted by

Eman Maher Othman Sholkamy

From

Minia, Egypt

Würzburg, April 2013

Submitted on:

Members of the Promotionskomitee:

Chairperson: Prof Dr Jörg Schultz

1. **Primary Supervisor:** Prof Dr Helga Stopper
2. **Supervisor:** Prof Dr Klaus Brehm
3. **Supervisor:** Prof Dr Ulric Holzgrabe
4. **Supervisor:** PD Dr Robert Hock

Date of public Defense

Index

Index

Index	I
Abbreviations	IV
1- Introduction	1
1.1 Genotoxicity	1
1.1.1 The Single Cell Gel Electrophoresis (Comet assay)	1
1.1.2 Micronucleus frequency test.....	5
1.2 Genomic damage and cancer etiology.....	6
1.3 Free Radicals, Reactive Oxygen Species and Oxidative Stress.....	8
1.3.1 ROS source.....	9
1.3.2 Cellular defense against ROS.....	12
1.3.3 ROS measurement.....	12
1.4 Genotoxicity and endogenous hormones.....	14
1.5 Insulin.....	14
1.5.1 Insulin action and signaling mechanism.....	15
1.5.2 Hyperinsulinemia and diseases.....	17
1.5.3 Insulin and oxidative stress.....	18
2- Objectives	20
3- Material and methods	22
3.1 Chemicals and reagents.....	22
3.2 Antibodies.....	22
3.3 siRNA oligonucleotides.....	23
3.4 PCR primers.....	23
3.5 Cell lines and cell culture reagents.....	24
3.6 Isolation of peripheral lymphocytes.....	26
3.7 Rho0 cells.....	27
3.8 Animal model and treatment.....	27
3.9 Human subjects.....	28
3.10 Apoptosis assay.....	29
3.11 Comet assay.....	30
3.12 Micronucleus frequency test.....	31
3.13 Flow cytometric quantification of oxidative stress.....	31
3.14 Microscopic analysis of reactive oxygen species.....	32
3.15 Western blot analysis.....	32
3.16 siRNA transfection.....	33
3.17 Determination of insulin concentration by HPLC.....	33
3.18 Quantification of 8-oxodG by LC-MS/MS.....	34
3.19 RNA and DNA isolation and PCR.....	35
3.20 Statistics.....	35

Index

4- Results	36
4.1 Insulin mediated oxidative stress and DNA damage in mammalian colon cells.....	36
4.1.1 Insulin induces genotoxicity in colon cells.....	36
4.1.2 Insulin stimulates ROS production and mediates oxidative stress.....	42
4.1.3 Insulin mediates oxidative damage and antioxidants offer protection...	45
4.1.4 Signaling pathway of insulin-mediates oxidative stress and DNA damage in colon.....	48
4.1.5 Insulin genotoxicity in Caco-2 cells and the primary rat colon cells.....	67
4.2 Insulin mediated oxidative stress and DNA damage in mammalian kidneys in vitro and in vivo.....	69
4.2.1 Insulin induces genotoxicity in kidney cells.....	69
4.2.2 ROS production and antioxidants.....	74
4.2.3 Role of insulin and insulin-like growth factor receptors in insulin genotoxicity.....	78
4.2.4 Activation of PI3 kinase and AKT.....	80
4.2.5 ROS sources.....	83
4.2.6 Insulin effect in primary rat kidney cells.....	85
4.2.7 Signaling pathway of insulin genotoxicity in kidney using HK2 cells.....	86
4.2.8 Zucker diabetic fatty rats (ZDF).....	99
4.3 Insulin mediated oxidative stress and DNA damage in mammalian hemopoietic system cells.....	101
4.3.1 Insulin induces oxidative stress and DNA damage in HL60.....	101
4.3.2 Insulin induces DNA damage in peripheral lymphocytes.....	103
4.3.3 Micronucleus frequency elevation in type II diabetes mellitus patients.....	104
4.4 Insulin mediated DNA damage in different mammalian cells.....	105
5- Discussion	106
5.1 Insulin-mediated oxidative stress and DNA damage in mammalian colon cells.....	107
5.2 Signaling pathway of insulin genotoxicity in colon cells.....	109
5.3 Insulin-mediated oxidative stress and DNA damage in mammalian kidney cells.....	113
5.4 Signaling pathway of insulin genotoxicity in kidney cells.....	113
5.5 Insulin-mediated oxidative stress and DNA damage in ZDF rats.....	115
5.6 Insulin-induced DNA damage in HL60, cultured peripheral lymphocytes and type II diabetic patients' lymphocytes.....	119
6- Summary	121
7- Zusammenfassung	124
8- References	127
9- Acknowledgment	136
Curriculum Vitae	138

Index

Dedication.....	141
Affidavit.....	142

Abbreviations

Abbreviations

·OH	Hydroxyl radical
8-OxodG:	8-oxo-2'-deoxyguanosine
Ames Test	Reverse Mutation Assay
ATP	Adenosine-5'-triphosphate
bp	Base pair
BSA	Bovine serum albumin
BT-474	Human breast carcinoma cell line
Caco-2	Heterogeneous human epithelial colorectal adenocarcinoma cell line
CAs	Chromosomal aberrations
CBPI	Cytokinesis block proliferation index
DABCO	Diazabicyclo octane
DCF	Dichlorofluorescein
DHE	Dihydroethidium
DHR	Dihydrorhodamine
DMEM	Dulbecco modified Eagle's minimal essential medium
DMSO	Dimethyl sulfoxide
DNA	Deoxyribonucleic acid
DSB	Double strand break
EDTA	Ethylenediamine-tetraacetic acid disodium salt
ERK1/2	Extracellular signal-regulated kinase
FCS	Fetal calf serum
FITC	Fluorescein isothiocyanate
FPG	Formamidopyrimidine DNA glycosylase
γ-H2AX	Phosphorylated histone 2AX
GSH	Reduced form of glutathione
GSSG	Oxidized form of glutathione
H2DCF-DA	2',7'-dichlorofluorescein diacetate
H₂O₂	Hydrogen peroxide
HCl	Hydrochloric acid

Abbreviations

HEPES	4-(2-hydroxyethyl)-1-piperazineethanesulfonic acid
HK-2	Human kidney 2 cell line
HL60	Human promyelocytic cell line
HNMPA-(AM)₃	Hydroxy-2-naphthalenylmethyl phosphonic acid acetoxymethyl ester
HO-1	Hemeoxygenase-1
hOGG1	8-oxodG DNA glycosylase 1
HPLC	High performance liquid chromatography
hr	Hour
HRP	Horse radish peroxidase
HSM	Human small mitoDNA
IGF1	Insulin-like growth factor1
IGF1R	Insulin-like growth factor1 receptor
IR	Insulin receptor
IRS	Insulin receptor substrate
LC-MS	Liquid chromatography-mass spectrometry
Lectin/PHA L8902	Phytohaemagglutinin
LLC-PK1	Porcine kidney cell line
M	Mole per liter
MAPK	Mitogen-activated protein kinase
MCF-7	Human breast adenocarcinoma cell
metformin	(1,1-dimethylbiguanide hydrochloride)
min	Minute
MN	Micronuclei
Mn-cells	Cells with one or more micronucleus/i
mtDNA	Mitochondrila DNA
NaCl	Sodium chloride
NADH	Nicotinamide adenine dinucleotide, reduced form
NADPH	Nicotinamide adenine dinucleotide phoshate, reduced form
NaOH	Sodium hydroxide
ONOO⁻	Peroxynitrite

Abbreviations

Rho0 cells	Mitochondria depleted cells
RNA	Ribonucleic acid
RPMI	Roswell Park Memorial Institute medium
RT-PCR	Reverse transcription polymerase chain reaction
SCGE	Single Cell Gel Electrophoresis
SD rat	Sprague Dawley rat
SOD	Superoxide dismutase enzyme
UV	Ultra violet
XOD	Xanthine oxidase

Introduction

1. Introduction

1.1 Genotoxicity

Genotoxicity describes a deleterious action on cellular genetic material affecting its integrity. Genotoxic substances are those with affinity to interact with DNA, which can lead to mutagenic or carcinogenic effects. The aim of genotoxicity testing is to evaluate whether the substance, product or environmental sample is able to induce genetic damage or not. With genotoxicity testing, potential hazard for human health and environmental organisms can be identified due to DNA damage and mutation induction. Many tests were reported to investigate the compounds genotoxicity such as the Bacterial Reverse Mutation Assay (Ames Test) which is used to investigate the ability of testing substance or sample to induce point mutations [1-2]. Another test is the SOS/umu test with *Salmonella typhimurium* TA1535/pSK1002, which determines the ability of the testing substance or sample to induce DNA damage [3].

1.1.1 The Single Cell Gel Electrophoresis (Comet assay)

The comet assay is a rapid, sensitive, versatile and economic method for detection of DNA single, double-strand breaks and alkali labile sites (incomplete excision repair sites, and apurinic or apyrimidinic sites, which are alkali labile and are translated into a strand break when exposed to the alkaline buffers of the comet assay), that are the consequences of direct DNA damage or occur as intermediates formed during the repair of DNA lesions. The method is appropriate for testing of the damaging effect of various compounds and environmental samples. Pictures of damaged (treated with insulin) as well as undamaged cells (treated with the solvent) measured by the comet assay are illustrated in figure 1.

Introduction

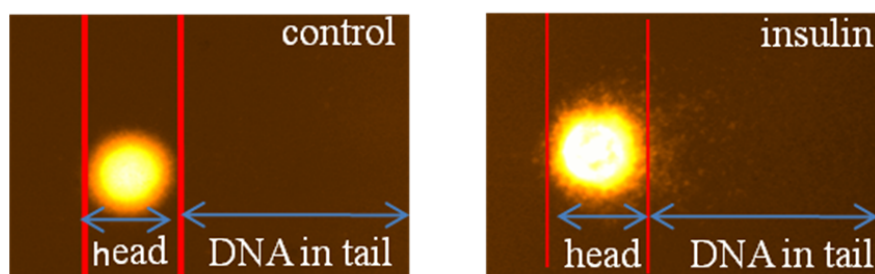


Figure1. Two representative cells in the comet assay. Cells are embedded in agarose and exposed to an electrical field. From cells with damaged DNA (right picture), more DNA can migrate than from cells with intact nuclear DNA (left picture).

During the past decade, the comet assay, or single-cell gel electrophoresis (SCGE) has become one of the standard methods for assessing DNA damage, with a wide array of applications in genotoxicity testing, human biomonitoring, molecular epidemiology, ecogenotoxicology as well as fundamental research in DNA damage and repair. It is an essential technique for measuring DNA breaks, the introduction of lesion-specific endonucleases permitting the detection of ultraviolet (UV)-induced pyrimidine dimers, oxidized bases, and alkylation damage [4].

In the 1970s, Peter Cook and colleagues [5] developed an approach for investigating the nuclear structure based on the lysis of cells with nonionic detergent and high-molarity using sodium chloride. This treatment removes membranes, cytoplasm, and nucleoplasm, and disrupts the nucleosomes resulting in solubilization of almost all histones by the high salinity. The remained nucleoid consists of a nuclear matrix or scaffold composed of ribonucleic acid (RNA) and proteins, together with the DNA which is negatively supercoiled as a consequence of the turns made by the double helix around the histones of the nucleosome. The survival of the supercoils implies that free rotation of the DNA is not possible. For that, Cook et al. [5] proposed a model with the DNA attached to the matrix so that it is effectively arranged as a series of loops, rather than as a linear molecule. When the negative supercoiling was unwound by adding the intercalating agent ethidium bromide, the loops expanded out from the nucleoid core to form a "halo." A similar effect was observed when ionizing radiation was applied to relax the loops-one single-strand break being sufficient to relax the supercoiling in that loop. The comet assay, too, in its most commonly used form involves lysis with detergent and

Introduction

high salt after embedding cells in agarose so that the DNA is immobilized for subsequent electrophoresis. The first description of comet was by Östling and Johanson [6], who described the tails in terms of DNA with relaxed supercoiling and referred to the nucleoid model of Cook et al. Interestingly, the comet tail seems to be simply a halo of relaxed loops pulled to one side by the electrophoretic field. Östling and Johanson employed a pH of less than 10. Although the most common variant now employed is alkaline SCGE, a high pH is not essential to detect single-strand breaks. The comet assay is most commonly applied to animal cells, whether in culture or isolated from the organism (e.g. lymphocytes separated from blood, or cells from disaggregated tissues). However, methods have also been developed to examine the damage in the DNA of plant cells [7].

Versions of comet assay according to the purpose of the experiment

1. Alkaline Single-Cell Gel Electrophoresis

The procedure of Östling and Johanson was not widely adopted. A few years later, two research groups independently developed procedures involving treatment at high pH. Singh et al. [8] lysed cells at pH 10 with 2.5 M NaCl, Triton X-100, and Sarkosyl for 1 hour, then treatment with alkali (0.3 M NaOH) and electrophoresis at the resulting high pH (>13). Olive et al. [9] lysed cells in weak alkali (0.03 M NaOH) for 1 hour before electrophoresis. Thus the idea was that the comet assay is in the same category as alkaline unwinding, alkaline elution, or alkaline sucrose sedimentation, where separation of two DNA strands around a break by alkaline denaturation is essential to reveal the break. The use of alkali makes comet tails more pronounced and extends the useful range of damage that can be detected [10], but it does not increase the sensitivity. The protocol introduced by Singh et al. has been simplified [11]. It is now common practice to embed cells in a single layer of agarose on a plain glass slide precoated with agarose and dried (in the original method, the cells were in the middle of three agarose layers on a frosted glass slide), sarkosyl is frequently omitted from the lysis solution.

Introduction

2. Neutral Single-Cell Gel Electrophoresis

After the example of Östling and Johanson [6], Collins et al demonstrated the ability of a neutral electrophoresis procedure to detect low levels of DNA breaks [10]. Olive et al. [12] modified the procedure to facilitate the detection of double-stranded breaks without interference from single-strand breaks. Their procedure employed extended treatment of lysed cells in agarose at 50°C. Under these conditions, it is likely that the nuclear matrix is disrupted so that we are truly looking at the behavior of double-stranded pieces of DNA (or the free ends of these fragments).

3. Use of Lesion-Specific Enzymes

Limited information is obtained from measuring the DNA strand breaks. Breaks might represent the direct effect of some damaging agents, but they are generally quickly rejoined. In fact, they might be apurinic/apyrimidinic sites (i.e., AP sites or baseless sugars), which are alkali labile and therefore appear as breaks. They might be also intermediates in cellular repair, because both nucleotide and base excision-repair processes cut out the damage and replace it with new nucleotides. To make the assay more specific as well as more sensitive, Collins group introduced the extra step of digesting the nucleoids with an enzyme that recognizes a particular kind of damage and creates a break. Thus endonuclease III is used to detect oxidized pyrimidines [13], formamidopyrimidine DNA glyco-sylase (FPG) for detecting the major purine oxidation product 8-oxoguanine as well as other altered purines [4], T4 endonuclease V to recognize-UV induced cyclobutane pyrimidine dimers [14], and Alk A incises DNA at 3-methyladenines [15]. In each case, the enzyme-sensitive sites are converted to additional DNA breaks increasing tail intensity.

4. Less common versions of comet assay

Different modifications for the comet assay were presented, such as Bromodeoxyuridine Labeling [16], which detects intermediates in DNA repair [17] and FISH Comets [18].

Introduction

1.1.2 Micronucleus frequency test

The in vitro micronucleus frequency test is used for detection of substances and samples that can cause structural and numerical chromosomal aberrations (clastogenic and aneugenic substances). Increased micronucleus formation can reflect the formation of chromosomal breaks or incorrect separation of chromosomes during the cell division. The in vitro micronucleus frequency test can be used as a replacement method for the standardized in vitro chromosomal aberration assay, especially as a screening method as it is cheaper and faster to perform on a wide variety of cell lines [19].

A schematic picture of micronucleus formation and representative cells containing micronuclei are illustrated in figure 2.

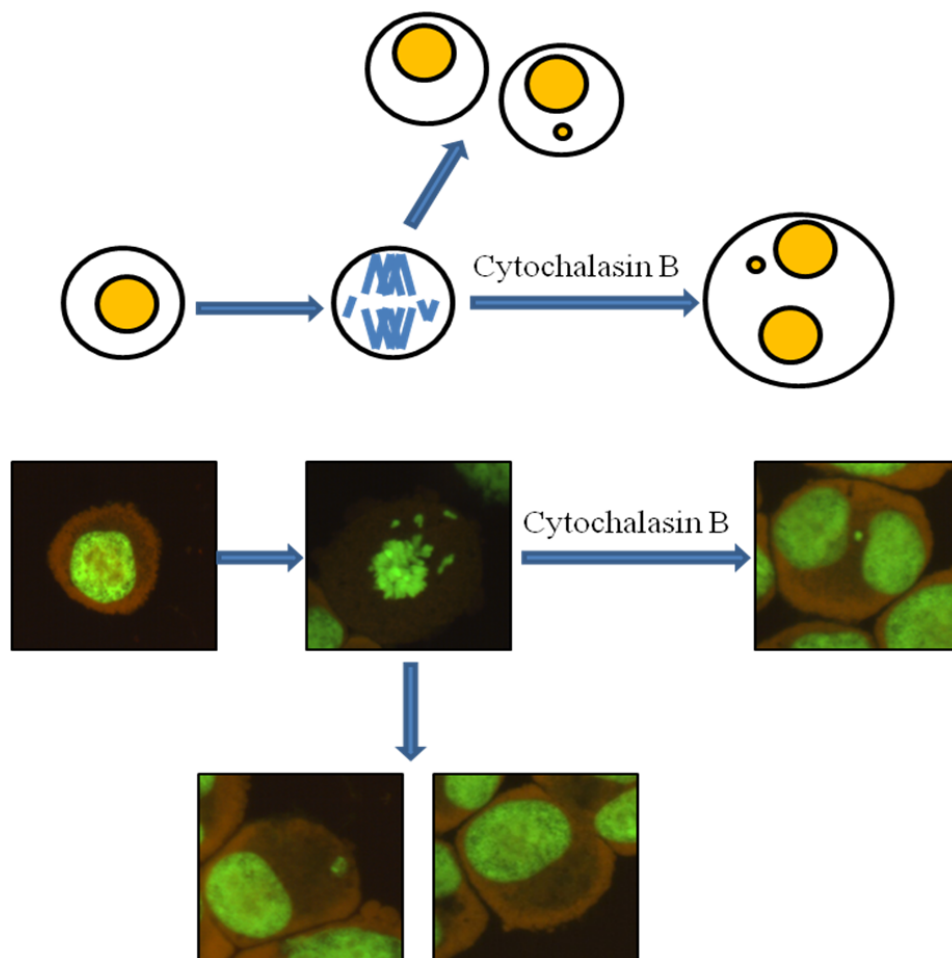


Figure2. A micronucleus contains a broken part of a chromosome or a whole chromosome which is unable to migrate toward the spindle poles during mitosis. Above is the schematic illustration of micronuclei formation. The lower part of the picture shows microscopic pictures representing the process.

Introduction

Because formation of micronuclei only occurs when cells go through cell division, it is important to observe only the population of the cells which are actively dividing during or after the desired treatment. One possibility to achieve this goal is to perform the cytokinesis-block micronucleus technique using cytochalasin B. This inhibitor of actin polymerization blocks the separation of daughter cells but not of daughter nuclei, yielding binucleated cells. By limiting the analysis to such binucleated cells, it can be ensured that these cells have actively divided since the treatment. On the other hand, mononucleated cells with micronucleus can also be analyzed without cytochalasin B addition.

1.2 Genomic damage and cancer etiology

Cancer is a genomic disease associated with accumulation of genetic damage. The majority of solid tumors show a large number of complex chromosomal aberrations (CAs) that are not always shared by all cells of the same tumor and may be not necessarily linked to a particular tumor type [20]. These chromosomal alterations occur in benign and malignant lesions as well as in pre-neoplastic stages and include structural and numerical aberrations. Cancer development has been considered as result of the process of Darwinian evolution based on two constituent events including the continuous acquisition of heritable mutations and the natural selection of the resultant phenotype [21]. The acquisition of genomic instability is a condition that predisposes a cell to accumulate stable genome mutations, representing an early step in the process of carcinogenesis [21]. A complex interaction of cellular processes characterizes the maintenance of genome stability ensuring cellular homeostasis and consistent genetic inheritance and continuity in multicellular organisms. However, cellular genomes are continuously exposed to endogenous and exogenous insults causing structural alterations to chromosomes leading to altered gene dosage and expression. Mutations in tumor suppressor genes oncogenes and other genes involved in genome maintenance could therefore lead to a mutator phenotype that increases the risk of new mutations including those associated with cancer [22]. Over the last decades, many research groups applied different biomarker-based approaches in the assessment of genotoxic agents and the increases of these biomarkers are considered

Introduction

early events, associated with the disease-related consequences. Assuming that the mechanisms for the induction of chromosomal damage are similar in different tissues, the extent of chromosomal damage evaluated in lymphocytes and other surrogate tissues is likely to reflect the level of damage in cancer-prone tissues and in turn cancer risk [23].

Micronucleus (MN) and other nuclear anomalies such as nucleoplasmic bridges (NPBs) and nuclear buds (NBUDs) are biomarkers of genotoxic events and manifestations of chromosomal instability that are often associated to cancer. The development of the cytokinesis-block micronucleus cytome (CBMNcyt) assay allowed a more accurate and precise measurement of these events in lymphocytes and more recently in exfoliated cells. The CBMNcyt assay provided deeper insights into the underlying molecular mechanisms contributing to those genome damage events that could increase risk of developmental and degenerative diseases. Genetic damage events such as MN, NPB or NBUDs provide valid measures of misrepaired DNA breaks, dysfunctional telomeres or lack of telomeres as well as defective separation of sister chromatids at anaphase due to failure of decatenation, DNA amplification and formation of DNA repair complexes [24]. The susceptibility of an individual's cells to accumulate chromosomal mutations can be measured after appropriate genotoxic stress in vitro. Indirect measurement of individual cancer susceptibility was described as mutagen sensitivity phenotype and could be measured by quantifying the genotoxic events induced by chemical or physical agents in short-term cultures of lymphocytes. A large number of epidemiologic studies reported a positive association between mutagen sensitivity and an increased risk of major cancers, including lung, breast, prostate, bladder, colorectal, brain, skin, head and neck and soft tissues [25-28]. Recent studies examined the role of genetic and environmental factors on the mutagen sensitivity phenotype and provided compelling evidence that mutagen sensitivity is highly heritable [29]. Several reports are available in the literature evaluating the baseline frequency of MN and other end points of the CBMNcyt assay in subjects affected by different types of cancer, confirming the presence of a higher level of genetic instability in cancer patients. Similarly, the much higher response of cancer patients in term of MN, NPB and NBUDs to various

Introduction

challenges is in keeping with an increased sensitivity to mutagens in these subjects [30-31].

1.3 Free Radicals, Reactive Oxygen Species and Oxidative Stress

A free radical is any species that is capable of independent existence (therefore called free) and contains one or more unpaired electrons [32]. An unpaired electron is one that occupies an atomic or molecular orbital by itself. The simplest free radical is atomic hydrogen. Since a hydrogen atom has only one electron, it must be unpaired. Many free radicals exist in living systems, although most molecules in vivo are non-radicals. Radicals can be formed by several mechanisms such as adding a single electron to a non-radical. They could also result when a covalent bond is broken if one electron from the bonding pair remains on each atom (homolytic fission) [33].

Another example, the O–O bond in H₂O₂, is readily split by exposing it to UV light, generating OH·.



Homolytic fission of one of the O–H covalent bonds in water requires more energy (γ -rays or x-rays) and yields H· and a hydroxyl radical. Formation of hydroxyl radical (OH·) accounts the most common reason for damage that happen to living organisms by ionizing radiation [34].

Molecular oxygen (O₂) is essential for the survival of all aerobic organisms. Aerobic energy metabolism is dependent on oxidative phosphorylation, a process by which the oxidoreduction energy of mitochondrial electron transport (via a multicomponent NADH dehydrogenase enzymatic complex) is converted to the high-energy phosphate bond of ATP. O₂ serves as the final electron acceptor for cytochrome-c oxidase, the terminal enzymatic component of this mitochondrial enzymatic complex that catalyzes the four-electron reduction of O₂ to H₂O. Partially reduced and highly reactive metabolites of O₂ may be formed during these and other electron transfer reactions. These O₂ metabolites include superoxide anion (O₂^{·-}) and hydrogen peroxide (H₂O₂), formed by one- and two-electron reductions of O₂, respectively. In the presence of transition metal ions, the even more reactive hydroxyl radical (OH·) can be formed. These partially reduced metabolites

Introduction

of O_2 are often referred to as “reactive oxygen species” (ROS) due to their higher reactivities relative to molecular O_2 . ROS from mitochondria and other cellular sources have been traditionally regarded as toxic by-products of metabolism with the potential to cause damage to lipids, proteins, and DNA [35].

Oxidative stress is broadly defined as an imbalance between oxidant production and the antioxidant capacity of the cell to prevent oxidative injury. Oxidative stress has been described in a large number of human diseases including atherosclerosis, pulmonary fibrosis, cancer, neurodegenerative diseases, and aging [36-37]. The relationship between oxidative stress and the pathobiology of these diseases is not clear, mainly due to the lack of understanding the mechanisms by which ROS function in both normal physiological and disease states. Accumulating data suggested that ROS are not only injurious by-products of cellular metabolism but also essential participants in cell signaling and regulation [38-39]. Although this role for ROS is a relatively novel concept in vertebrates, there is strong evidence of a physiological role for ROS in several non-mammalian systems [40-41]. The apparent paradox in the roles of ROS as essential biomolecules in the regulation of cellular functions and as toxic by-products of metabolism is related to differences in the concentrations of ROS produced. ROS elevation during a short time may cause increased DNA oxidization, like formation of the mutagenic base 8-oxodG, which is then present until removal by DNA-repair until replication. Repair attempts can lead to strand breakage, and replication may result in gene mutation because of mispairing of the oxidized DNA-base 8oxodG. Moreover, ROS can directly induce single and double strand breaks [42], which are also mutagenic events. The potential connection to cancer induction was recently reviewed by Kryston et al. [43].

1.3.1 ROS sources

The main two important sources for ROS production in the cell are mitochondria and the NADPH oxidase enzyme complex. Free radicals are mainly produced inside organelles, such as the mitochondrion, and released toward the cytosol. Mitochondria convert energy for the cell into a usable form, adenosine triphosphate (ATP). The process in which ATP is produced, called oxidative phosphorylation which involves the transport of

Introduction

protons (hydrogen ions) via the inner mitochondrial membrane by means of the electron transport chain. In the electron transport chain, electrons are passed through a series of proteins via oxidation-reduction reactions, with each acceptor protein along the chain having a greater reduction potential than the previous. The last destination for an electron along this chain is an oxygen molecule. In normal conditions, the oxygen is reduced to yield water; however, in about 0.1–2 % of electrons passing through the chain, oxygen is instead incompletely reduced to give the superoxide radical ($O_2^{\cdot-}$), most well documented for Complex I and Complex III. Superoxide can inactivate specific enzymes or initiate lipid peroxidation in its protonated form, hydroperoxyl HO_2 . The pKa of hydroperoxyl is 4.8. Thus, at physiological pH, the majority will exist as superoxide [44].

The second important sources for ROS production are NADPH oxidase enzymes, a family of multi-subunit enzyme complexes that catalyze the production of reactive oxygen species (ROS). In addition to the first NADPH oxidase found in phagocytes, other non-phagocytic NADPH oxidase isoforms were identified (fig.3), which all differ in their catalytic subunit (Nox1-5 and DOUX1 and 2) and tissue distribution [45-46].

NADPH oxidases consist of membrane proteins (i.e. the catalytic flavin–heme protein); NOX, of which five isoforms exist (NOX1–5); and the non-catalytic 22 kDa binding protein, p22phox [47]. Other components of the NADPH oxidase complex can include a cytosolic organizer (p47phox or NOXO1), an activator (p67phox or NOXA1) and other proteins (p40phox and Rac). These cytosolic subunits vary with the different NOX isoforms [48]. Upon phosphorylation, cytosolic subunits translocate to the NOX-containing membrane resulting in ROS formation. However, NOX4 and NOX5 may be independent of cytosolic subunits and constitutively active [48-51] or regulated by the intracellular free calcium [50]. The only known function of NADPH oxidases is to generate ROS making them distinct from other sources of ROS such as xanthine oxidase (XOD) or uncoupled NOS as these enzymes produce ROS only after conversion to a dysfunctional state. This is triggered by ROS derived from a primary source. NADPH oxidases might be the primary source of ROS, initiating oxidative stress and converting other enzymes into ROS producing state [52]. Nox isoforms are distributed unequally through the body tissues, and play different roles according to the

Introduction

tissues need. Nox1 is predominantly present in the colon, where it contributes to the host defense process while Nox2 is the phagocyte NADPH oxidase which was found to be the clear host defense enzyme. Nox3 is localized in the inner ear, where it is involved in the otoconia morphogenesis but according to its localization it may also play a role in the auditory system. Nox4 is expressed in the kidney, vascular cells and osteoclasts, and it is an active enzyme regulated on the level of gene expression. Nox5, a calcium activated enzyme, is predominantly expressed in the lymphoid tissues and testis, where it may contribute in the signaling process. DOUX1 is expressed in the thyroid and respiratory epithelia where DOUX2 presents in the thyroid and gastrointestinal glandular epithelia, both DOUX enzymes are involved in the thyroid hormone synthesis and epithelial host defense [50, 53].

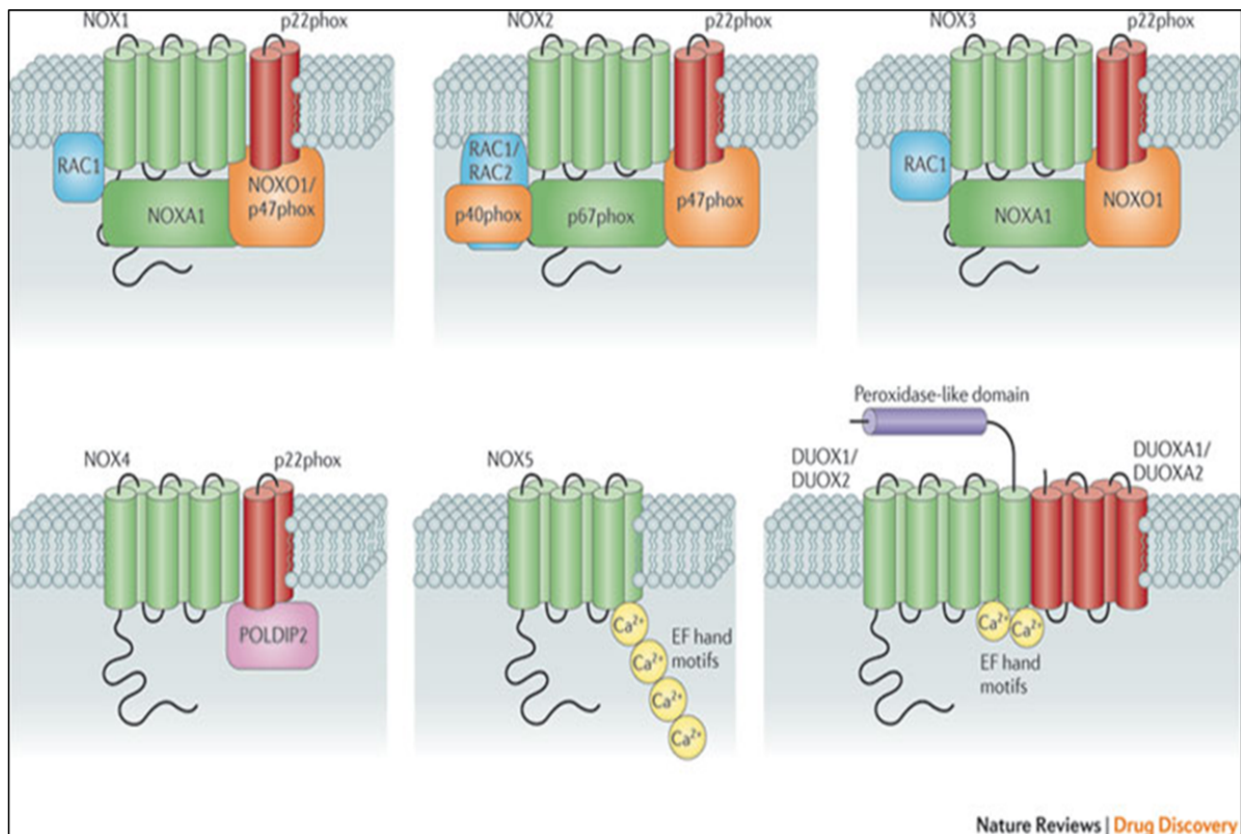


Figure 3 : Schematic representation of the NADPH oxidase enzyme and its isoforms [46].

Introduction

1.3.2 Cellular Defense against ROS

Detoxification of reactive oxygen species (ROS) is important for the survival of all aerobic life forms. As such a number of defense mechanisms have evolved to suits this need and provide a balance between the production and removal of ROS. An imbalance toward the pro-oxidative state is often referred to as “Oxidative stress”.

Cells have a variety of defense mechanisms to ameliorate the harmful effects of ROS. Superoxide dismutase (SOD) catalyzes the conversion of two superoxide anions into a molecule of hydrogen peroxide (H_2O_2) and oxygen (O_2) [54]. In the peroxisomes of eukaryotic cells, the enzyme catalase converts H_2O_2 to water and oxygen, and thus completes the detoxification initiated by SOD. Glutathione peroxidase is a cluster of enzymes containing selenium, which also catalyze the degradation of hydrogen peroxide, as well as organic peroxides to alcohols.

There are number of non-enzymatic small molecule antioxidants that play a role in the detoxification process. Glutathione may be the most important intracellular defense against the deleterious effects of reactive oxygen species. This tripeptide (glutamyl-cysteinyl-glycine) provides an exposed sulfhydryl group, which serves as an abundant target for attack. Reactions with ROS molecules oxidize glutathione but the reduced form is regenerated in a redox reaction by an NADPH-dependent reductase. Vitamin C or ascorbic acid is a water soluble molecule capable of reducing ROS, while vitamin E (α-tocopherol) is a lipid soluble molecule that has been suggested to play a similar role in membranes. The ratio of the oxidized form of glutathione (GSSG) and the reduced form (GSH) is a dynamic indicator of the oxidative stress of an organism [55].

1.3.3 ROS measurement

Establishing a precise role for ROS in vivo or in vitro requires the ability to measure them and the oxidative damage that they cause. Different methods were applied to detect and quantify ROS, some of them used in vivo and others in vitro. Whatever the applied method to trap ROS, it is necessary to evaluate how the method works, what is likely to confound and how the quantification will be achieved.

One of the techniques that is used for ROS measurement is L-band electron spin resonance (ESR) with nitroxyl probes and magnetic resonance imaging spin trapping

Introduction

which detects the presence of unpaired electrons, recently it is under development to measure ROS in the whole animal [56-57].

Fluorescence-based probes are commonly used to detect the cellular production of RS such as dichlorofluorescein diacetate (DCFDA), which is the most popular among these probes. DCFDA is deacetylated by esterases to the non-fluorescent product, dichlorofluorescein (DCFH). DCFH is then converted by reactive species (RS) into DCF, which can be easily visualized by strong fluorescence at 525 nm when excited at around 488 nm, the drawback in DCFDA is that it is not specific for certain RS [58].

Dihydrorhodamine (DHR) is a dye commonly used to detect several RS (OH^\cdot , ONOO^- , NO_2^\cdot derived species), but it is poorly sensitive to O_2^\cdot , H_2O_2 or NO^\cdot [59]. DHR is oxidized to rhodamine 123, which is highly fluorescent around 536 nm when excited at about 500 nm [58].

Dihydroethidium (dihydroethidine, DHE), is frequently used as an indicator probe for superoxide radical ($\text{O}_2^{\cdot-}$) detection. It is oxidized to a fluorescent product and the more generally used excitation at 520 ± 10 nm enables the detection of at least two oxidation products of DHE. UV excitation is thought to be rather specific for the superoxide-DHE reaction product [60-61]. Dihydroethidium is a reduced form of the commonly used DNA dye ethidium bromide. It has been applied extensively in tissue culture experiments to evaluate reactive oxygen species (ROS) production. Dihydroethidium (DHE), by virtue of its ability to freely permeate cell membranes is used extensively to monitor superoxide production. It had long been postulated that DHE upon reaction with superoxide anions forms a red fluorescent product (ethidium) that intercalates with DNA. However, more recent studies have suggested that the product is actually 2-hydroxyethidium. DHE which is perhaps the most specific and least problematic dye as it detects essentially superoxide radicals, is retained well by cells, and may even tolerate mild fixation. Dihydroethidium itself is blue fluorescent in cell cytoplasm while the oxidized form ethidium is red fluorescent upon DNA intercalation. Many other techniques and probes are used for detection of RS in vivo and in vitro, according to the aim of the investigation [58].

Introduction

1.4 Genotoxicity and endogenous hormones

Increased levels of endogenous hormones such as angiotensin II and steroidal hormones can result in genomic damage [62-65]. One of the most important hormones in the body is insulin which controls different metabolic pathways and plays a critical role in cell proliferation [66].

1.5 Insulin

The Latin word *insula* means "island", from which the name is derived. It is a polypeptide hormone which is synthesized and secreted by pancreatic beta cells, so called "island-cells". The structure of insulin structure varies slightly between species of animals; insulin from animal sources differs somewhat in "strength" (in carbohydrate metabolism control effects) from that of humans because of those variations. Porcine insulin is especially close to the human version. The human insulin protein is composed of 51 amino acids, and has a molecular weight of 5808 Da. Insulin consists of 2 polypeptide chains A (with 21 amino acid residues) and B (with 30 amino acid residues) that are linked through disulfide bridges. Additionally, chain A contains an intra-chain disulfide bridge linking residue 6 and 11. C-chain, which connects A and B chains, is liberated along with insulin after breakdown of proinsulin [67].

Insulin is synthesized in the pancreas in the form of preproinsulin and within a minute after synthesis, it is discharged into cisternal space of rough endoplasmic reticulum where it is cleaved into proinsulin by proteolytic enzymes. Proinsulin with a C-chain linking A and B chains is then transported by microvesicles to the Golgi apparatus. Proinsulin is released in vesicles. Conversion of proinsulin to insulin continues in maturing granules through the action of prohormone convertase 2 and 3 and carboxy peptidase H. Maturing granules are translocated with the help of microtubules and microfilaments [68].

Insulin is essential for appropriate tissue development, growth, and maintenance of whole-body glucose homeostasis. This hormone is secreted in response to increased circulating levels of glucose and amino acids after a meal. Insulin regulates glucose homeostasis at many sites, reducing hepatic glucose output (via decreased

Introduction

gluconeogenesis and glycogenolysis) and increasing the rate of glucose uptake, primarily into striated muscle and adipose tissue. In muscle and fat cells, the clearance of circulating glucose depends on the insulin-stimulated translocation of the glucose transporter GLUT4 isoform to the cell surface [69]. Moreover, insulin stimulates the transport of potassium and magnesium into the cell. Insulin stops the use of fat as an energy source by inhibiting the release of glucagon. With the exception of the metabolic disorder diabetes mellitus and metabolic syndrome, insulin is provided within the body in a constant proportion to remove excess glucose from the blood, which otherwise would be toxic. As a central metabolic control mechanism, insulin status is also used as a control signal to other body systems (such as amino acid uptake by body cells). In addition, it has several other anabolic effects throughout the body.

1.5.1 Insulin action and signaling mechanism

Insulin is the most potent anabolic hormone known; its action begins with the binding of insulin to heterotetrameric receptors (insulin receptors) on the cell membrane of the target cells. Insulin receptors are membrane glycoproteins composed of two separate insulin-binding (alpha-subunits) and two signal transduction (beta-subunits) domains [70]. Binding of insulin to the receptors results in conformational changes in the alpha-subunits that promote ATP binding to the intracellular domain of the beta-subunit. ATP binding leads to the activation of a tyrosine kinase in the beta-subunit that autophosphorylates the receptor, the receptor then undergoes a series of intramolecular transphosphorylation reaction cascades in which one β subunit phosphorylates its adjacent partner on specific tyrosine residues. Some evidence suggests that different tyrosine residues account for distinct functions. For example, phosphorylation of COOH-terminal tyrosines mediates the mitogenic actions of insulin. The phosphorylated tyrosines in the juxtamembrane domain may participate in the substrate binding, whereas those found within the kinase domain regulate the catalytic activity of the insulin receptor β subunit. Activated insulin receptor phosphorylates a number of important proximal substrates on tyrosine, including members of the insulin receptor substrate family (IRS1/2/3/4), the Shc adapter protein isoforms, SIRP family members, Gab-1, Cbl, and APS. Tyrosine phosphorylation of the IRS proteins creates recognition

Introduction

sites for additional effector molecules containing Src homology 2 (SH2) domains. These include the small adapter proteins Grb2 and Nck, the SHP2 protein tyrosine phosphatase and, most importantly, the regulatory subunit of the type 1A phosphatidylinositol 3-kinase (PI3-kinase) [70-73]. The insulin signal is further propagated through a phosphorylation network involving other intracellular substances. Through activation of these signaling pathways, insulin acts as a powerful regulator of metabolic function. Furthermore, insulin receptor-mediated activation of the mitogen-activated protein (MAP) kinase pathway has been implicated in effects on growth and proliferation [73].

Several studies have suggested that the interaction of IRS with PI3-kinase is necessary for the appropriate activation and/or targeting of the enzyme to a critical intracellular site, perhaps including its association with GLUT4 vesicles. However, expression of the dominantly interfering IRS PH and PTB domains completely prevents insulin-stimulated IRS tyrosine phosphorylation and DNA synthesis but have no significant effect on GLUT4 translocation [70]. The targets of PI3-kinase action are likewise controversial. Two classes of serine/threonine kinases are known to act downstream of PI3-kinase, namely the serine/threonine kinase AKT, also known as protein kinase B (PKB), and the atypical protein kinase C isoforms ζ and λ (PKC ζ/λ). Stable expression of a constitutively active, membrane-bound form of AKT in 3T3L1 adipocytes results in increased glucose transport and persistent localization of GLUT4 to the plasma membrane [74-75]. Similarly, PKC ζ is also activated by the formation polyphosphoinositides, which accumulate in insulin-treated cells; PKC ζ is therefore also sensitive to pharmacologic PI 3-kinase inhibitors, such as wortmannin [76]. Expression of PKC ζ or PKC λ are also reported to induce GLUT4 translocation, whereas expression of a dominant-interfering PKC λ inhibited GLUT4 translocation [77-78]. Thus, although PI3-kinase activation is essential, the protein kinase targets that mediate the effects of this pathway remain uncertain [70].

Recent studies have shown that insulin can also rapidly induce the tyrosine phosphorylation of the Cbl proto-oncoprotein, but only in insulin-responsive cells [79]. This phosphorylation requires the presence of the adapter protein CAP, which associates with a proline-rich domain in Cbl through its COOH-terminal SH3 domain.

Introduction

CAP appears to be important in insulin signaling, as it is markedly induced during adipocyte differentiation and is transcriptionally regulated by the thiazolidinedione family of insulin-sensitizing PPAR γ agonists [80]. These data suggest that the insulin-dependent tyrosine phosphorylation and/or compartmentalization of CAP/Cbl complex may provide a necessary second signal that functions in parallel with the activation of the PI3-kinase–dependent signaling pathway.

1.5.2 Hyperinsulinemia and other diseases

Hyperinsulinemia is a condition involving an excessively high level of insulin in the blood stream. Research has recently identified hyperinsulinemia in the context and as possible cause of several illnesses. One of the most common diseases accompanied by hyperinsulinemia is diabetes mellitus. Indeed, most patients with type I and type II diabetes are exposed to high insulin, however the physiologic and therapeutic conditions are very different between both types of diabetes. Because of autoimmune destruction of pancreatic β -cells, type I diabetic patients have an absolute requirement for exogenous insulin. In these patients, insulin administration cannot replace the physiologic insulin secretion exactly, leading to different temporal patterns and compartment distribution [81-82]. Circulating insulin may sometimes reach two- to five folds higher concentrations than its normal endogenous levels. On the contrary, in most type II diabetic patients, hyperglycemia is associated with endogenous hyperinsulinemia, a compensatory state caused by insulin resistance. This condition often persists for many years before the insulin production is exhausted and reduced insulin levels develop. Over 40% of those with Type 2 diabetes require insulin as part of their diabetes management plan [81].

Polycystic ovarian syndrome (PCOS) is a prevalent disorder affecting approximately 6% of women of reproductive age, and is characterized by anovulation and hyperandrogenism. It has also become apparent that a frequent feature of women with PCOS is insulin resistance accompanied by compensatory hyperinsulinemia, and increasing evidence suggests that hyperinsulinemia plays an important role in the pathogenesis of PCOS [83].

Introduction

High baseline and continuously increasing fasting insulin levels were the independent determinants for future development of nonalcoholic fatty liver disease during a 5-year follow-up in nondiabetic healthy adults [84]. Hyperinsulinemia is linked to high blood pressure and arteriosclerosis and it is a bigger risk factor for cardiovascular disease than excess cholesterol [85]. It is also a major cause of obesity [86].

Furthermore, epidemiological studies indicated that the risk of several types of cancer is increased in patients suffering from diabetes type II and obesity. This includes esophageal adenocarcinoma [87-88], as well as cancers of the pancreas, liver, breast, urinary tract, kidney and female reproductive organs [81, 89-90]. One of the most common cancers associated with hyperinsulinemia is colon cancer, for which an impressive body of epidemiological and research data collected over the past decade indicate that the risk is elevated in patients suffering from different diseases which are all characterized by hyperinsulinemia, such as metabolic syndrome, diabetes mellitus and obesity [91-94]. People with type II diabetes are nonetheless more likely to develop cancer and to die from it than members of the general population, so cancer should be numbered among the complications of diabetes [95]. Interestingly metformin, the first choice for oral pharmaceutical treatment of type II diabetes, is not only an insulin sensitizer [96-97] but it also seems to reduce the cancer risk associated with type II diabetes [98-101]. Obesity, insulin resistance, and/or increased levels of IGF-1 and insulin are strongly associated with most (but not all) of the diabetes-related cancers in the nondiabetic population [95]. Insulin and IGF-1 offer a plausible mechanistic explanation for the overlapping risk of cancer in the nondiabetic and diabetic populations. Both hormones are mitogenic and present at high levels in insulin-resistant states, and their receptors are over expressed on the surface of cancer cells associated with diabetes. They thus have the potential to act as tumor growth factors in vivo as well as in vitro [102-103]. Accordingly, drugs used to treat diabetes might influence the risk of cancer by modulating the insulin/IGF axis [95].

1.5.3 Insulin and oxidative stress

It is known that reactive oxygen species (ROS) are important mediators during insulin dependent cellular signaling [104-106]. One of the suggested signaling mechanisms for

Introduction

insulin-induced ROS stimulation is the activation of NADPH-dependent H₂O₂ generation [104]. This seems to be involved in the insulin-mediated ROS production in colon cells [107]. Another source for insulin-dependent ROS formation seems to be mitochondria, which were observed to play a role in ROS production in hepatocytes [108]. In 2011, Aggeli et al reported that insulin-induced oxidative stress up-regulates heme oxygenase-1 via diverse signaling cascades in the C2 Skeletal Myoblast Cell line [109]. Low levels of ROS, including superoxide and H₂O₂, are produced in a rapid temporal response to cellular growth factor and cytokine stimulation and are integral to the regulation of a variety of intracellular signaling pathways [110-114], this is also true for insulin [104-106] for which many studies also reported that it stimulates the production of ROS [115-117]. Therefore, excess ROS may be produced under hyperinsulinemia. The damaging effects of excess ROS have been well described and ROS can affect almost all biological macromolecules of cells [118]

Objectives

2. Objectives

Oxidative stress, DNA damage and cancer, are three terms which have recently appeared to be linked strongly to each other. Oxidative stress which results from the imbalance between oxidant production (such as ROS) and antioxidant levels in the body, is observed in different diseases such as diabetes mellitus and obesity. These are diseases which also exhibit cancer risk. The damaging effects of ROS are reported frequently, varying between effects on macro and micro molecules in the cells reaching the DNA and resulting in DNA oxidization, chromosome aberrations, DNA single and double strand breaks, base modifications and other kinds of DNA damage, which can play a role in development and progression of malignancy.

Many diseases such as diabetes mellitus, metabolic syndrome, obesity and polycystic ovarian syndrome are characterized by hyperinsulinemia, a term describing high blood insulin levels. Patients suffering from hyperinsulinemia are found to exhibit higher cancer risk than healthy individuals.

Many studies showed that insulin in high level can stimulate ROS production causing oxidative stress which in turn can lead to different deleterious consequences.

According to the previous knowledge, the aim of this study was designed to characterize the genomic damage induced by insulin at high levels in vitro in different tissues, mainly colon (represented as HT29, Caco-2 and rat primary colon cells), kidney (represented as LLC-PK1, HK2 and rat primary kidney cells) and lymphocytes (represented as cultured peripheral lymphocytes) and the pathways which lead to the genotoxicity of insulin in vitro. As an in vivo model kidneys from ZDF rats infused with insulin and peripheral lymphocytes from diabetic patients were used.

First the genotoxicity of insulin in the cells in vitro have to be investigated by the most common genotoxicity tests, comet assay and micronucleus frequency test, and on the protein level, accumulation of p53 protein had to be investigated as a marker for DNA damage.

To elucidate the link between insulin and DNA damage, stimulation of ROS production upon treatment of the cells with insulin had to be measured using H₂DCF-DA and DHE staining, and the protective effect of antioxidants (tempol and apocynin) had to be investigated. The sources of the produced ROS (mainly mitochondria and NADPH

Objectives

oxidase enzyme) had to be identified by using different inhibitors. The pathway which starts with the stimulation of the insulin receptor and insulin-like growth factor 1 receptor, followed by activation of different proteins and ultimately resulting in the production of ROS had to be identified.

In the ZDF rats kidneys, p53 level and 8-oxo-7, 8-dihydro-2'-deoxyguanosine (8-oxodG) had to be measured as markers for DNA damage and DHE staining was to be used as indicator for oxidative stress in two groups of rats. The first group was infused with different insulin concentrations leading to normal postprandial and pathophysiological insulin levels and the second group was treated to evaluate the effect of metformin treatment. In the diabetic patients' peripheral lymphocytes, micronucleus frequency had to be measured and compared to healthy individuals.

Materials and methods

3. Materials and methods

3.1 Chemicals and reagents

Bovine insulin, tempol, apocynin, plumbagin, wortmannin, rotenone, Histopaque 1077 and Lectin/PHA L8902 and metformin D-150959 were purchased from Sigma--Aldrich (Munich, Germany). Basic laboratory chemicals were purchased from Sigma--Aldrich (Munich, Germany) and Merck Biosciences GmbH (Schwalbach, Germany). Human insulin and PPP (sc-204008) were purchased from Santa Cruz biotechnology (Heidelberg, Germany), HNMPA-(AM)₃ was purchased from Enzo life sciences (Loerrach, Germany), FPG enzyme and FPG buffer were purchased from New England Biolabs (Frankfurt, Germany), VAS2870 was a gift from Vasopharm GmbH (Würzburg, Germany). Dihydroethidium (DHE) was purchased from Merck Biosciences GmbH (Schwalbach, Germany). Gel Red and Gel Green were purchased from Biotrend (Köln, Germany). H2DCF-DA was purchased from Invitrogen Life Technologies (Darmstadt, Germany), Annexin-V-Fluos Stock (Cat. 1828681) was purchased from Roche Applied Science (Germany). Cell culture media and reagents were obtained from PAA Laboratories GmbH (Pasching, Austria) and Invitrogen Life Technologies (Darmstadt, Germany).

3.2 Antibodies

Anti-AKT (pS473) antibody (22650) was purchased from Rockland (Gilbertsville, PA, USA). Anti-pIR (Tyr1150/1151) and anti pIGF-1R (Tyr1161/tyr1165/Tyr1166) were purchased from MerckMillipore (Darmstadt, Germany), the anti p85 (19H8) was purchased from Cell Signaling Technology Inc (Beverly, USA), the anti β -actin antibody (T6199) was purchased from Sigma-Aldrich (Taufkirchen, Germany), the anti p53 (Pab 240, sc-99), anti-Nox4 (3187-1) was from Epitomics (Burlingame, USA), anti-Nox1 (sc-25545), anti-Nox2 (sc-130543) antibodies and the secondary antibodies (sc-2004, sc-2005, sc-2020) were from Santa Cruz Biotechnology (Heidelberg, Germany).

Materials and methods

3.3 siRNA oligonucleotides

The siRNA oligonucleotides for Nox2 (sc-35503), Nox4 (sc-41586), Nox1 (sc-43939) and control siRNA (sc-37007) were purchased from Santa Cruz Biotechnology (Heidelberg, Germany).

3.4 PCR primers

Primers for PCR were taken from the literature or designed using the program Primer3 (<http://frodo.wi.mit.edu/primer3>) and ordered from MWG Biotech (Ebersberg, Germany).

Human Insulin receptor (IR) [119]

Forward: 5'-AAC CAG AGT GAG TAT GAG GAT-3'

Reverse: 5'-CCG TTC CAG AGC GAA GTG CTT-3'(125 bp)

Annealing temperature for IR 58 °C

Human Insulin-like growth factor1 receptor (IGF-1R)

Forward: 5'-AGG GCG TAG TTG TAG AAG AGT TTC C-3'

Reverse: 5'-TAC TTG CTG CTG TTC CGA GTG G-3' (101 bp)

Annealing temperature for IGF1R 58 °C

Sus scrofa Insulin receptor (IR)

Forward: 5'-AGA GCG GAT CGA GTT TCT CA-3'

Reverse: 5'-CCA TCC CAT CAG CAA TCT CT-3' (245)

Annealing temperature for IR 52 °C

Sus scrofa Insulin-like growth factor1 receptor (IGF-1R)[120]

Forward: 5'-TGG AGA TCA GCA GCA TC-3'

Reverse: 5'-TCA GCC TTG TGT CCT GAG TG-3' (199 bp)

Annealing temperature for IGF-1R 50 °C

Nox1

Forward: 5'-GGA TGA TCG TGA CTC CCA CT-3'

Reverse: 5'-AGG TTG TGG TCT GCA CAC TG-3' (458 bp)

Annealing temperature for Nox1 59.5 °C

Materials and methods

Nox2

Forward: 5'-TGC AGC CTG CCT GAA TTT CAA C-3'

Reverse: 5'-GAG GCA CAG CGT GAT GAC AAC-3' (391 bp)

Annealing temperature for Nox2 56 °C

Nox4

Forward: 5'-CTG GTG AAT GCC CTC AAC TT-3',

Reverse: 5'-CTG GCT TAT TGC TCC GGA TA-3' (556 bp)

Annealing temperature for Nox4 52 °C

Human small mitoDNA (HSM) [121]

Forward: 5'-CCC CAC AAA CCC CAT TAC TAA ACC CA-3'

Reverse: 5'-TTT CAT CAT GCG GAG ATG TTG GAT GG-3' (220 bp)

Annealing temperature for HSM 58 °C

β -actin

Forward: 5'-CTC TTC CAG CCT TCC TTC CT-3',

Reverse: 5'-AGC ACT GTG TTG GCG TAC AG-3' (610 bp)

Annealing temperature 56 °C

3.5 Cell lines and cell culture reagents

LLC-PK1, a pig kidney cell line with many properties of proximal tubular cells was obtained from the American Type Culture Collection (ATCC, Rockville, MD;HPACC, Salisbury, UK). LLC-PK1 cells were cultured at 37 °C, 5% (v/v) CO₂ in Dulbecco's modified Eagle medium (DMEM) low glucose (1 g/L) supplemented with 10% (v/v) fetal bovine serum (FBS), 1% (w/v) L-glutamine, 2.5% (w/v) HEPES and 0.4% (w/v) antibiotics (50 U/ml penicillin, 50 mg/ml streptomycin). They were subcultured twice per week.

HK-2, a human kidney cell line with many properties of proximal tubular cells, were obtained from Dr. G. Garibotto, Nephrology Division, Department of Internal Medicine and Urology Division, University of Genoa, Genoa, Italy and cultured in DMEM/F12 medium supplemented with 5 % fetal calf serum, 2 mM of L-glutamine, 1 % antibiotics,

Materials and methods

10 µg/l epidermal growth factor, 5 µg/l hydrocortisone, 5 µg/l sodium selenate, 5 ng/l bovine pituitary extract, 5 mg/l transferrin, 5 mg/l insulin and 5 ng/l T3. They were subcultured two times per week.

HT29 (Human colon adenocarcinoma cell line) cells were obtained from the American Type Culture Collection (ATCC, Rockville, MD; HPACC, Salisbury, UK). HT29 cells were cultured at 37 °C, 5% (v/v) CO₂ in DMEM high glucose (4.5 g/L) supplemented with 10% (v/v) fetal bovine serum (FBS), 1% (w/v) L-glutamine, and 0.4% (w/v) antibiotics (50 U/ml penicillin, 50 mg/ml streptomycin). They were subcultured two times per week.

Caco-2 (Heterogeneous human epithelial colorectal adenocarcinoma cell line) cells were obtained from the American Type Culture Collection (ATCC, Rockville, MD; HPACC, Salisbury, UK). They were cultured at 37 °C, 5% (v/v) CO₂ in modified Eagle medium (MEM) with Earle's salts and supplemented with 20% (v/v) fetal bovine serum (FBS), 1% (w/v) L-glutamine, 1% (v/v) sodium pyruvate, 1% (v/v) non-essential amino acids and 0.4% (w/v) antibiotics (50 U/ml penicillin, 50 mg/ml streptomycin). They were subcultured two times per week.

HL60, a human promyelocytic cell line was kindly donated by Prof. Schinzel, Vasopharm, Wuerzburg, Germany. HL60 cells were cultured at 37 °C, 5% (v/v) CO₂ in Roswell Park Memorial Institute medium (RPMI) 1640 medium, supplemented with 10% (v/v) fetal bovine serum (FBS), 1% (w/v) L-glutamine, and 0.4% (w/v) antibiotics (50 U/ml penicillin, 50 mg/ml streptomycin). They were subcultured twice per week.

MCF-7 (Human breast adenocarcinoma cell) cells were obtained from the American Type Culture Collection (ATCC, Rockville, MD; HPACC, Salisbury, UK). MCF-7 cells were cultured at 37 °C, 5% (v/v) CO₂ in RPMI 1640 medium, supplemented with 5% (v/v) fetal bovine serum (FBS), 1% (w/v) L-glutamine, 1% sodium pyruvate and 0.4% (w/v) antibiotics (50 U/ml penicillin, 50 mg/ml streptomycin). They were subcultured twice per week.

Materials and methods

BT-474 (Human breast carcinoma cell) cells were kindly donated by PD Dr Jörg Wischhusen, Frauenklinik, Wuerzburg, Germany. BT-474 cells were cultured at 37 °C, 5% (v/v) CO₂ in RPMI 1640 medium, supplemented with 10% (v/v) fetal bovine serum (FBS), 1% (w/v) L-glutamine, 0.5 % sodium pyruvate and 1% (w/v) antibiotics (50 U/ml penicillin, 50 mg/ml streptomycin). They were subcultured twice per week.

Primary rat cells, Primary rat cells were isolated from freshly obtained rat (kidney, colon, fatty and liver) tissues (n= 3, 12 week old female SD rats) were washed once in ice-cold PBS. They were transferred into 3 ml of an ice-cold medium (LLC-PK1, HT29, HK2 (the same medium is used for the fatty tissue), HepG2 media respectively) and minced on ice into small pieces very fast. The extracted primary cells were sifted through a cell strainer with a mesh pore size of 100 µm (BD, Heidelberg, Germany), centrifuged for 5 minutes at 1000 rpm and 4°C, and were finally resuspended in 1 ml of the above-mentioned medium.

3.6 Isolation of peripheral lymphocytes

Whole blood (10 ml) was collected into Heparin-EDTA tubes. Peripheral blood mononuclear cells (PBMC) were isolated by density gradient centrifugation on histopaque. Whole blood was added on the same amount of warmed up histopaque slowly and centrifuged 30 minutes, 1600 rpm at room temperature, then PBMC layer was placed in a tube containing 10 ml lymphocyte culture medium (RPMI 1640 medium and supplemented with 15% (v/v) fetal bovine serum (FBS), 1% (w/v) L-glutamine, 1% (v/v) sodium pyruvate, 1% (v/v) non-essential amino acids, 0.4% (w/v) antibiotics (50 U/ml penicillin, 50 mg/ml streptomycin) and 0,1% tylosin). PBMCs were washed two times with fresh medium for 10 minutes, RT at 1300 rpm, and were then resuspended in fresh medium and transferred into a 24 well plate where PHA (final concentration 10 µg/ml) was added to each well. After 42-44 hours at 37 °C, 5% (v/v) CO₂ cells were treated for 24 hours with insulin for comet assay analysis and for 24 hours with insulin and 3 µg/ml cytochalasin B for the micronucleus frequency test (the isolation

Materials and methods

procedures were done by the medical PhD student Annekathrin Leyh and the results will appear also in her thesis).

3.7 Rho0 cells (cells depleted of mtDNA)

HT29 and HK2 Rho0 cell lines were established by treating cells with low concentration of ethidiumbromide (0.4µg/ml). Cells were cultured at 37 °C, 5% (v/v) CO₂ in Dulbecco's modified Eagle medium high glucose (DMEM) (4.5 g/L) supplemented with 10% (v/v) fetal bovine serum (FBS), 1% (w/v) L-glutamine, 1% sodium pyruvate and 50 µg/ml uridine. They were subcultured two times per week.

3.8 Animal model and treatment

Rat kidneys were obtained from Dr Michael C. Kreissl (Department of Nuclear Medicine, University Hospital of Wuerzburg, University of Wuerzburg, Würzburg, Germany), the kidneys were from lean healthy rats (ZDF lean) which had been purchased from Charles River laboratories at 8 weeks of age. The animals were fed with a managed diet of Purina 5008 and were kept in an environmentally controlled room with a 12 hours light/dark cycles, and free tap water access. All procedures were approved by the Local Ethics Committee. Organ collection was made at 14 weeks of age under sodium pentobarbital anesthesia. The animals were sacrificed by decapitation and the kidneys were immediately frozen. Parts of the kidneys were used for analysis of p53 protein by western blot analysis and slices were prepared from the remaining tissue for DHE staining (ROS quantification). Before organ collection the rats were fasted for 14 hours and received a hyperinsulinemic euglycemic clamp, consisting of a glucose primer infusion followed by a continuous insulin infusion through a sterile silicon rubber catheter placed in the tail vein. Blood glucose levels were titrated to normal levels (5.5 mM) in all animals using an "Accutrend" sensor (Roche, Germany). Different amounts of insulin were infused, resulting in normal postprandial blood insulin levels (0.28 ± 0.179 ; control) in three animals and in high blood insulin levels (1.67 ± 0.67 nM) reflecting pathophysiological conditions in six animals. In addition, male obese Zucker diabetic fatty rats (ZDF, fa/fa n=10) were purchased and at 10 weeks of age the fa/fa rats were

Materials and methods

randomized in 2 groups with 5 animals in each group (ZDF fa/fa placebo; ZDF fa/fa metformin). The treatment consisted of 4 weeks of daily gavage feeding with either placebo solution (0.5% carboxymethylcellulose sodium salt solution 1ml/kg body weight/day) or metformin (1,1-dimethylbiguanide hydrochloride 97% SIGMA D-150959, dissolved in carrier solution at a concentration of 250 mg/ml to achieve a daily doses of 250 mg/kg/day). The animals sacrificed at the age of 14 weeks after the same treatment (application of the same clamp procedure and preparation of organs) as the lean animals, parts of the kidneys were used for insulin measurement and for the isolation of DNA for 8-oxodG analysis, and slices were prepared from the remaining tissue for DHE staining (ROS quantification).

The animals used for the study were also employed to study cardiovascular metabolism in ZDF rats (Kreissl et al, unpublished data).

3.9 Human subjects

During a medical thesis (Ms Katrin Hacke, not yet submitted), blood samples from 35 type II diabetic patients and 15 control were collected. In the present study, slides prepared from the peripheral lymphocytes of both groups for micronucleus frequency analysis were used and analyzed again by the author of this thesis. Characteristics of the patients and control group were summarized in table 1.

Group	Number and sex	Age
Control	10 females	67.10 ± 7.96
	5 males	68.4 ± 9.70
Type II diabetic patients	18 females	56.40 ± 9.20
	17 males	56.90 ± 9.80

Table 1: Characteristics of the patients and control group

Materials and methods

Further medications which administered by the patients were summarized in table 2.

Medicaments	No. of patients
ACE-inhibitor, AT1-Antagonist	8
Aldosterone antagonist	2
β-Blocker	5
Calcium antagonist	3
Diuretics	7
Statins	8
Oral anti- diabetic	14
Insulin	3
Acetylacetic acid (ASS)	6

Table 2: List of the medications administered by the type II diabetic patients in the study.

3.10 Apoptosis Assay

1×10^6 cells were cultured one day before the experiment, on the day of the experiment, cells were treated with insulin for the desired incubation time then trypsinized and collected, washed one time with the 1x binding buffer (10x binding buffer: 0,1 M HEPES/NaOH, 140 mM NaCl, 25 mM CaCl₂, pH 7,4, sterilized) followed by centrifugation then one time washing with PBS and centrifugation again. 100 µl AnnexinV/PI (propidium iodide) suspension (20 µl Annexine V-Fluos Stock, 20 µl PI stock (50 µg/ml), 960 µl 1x binding buffer) was added for 15 minutes in room temperature in dark. After staining, 900 µl 1x binding buffer were added and 10000 cells were examined by flow cytometry using a FACS LSR I (Becton-Dickinson, FACScan, USA).

Materials and methods

3.11 Comet assay

The alkaline version of the comet assay was performed in all the experiments. This endpoint detects single and double strand breaks as well as alkali-labile lesions on an individual cell basis. It is a standard test for genotoxicity testing in the development of substances [122]. After treatment of 1×10^6 cells/5ml for 2 hours with insulin (in the 6 days treatment experiment a daily exchange of 50% of the medium and a daily addition of 100 nM or 10 nM fresh insulin was performed) or other test compounds (5 minutes to 4 hours for time course experiment or 6 days for long exposure experiment) in the case of cell lines, 30 minutes for the primary rat cells and 24 hours for the cultured peripheral lymphocytes, the cells were harvested and 20 μ l of the treated cell suspension were mixed with 180 μ l of 0.5 % low melting agarose and added to fully frosted slides that had been covered with a bottom layer of 1 % normal melting point agarose. The slides were incubated in lysis solution (2.5 M NaCl, 0.1 M EDTA, 0.01 M Tris and 10 g/l N-lauroylsarcosine sodium adjusted to pH 10 with NaOH) with 1 % Triton X-100 and 10% dimethyl sulfoxide at 4 °C for at least 1 hour, when the comet assay was combined with bacterial FPG protein, slides were washed three times (for 5 minutes each) in enzyme buffer (40 mM HEPES, 100 mM KCl, 0.5 mM EDTA, 0.2 mg/ml BSA; pH 8.0) and covered with 1:1000 of either buffer or FPG protein in buffer, sealed with a cover slip and incubated for 30 minutes at 37 °C. After all treatment conditions, the slides were washed and then placed in the electrophoresis solution (300 mM NaOH, 1 mM EDTA, pH > 13.0) for 20 minutes. Then the electrophoresis was conducted for 20 minutes at 25 V (1.1 V/cm) and 300 mA. The slides were neutralized in 0.4 M Tris buffer (pH 7.5) and then dehydrated in methanol for 10 minutes at -20 °C. The slides were then left in 37 °C incubator to dry and stored at room temperature afterward. Before evaluation 20 μ l of Gel red /DABCO solution was added to each slide. Images of 50 randomly selected cells (25 per replicate slide) for each sample were analyzed with a fluorescence microscope (Labophot 2, Nikon, Germany) at 200-fold magnification using image analysis software (Komet 5, BFI Optilas, Germany). A representative picture of a damaged cell in the comet assay was shown in figure 1. The percentage of DNA in the tail was used to quantify DNA migration.

Materials and methods

3.12 Micronucleus frequency test

Micronuclei are small chromatin containing structures in the cytoplasm of cells which represent a subtype of chromosomal aberrations. This test is a standard assay in mutagenicity testing according to OECD guideline 487. 1×10^6 cells/5ml were incubated with insulin or other test substances in 5 ml medium. After 4 hours for cells or 24 hours for lymphocytes treatment, the medium was removed and replaced by fresh culture medium (with or without cytochalasine B) after washing with PBS. In the case of long-term experiments with 48 hours or 6 days insulin exposure, a daily exchange of 50% of the medium and a daily addition of 100 nM or 10 nM fresh insulin was performed. After a further 20-22 hours, cells were harvested, applied onto glass slides by cyospin centrifugation and fixed in methanol (-20°C) for at least two hours. Before counting, cells were stained for 3 minutes with Gel Green (10 μl stock solution in 990 μl distilled water), washed twice with PBS buffer and mounted for microscopy. A representative picture of a micronucleus containing cell was demonstrated in figure 2. From each of two slides, 1000 cells were evaluated for micronuclei and the average was calculated. For substance combinations, concentrations which were described as effective in the literature and had been found not toxic in preliminary experiments were applied.

3.13 Flow cytometric quantification of oxidative stress

To evaluate the formation of ROS, the cell-permeable fluorogenic probe 2',7'-dichlorodihydrofluorescein diacetate (H2DCF-DA) was used [123]. Oxidation of this probe can be detected by monitoring the increase in fluorescence using a flow cytometer with the appropriate filter FL1 488 (band width 25).

HT29 cells (5×10^5) were seeded one day before the experiment in 25 cm^2 flasks. Cells were incubated at 37°C in medium containing 10 nM insulin for 30 minutes and during the last 20 minutes, 10 μM H2DCF-DA was added. Afterwards, the medium was removed, cells were rinsed with PBS and trypsinized, and 1ml of 1% BSA/PBS was added per flask. Fluorescence of 30000 cells was measured by flow cytometry using a FACS LSR I (Becton-Dickinson, FACScan, USA).

Materials and methods

3.14 Microscopic analysis of the reactive oxygen species

To evaluate the formation of ROS, the cell-permeable fluorogenic probe dihydroethidium (DHE) was used. One day before the experiment, 2×10^5 cells were seeded on 24 mm cover slips in 6-well plates in 3 ml medium. 10 μ M DHE, antioxidant and inhibitors were added to the cells and incubated in the dark at 37°C for 30 minutes for all treatment. For the time course experiment, insulin was added in the time frame from 5 minutes to 2 hours, while 5 and 30 minutes insulin treatment was used for the dose response experiment with different insulin concentrations.

For the kidney sections from the ZDF rat, cryosections (5 μ m) were prepared with a Leica CM3050 Scryostat (Leica, Wetzlar, Germany). ROS production on cryosections was detected after staining the sections for 30 minutes with 10 μ M DHE at 37°C in the dark. After washing 3 times with PBS, the cover slips and the cryosections were mounted and observed under an Eclipse 55i microscope (Nikon GmbH, Düsseldorf, Germany) and a Fluoro Pro MP 5000 camera (Intas Science Imaging Instruments GmbH, Göttingen, Germany) at 200-fold magnification. All images of the DHE staining were taken using the same exposure time. Quantification was done by measuring grey values of 200 cells per treatment with ImageJ 1.40g (<http://rsb.info.nih.gov/ij/>).

3.15 Western Blot analysis

After treatment, the cells were harvested and lysed in homogenization buffer (0.2 M mannitol, 50 mM saccharose, 10 mM HEPES, pH: 7.5). The homogenization process was facilitated by disruption of the cell membranes mechanically and the yielded suspension was then centrifuged at 14000 rpm for 30 minutes at 4 °C. The protein containing supernatant was transferred to a clean tube and the concentration of protein in this solution was determined using Bradford's method. Generally, 30 μ g of protein per sample was loaded on a discontinuous acrylamide gel. After electrophoresis the gel was blotted on the PVDF membrane. The membrane was blocked overnight in either 1% bovine serum albumin (for pIGF-1R , pAKT, p85 and GAPDH) , 5 % nonfat milk powder (for p53 and β -actin) or 3% milk powder (pIR) in TBS-T buffer (5 mM TRIS, 150 mM NaCl, 0.05 % Tween-20) and then incubated with primary antibody (pIR (1:200), pIGF-

Materials and methods

1R (1:200), p85 (1:500), (pAKT (1:5000) and p53 (1:1000)) . After washing of the excess of primary antibody, the horse radish peroxidase (HRP) conjugated secondary antibody was added followed by washing. After incubation with HRP substrate, the membrane was exposed to an X-ray sensitive film and the film was developed afterward or by using FluorchemQ, Alpha Innotech, Biozyme (Hessisch, oldendorf, Germany).

For the kidney samples, a part of the kidneys was crushed in liquid nitrogen followed by lysis in homogenization buffer and the same procedure as mentioned before were applied to examine the presence of the protein in kidney.

3.16 siRNA transfection

The cells were seeded in antibiotic free medium in 6-well plates one day prior to the transfection. At the day of the experiment, the cells were washed with Transfection Medium (sc-36868, Santa Cruz Biotechnology). siRNA was diluted to 100 μ M in Transfection Medium. This solution was named solution A. Transfection Reagent (sc-29528, Santa Cruz Biotechnology) was also diluted to 100 μ M with Transfection Medium and named solution B. Solution A and B were gently mixed and incubated for 45 minutes at room temperature and then 800 μ l of Transfection Medium was added to this mixture. The cells were then covered with this solution and incubated for 18 hours at 37 °C. After this time, either the medium was changed and the cells were collected or treated with insulin and the proteins was extracted for confirming down regulation of the desired target or measure the desired protein activation.

3.17 Determination of insulin concentration by HPLC

Plasma insulin level in ZDF rat was determined according to standard RIA procedures before and after the clamp procedure.

From kidney tissue, tissular insulin was extracted using a minor modification of a published protocol [124]. Kidney tissue was lysed in homogenization buffer (0.2 M mannitol, 50 mM sucrose, 0.12g HEPES and Proteinase and phosphatase inhibitors, pH= 7.5) and centrifuged for 30 minutes at 4°C at 14.000 rpm. The protein containing supernatant was transferred to a clean tube and the concentration of protein in the

Materials and methods

solution was determined using Bradford's method. An aliquot equal to 500 µg total protein of the supernatant was mixed with double volume of 66 % acetonitrile and centrifuged for 1 minute at 4°C at 14.000 rpm. The supernatant was evaporated under nitrogen to dryness and reconstituted with 100 µl of 0.005 M HCl.

Preparation of mobile phase: Solution A was prepared by dissolving 28.4 g of anhydrous Na₂SO₄ and 9.8 g H₃PO₄ in Roth water; pH was then adjusted to 2.3 and the volume was completed to 1 L with Roth water. Solution B was acetonitril. Solutions (A and B) were filtered and sonicated before being introduced into the HPLC system.

HPLC analysis was performed using a Nucleosil 100-5 C18 (EC 250/4.6) analytical column (MACHEREY-NAGEL, Düren, Germany) using solutions A and B (20% MeCN: Na₂SO₄ to 80 % MeCN over 25 minutes at a flow rat 0.9 ml/min) and the detection was performed at 214 or 280 nm. Quantification was achieved by comparison to dilutions of a standard stock solution of insulin.

3.18 Quantification of 8-oxodG by LC-MS/MS

The genomic DNA was isolated from the ZDF rat kidney tissue according to a recently described protocol [125]. DNA concentration was measured by the absorbance at 260 nm. Protein contamination was checked using the absorbance ratio A₂₆₀/A₂₈₀; an absorbance ratio > 1.6 was acceptable. DNA hydrolysis was performed as described by Chao *et al.*[126]. The DNA samples (~20 µg) were spiked with 2.82 pmol of [15N5] 8-oxodG and 84.3 pmol of [15N5]-dG. Then, 10 µl of 1 U/µl nuclease P1 (in 300 mM sodium acetate and 1 mM ZnSO₄, pH 5.3) was added to the DNA solutions, and the DNA was incubated at 37°C for 2 hours. Thereafter, 10 µl of 10x alkaline phosphatase buffer (500 mM Tris/HCl, pH 8, and 1mM EDTA) containing 0.2 µl of alkaline phosphatase was added, and the incubation was continued at 37°C for 2 hours. Finally, 10 µl of 0.1 M HCl was added to neutralize the solution. The neutralized DNA hydrolysates were filtered through a cutoff filter tube (Ultrafree 5000 NMWL; Millipore, Schwalbach am Taunus, Germany) and centrifuged at 4°C and 7000 g for 45 minutes, then measured by online LC-MS/MS by Dr Oli RG. The column-switching operation method is described elsewhere [126-127]. 100 mL of DNA samples were loaded on the

Materials and methods

trap column using an auto sampler (Agilent 1100 series) and the content of 8-oxodG was quantified as reported elsewhere [126-127].

3.19 RNA and DNA extraction and RT-PCR

The expression of mRNA was detected using the reverse transcription polymerase chain reaction (RT-PCR). Total RNA was isolated from the cells with the RNeasy Mini Kit (Qiagen, Hilden, Germany) and 2.0 µg of RNA was used for cDNA synthesis using Verso cDNA Synthesis Kit (Thermo scientific, Schwerte, Germany), while total DNA was isolated using DNeasy tissue kit (Qiagen, Hilden, Germany) and 500 ng of DNA was used for the amplification step. The previous mentioned primers were used for amplification of Noxs (1, 2 and 4) (40 cycles), insulin receptor (IR) (40 cycles), insulin-like growth factor (IGF-1R) receptor (40 cycles), small mitochondrial DNA (HSM) (20 cycles) and β-actin (18 cycles). The PCR was performed using REDTaq™ ReadyMix™ PCR was used. Reaction Mix (Sigma-Aldrich, Taufkirchen, Germany) as Taq polymerase enzyme and thermal cycler PTC 200 MJ research (Watertown, MA, USA).

3.20 Statistics

Statistical calculations were performed using Statistica 8 (StatSoft (Europe) GmbH, Hamburg, Germany). Data are shown as averages ± standard deviation of the three single experiments. In the single experiments, means of % tail DNA calculated from all 50 cells per treatment were used in comet assays. Numbers of micronucleus containing cells per 1000 cells (derived from counting 2000 cells) were used in the micronucleus frequency test. Where relative values are shown, the average of all control values was set to 1.0, and then all individual experimental values calculated as alterations (x-fold) compared to that. Statistical significance among multiple groups was tested with Kruskal-Wallis test. Individual groups were then tested using the Mann Whitney U-test and results were considered significant if the *p*-value was ≤ 0.05.

Results

4. Results

4.1 Insulin mediated oxidative stress and genomic damage in mammalian colon cells.

4.1.1 Insulin-mediates DNA damage in colon cells

The genotoxicity of insulin was investigated by two assays, the comet assay and the micronucleus frequency test. Accumulation of p53 protein was also investigated as an indication for DNA damage.

Comet assay analysis of insulin-induced DNA damage was performed in HT29 colon cells treated with 10 nM insulin for different incubation times between 5 minutes and 4 hours (fig. 4), a significant induction of DNA damage was observed after all incubation conditions.

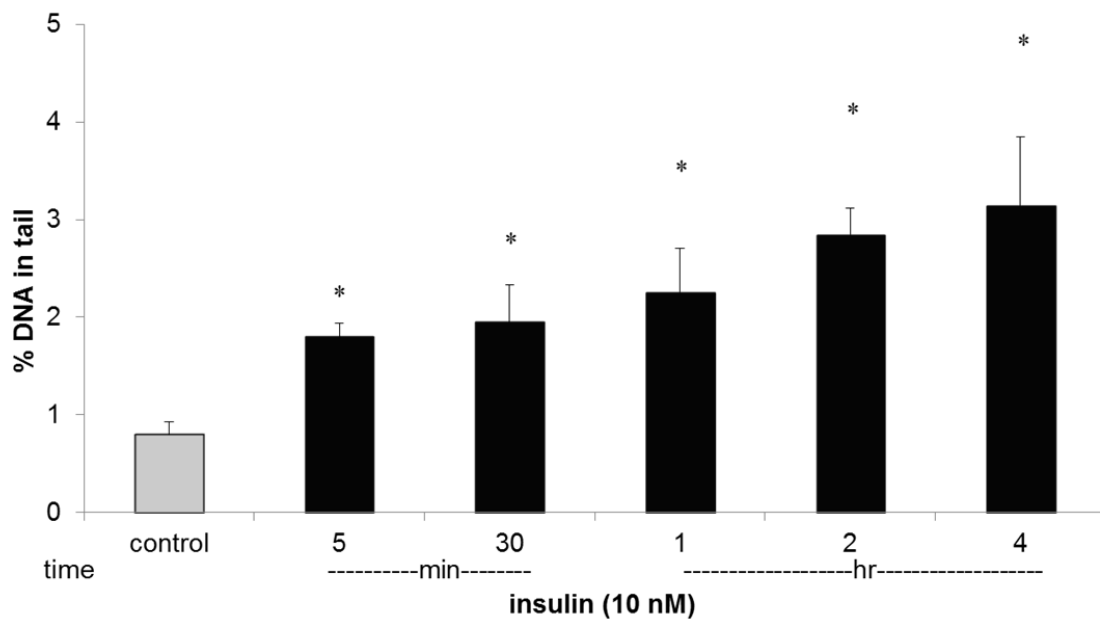


Figure 4: DNA damage (% DNA in tail) measured by comet assay analysis in the HT29 cells treated with 10 nM insulin for different incubation times (5 min to 4 hr) (* = significantly different from control).

Accumulation of p53 protein appears in many cellular events. One of those is DNA damage. P53 protein level was measured in HT29 cells treated with 10 nM insulin for

Results

different times (5 minutes to 4 hours) (fig. 5). The p53 level increased after 5 minutes of insulin stimulation.

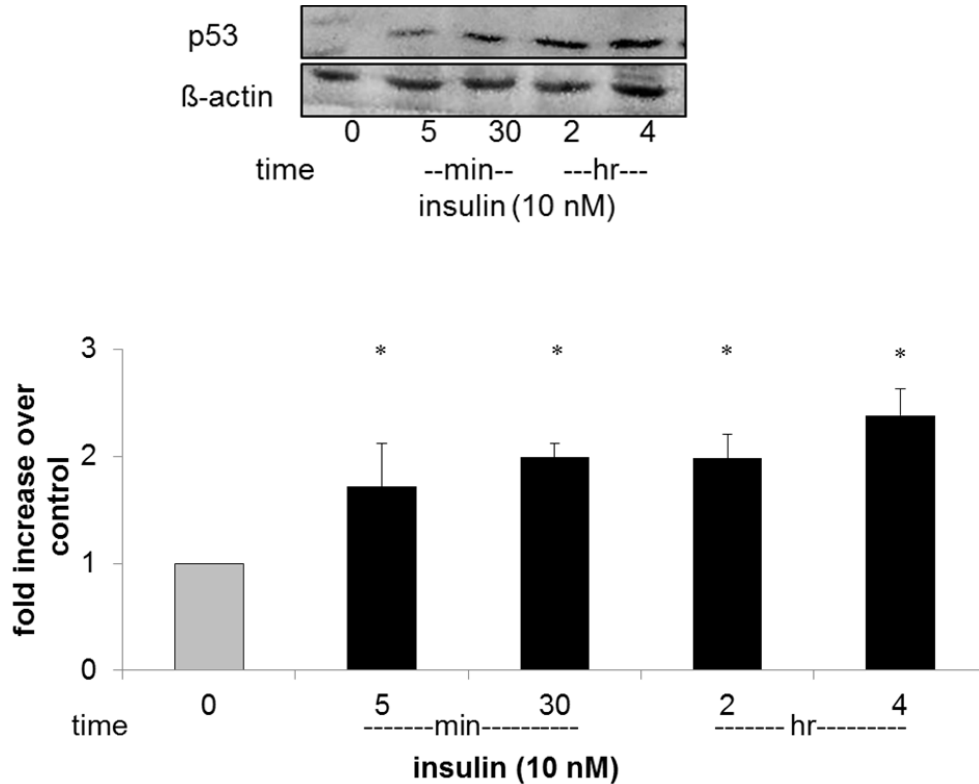


Figure 5: p53 levels in HT29 cells treated for with 10 nM insulin for different times (5 min to 4 hr) and measured by Western blot analysis, (* = significantly different from control)

To evaluate the concentration effect and to determine the concentration at which the DNA damage started to be measurable, HT29 cells were treated with different insulin concentrations ranging between 0.5 and 100 nM with a treatment duration of 2 hours (fig. 6), where the significant induction of DNA damage started at 5 nM insulin.

P53 level was also determined under the same conditions (fig. 7), in this case p53 started to accumulate after stimulation with 0.5 nM insulin.

Results

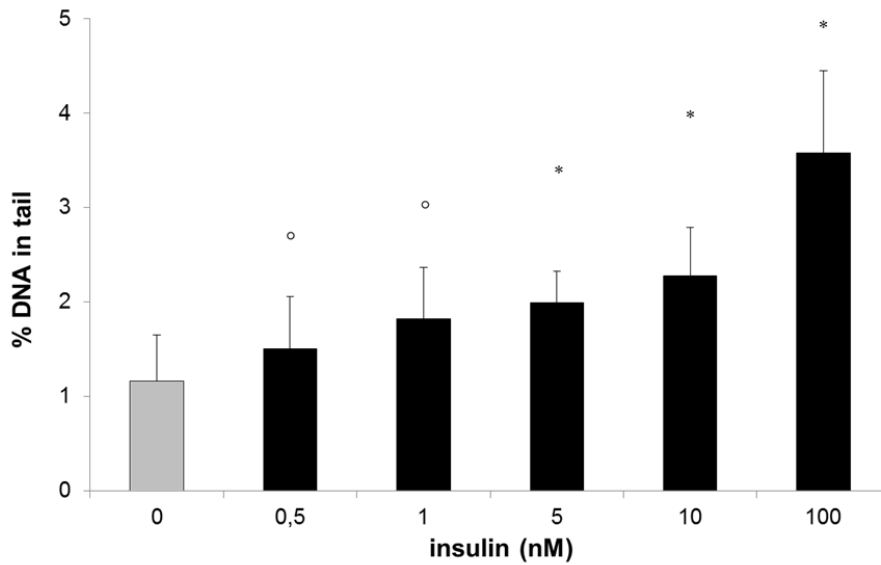


Figure 6: DNA damage (% DNA in tail) measured by comet assay analysis in the HT29 cells treated with different insulin concentrations for 2 hr (* = significantly different from control, ° = not significantly different from control).

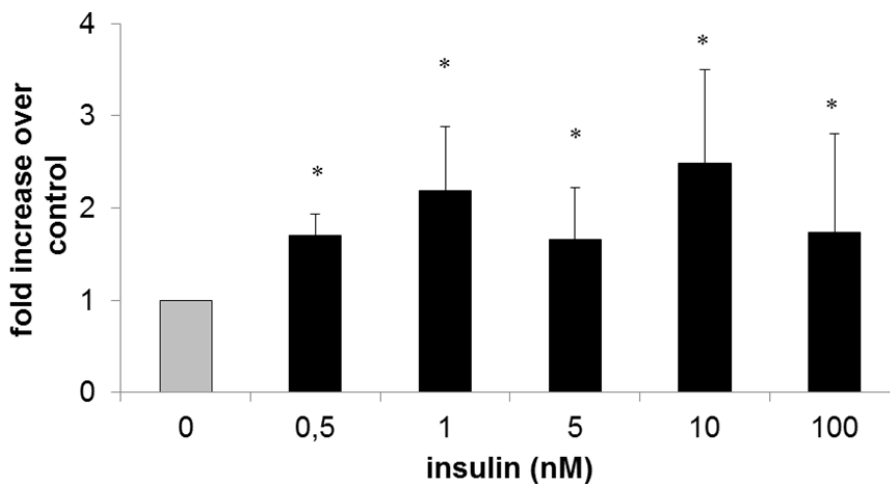
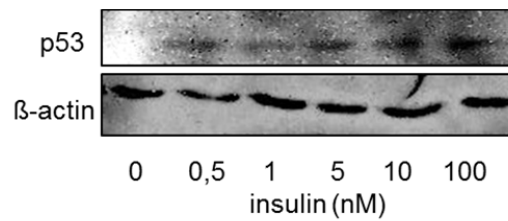


Figure 7: p53 levels in HT29 cells treated for 2 hr with different insulin concentrations (0.5 to 100 nM) and measured by Western blot analysis (* = significantly different from control).

Results

To evaluate the influence of both factors in the same experiment (exposure time and concentration); HT29 cells were treated with insulin for 6 days, the continuous exposure to 0.5-1 nM insulin for 6 days led to significant induction of DNA damage (fig. 8).

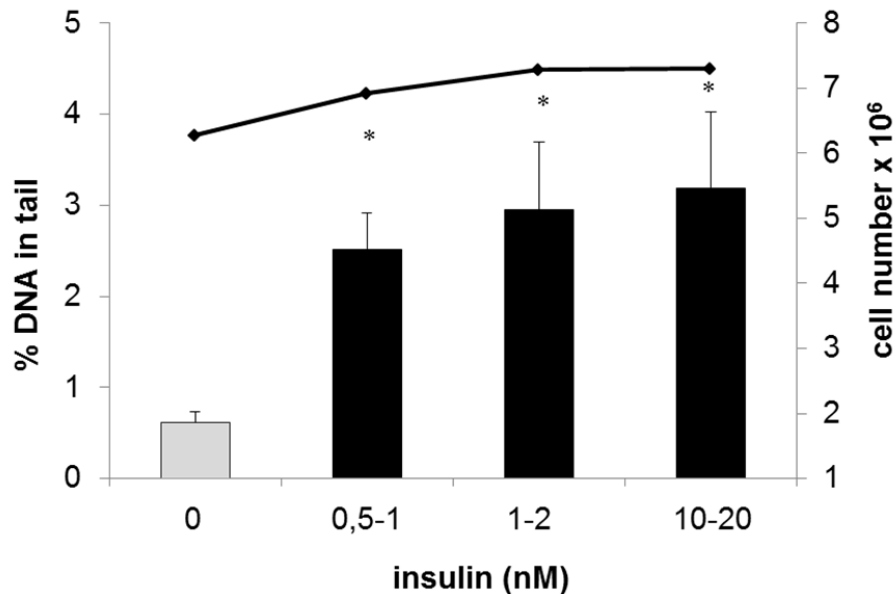


Figure 8: DNA damage (% DNA in tail) measured by comet assay analysis in the HT29 cell line treated with different insulin concentrations for 6 days, because of daily addition of fresh insulin, the concentration was 0.5-1 nM, 1-2 nM and 10-20 nM in the cultures during the 6 day treatment time, cell counts (straight line) at the time of harvest are shown on the second y-axis. (* = significantly different from control).

Overall, the cells reacted with significant induction of DNA damage to 10 nM insulin after 5 minutes, to 5 nM after 2 hours treatment and to 0.5-1 nM after 6 days treatment. In parallel to all comet assay experiments, vitality tests using activation of fluoresceine diacetate and membrane passage of Gel Red were performed and cell number was used as a marker for cell proliferation. The applied treatments did not result in significant reduction of vitality or increase in proliferation.

In the micronucleus frequency test, the formation of micronuclei was evaluated for an insulin concentration ranging between 0.5 to 100 nM in HT29 cells after treatment duration of 4 hours (plus an expression time of 20-22 hours (with addition of cytochalasin B) after treatment (fig. 9), a significant increase in micronucleus formation was observed at 1 nM insulin and higher.

Results

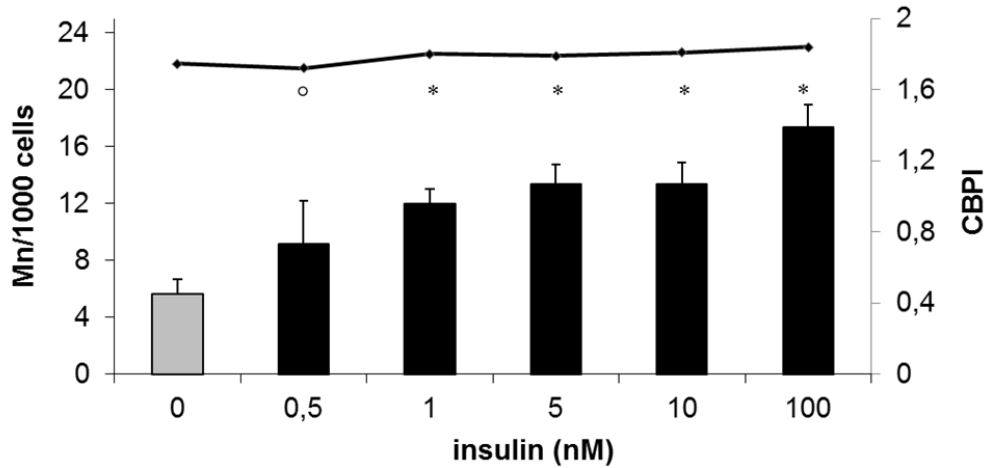


Figure 9: Chromatin damage (Mn/1000 cells) measured as micronucleus frequency in the HT29 cell line treated with different insulin concentrations for 4 hr with cytochalasin B addition for 20-22 hr after that, cell proliferation (CBPI) (straight line) is shown on the second y-axis. (* = significantly different from control, ° = not significantly different from control).

Experiments with insulin concentrations ranging between 0.5-1 nM to 10-20 nM insulin and treatment duration of 6 days (with cytochalasin B addition), plus an expression time of 20-22 hours after treatment was performed (fig.10).

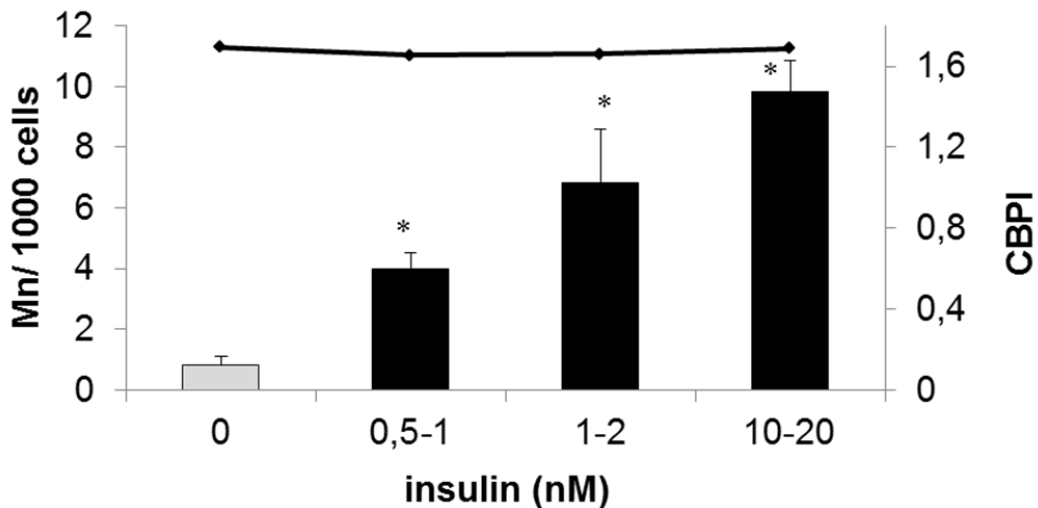


Figure 10: Chromatin damage (Mn/1000 cells) measured as micronucleus frequency in the HT29 cell line treated with different insulin concentrations for 6 days with cytochalasin B addition for the last 20-22 hr, cell proliferation (CBPI)(straight line) is shown on the second y-axis (* = significantly different from control).

Results

The same experiment was repeated without addition of cytochalasine B (fig. 11). In both experiments (fig.10, 11), a concentration dependent increase in micronucleus formation was observed with significant difference to the control at 0.5-1 nM and higher after treatment with insulin for 6 days.

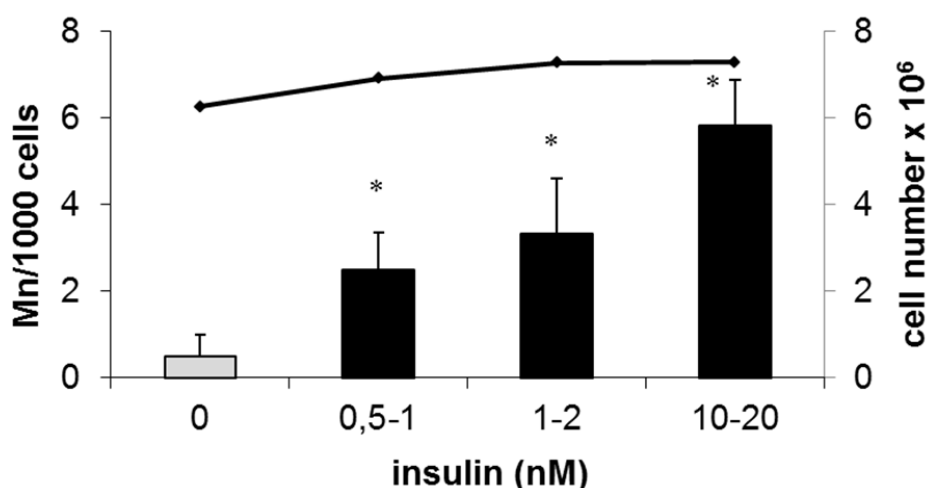


Figure 11: Chromatin damage (Mn/1000 cells) measured as micronucleus frequency in the HT29 cell line treated with different insulin concentrations for 6 days plus 20-22 hr expression time, cell number (straight line) is shown on the second y-axis (* = significantly different from control).

In parallel to the micronucleus frequency tests, the proliferation index and cell account were also assessed (fig. 9, 10) and (fig. 11) respectively. No alteration was observed under the tested conditions. Apoptotic cells were also quantified according to their nuclear morphology and no increase was observed after any of the treatments. To confirm further that insulin did not cause apoptosis under our treatment conditions, flow cytometric analysis of annexin V positive and propidium iodide negative early apoptotic cells was performed after treatment with 10 and 100 nM insulin. No significant increase compared to the control (0.05 ± 0.05 %) was observed after 8 hours treatment with 10 nM (0.08 ± 0.04 %) and 100 nM (0.07 ± 0.02 %) and 16 hours treatment with 10 nM (0.09 ± 0.04 %) and 100 nM (0.08 ± 0.01 %) insulin.

Results

Insulin and glucose are physiologically related. To evaluate if glucose plays a role in insulin genotoxicity, HT29 cells were treated with 5.5 and 25 mM glucose alone and in combination with 10 nM insulin for 2 hours (yielding 5.5 mM, 11 mM and 30.5 mM final glucose concentration because of the medium glucose) and the % DNA in tail was determined by comet assay. Glucose did not show any influence on insulin genotoxicity (fig. 12).

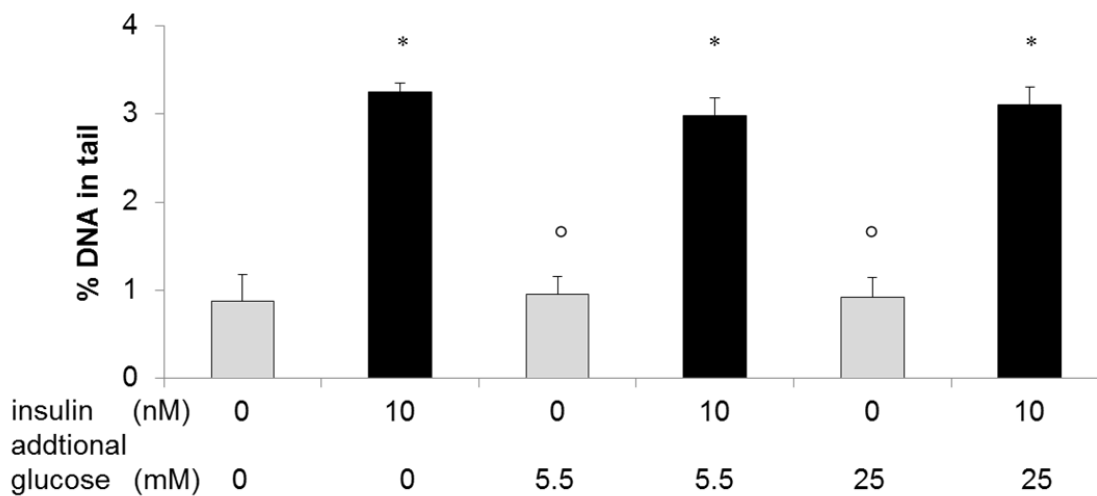


Figure 12: DNA damage (% DNA in tail) measured by comet assay analysis in the HT29 cell line treated with insulin for 2 hr with addition of 5.5 mM or 25 mM of glucose to the culture medium. Because of the glucose content of the culture medium the final glucose concentration was 5.5/11/30.5 mM, (* = significantly different from control, ° = not significantly different from control).

4.1.2 Insulin stimulates ROS production and mediates oxidative stress

Oxidative stress and ROS production were determined in HT29 cells using H2DCF-DA, which has been used extensively in tissue culture experiments to evaluate reactive oxygen species (ROS) production, but H2DCF-DA is not specific for detection of a particular ROS. Cells treated with 1 nM and more insulin for 5 minutes showed a positive response with H2DCF-DA dye (fig. 13).

Results

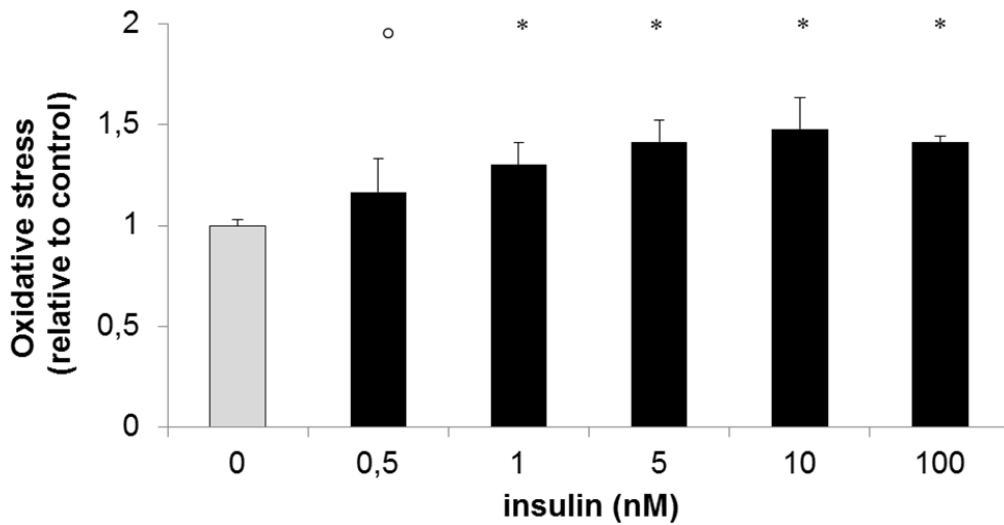


Figure 13: Flow cytometric oxidative stress measurement using the dye H2DCF-DA in HT29 cell treated for 30 min with different concentrations of insulin and 20 min H2DCF-DA (10 μ M), (* = significantly different from control, ° = not significantly different from control).

To focus on the superoxide radical as the probably most relevant product in insulin mediated oxidative stress, DHE staining with UV excitation was used with microscopic measurement (fig. 14).

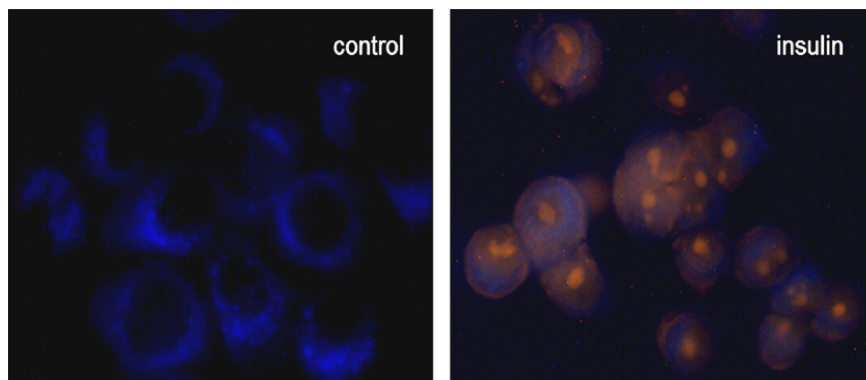


Figure 14: Representative pictures for DHE staining using UV excitation.

Cells which were treated with 10 nM insulin for 5 minutes and longer showed significant increase in superoxide production (fig. 15a) while 0.5 nM insulin and more showed a

Results

significant increase in superoxide production over control within 30 minutes treatment time (fig. 15b).

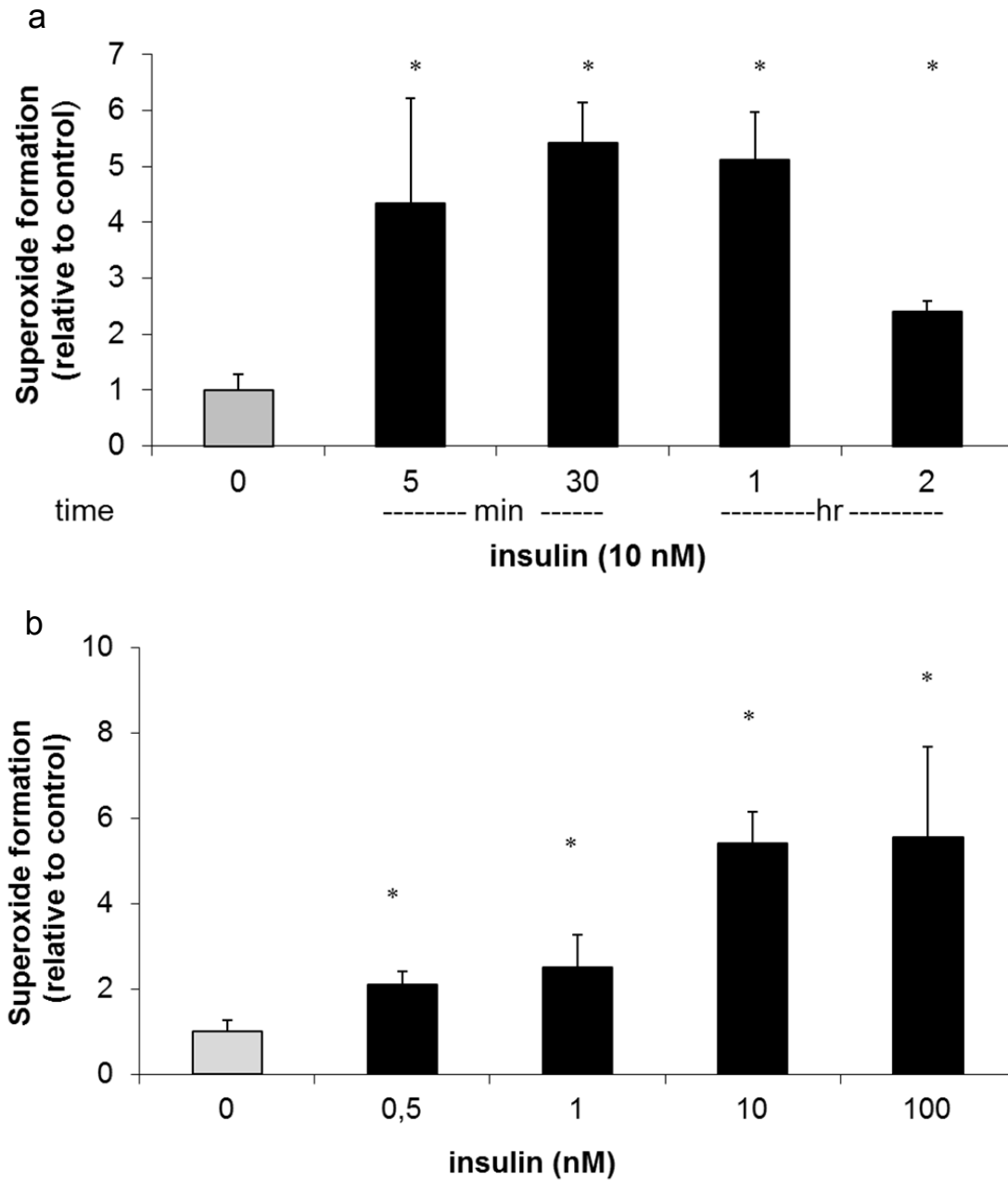


Figure 15: Microscopic detection of superoxide formation using the dye DHE in HT29 cell treated (a) with 10 nM insulin for different time (5 min to 2 hr) and (b) for 30 min with different concentrations of insulin, and 30 min DHE (10 μ M); (* = significantly different from control).

Results

4.1.3 Insulin mediates oxidative damage and the antioxidants offer protection

To elucidate the role of reactive oxygen species (ROS) production and oxidative stress in the insulin-induced DNA damage, two approaches were used; the application of FPG modified comet assay (fig.16) and the addition of the radical scavenger tempol (fig.17).

In the FPG modified comet assay, the enzyme treatment clearly led to an increased DNA damage detection compared to that without FPG enzyme, with the increase being higher in the insulin treated cells than in the control cells. The DNA damage was expressed as the difference between the % DNA in tail of FPG treated cells and % DNA in tail of FPG non-treated cells (fig.16).

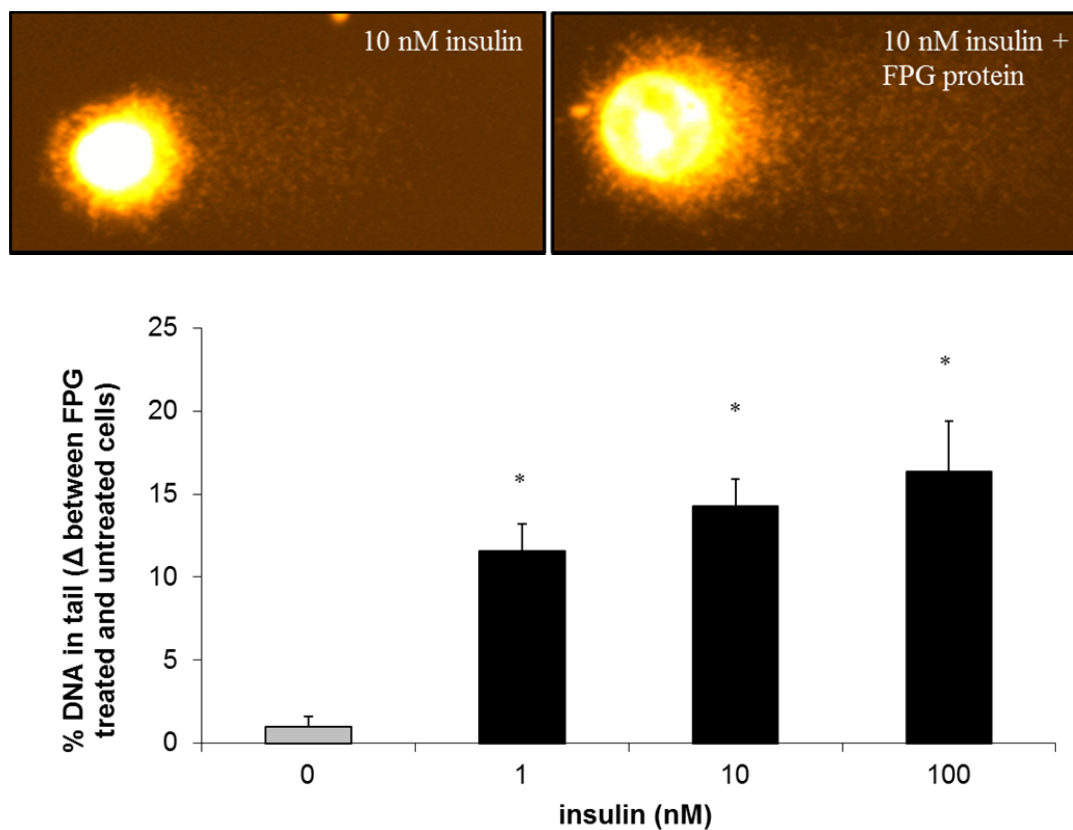


Figure 16: Effect of FPG post treatment on insulin-induced DNA damage in the comet assay in HT29 cells treated with different insulin concentrations for 2 hr, (* = significantly different from control).

Results

The DNA-damaging effect of insulin measured with the comet assay and micronucleus test was significantly reduced by combining 50 μM tempol with the insulin treatment (fig. 17 a and b).

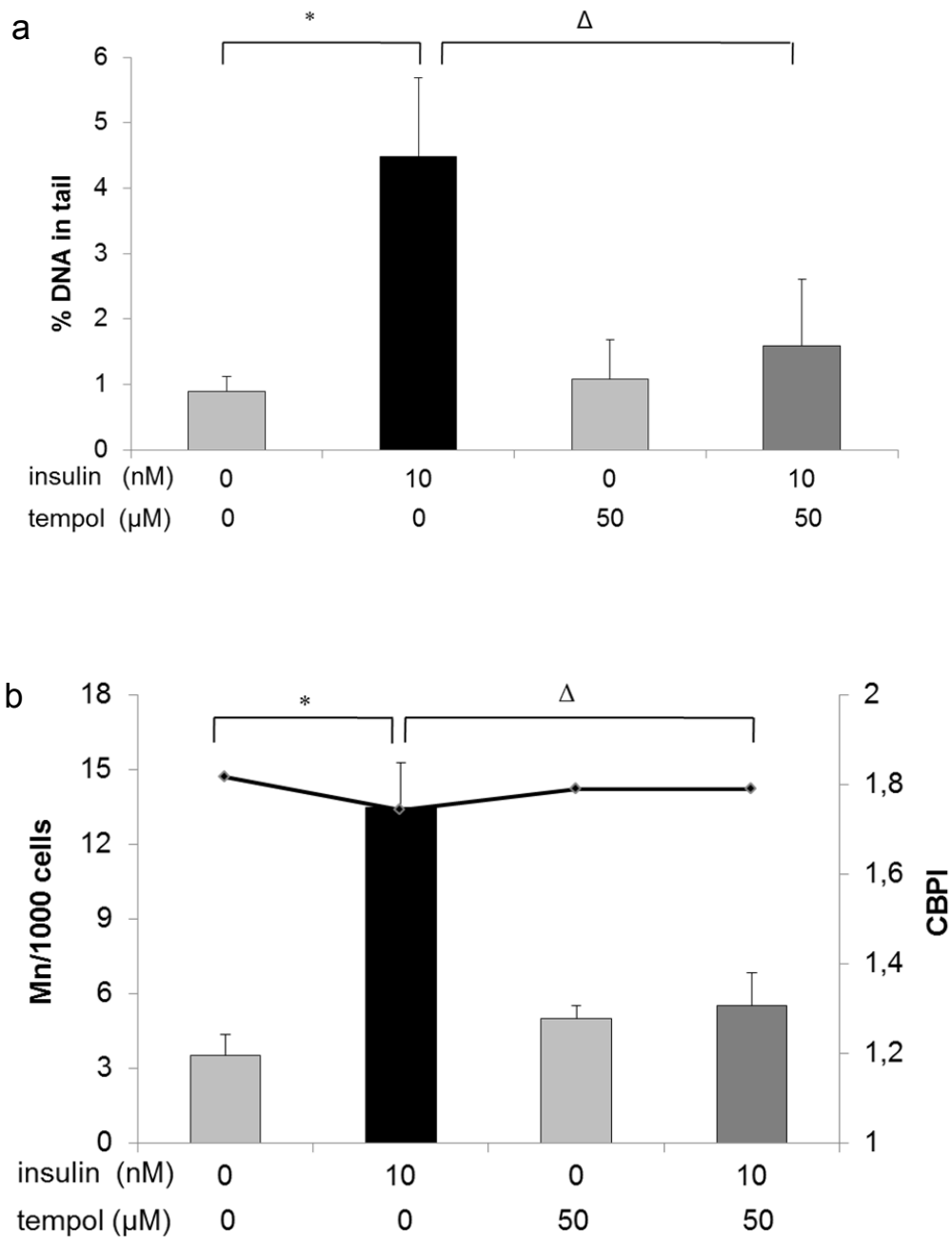


Figure 17: Influence of tempol on insulin-induced alterations in HT29 cells; a) DNA damage (% DNA in tail) in the comet assay after a 2 hr treatment with 10 μM insulin, 50 μM tempol and the combination, and b) micronucleus frequency after 4 hr treatment (plus 22 hr expression time) with 10 nM insulin, 50 μM tempol and the combination, (* = significantly different from control, Δ = significantly different from insulin).

Results

To further confirm the protective effect of antioxidants, the protection effect of the antioxidant and NADPH oxidase inhibitor apocynin (100 μM) was investigated in both comet assay and micronucleus frequency test which showed a decrease in insulin-induced genomic damage (fig.18).

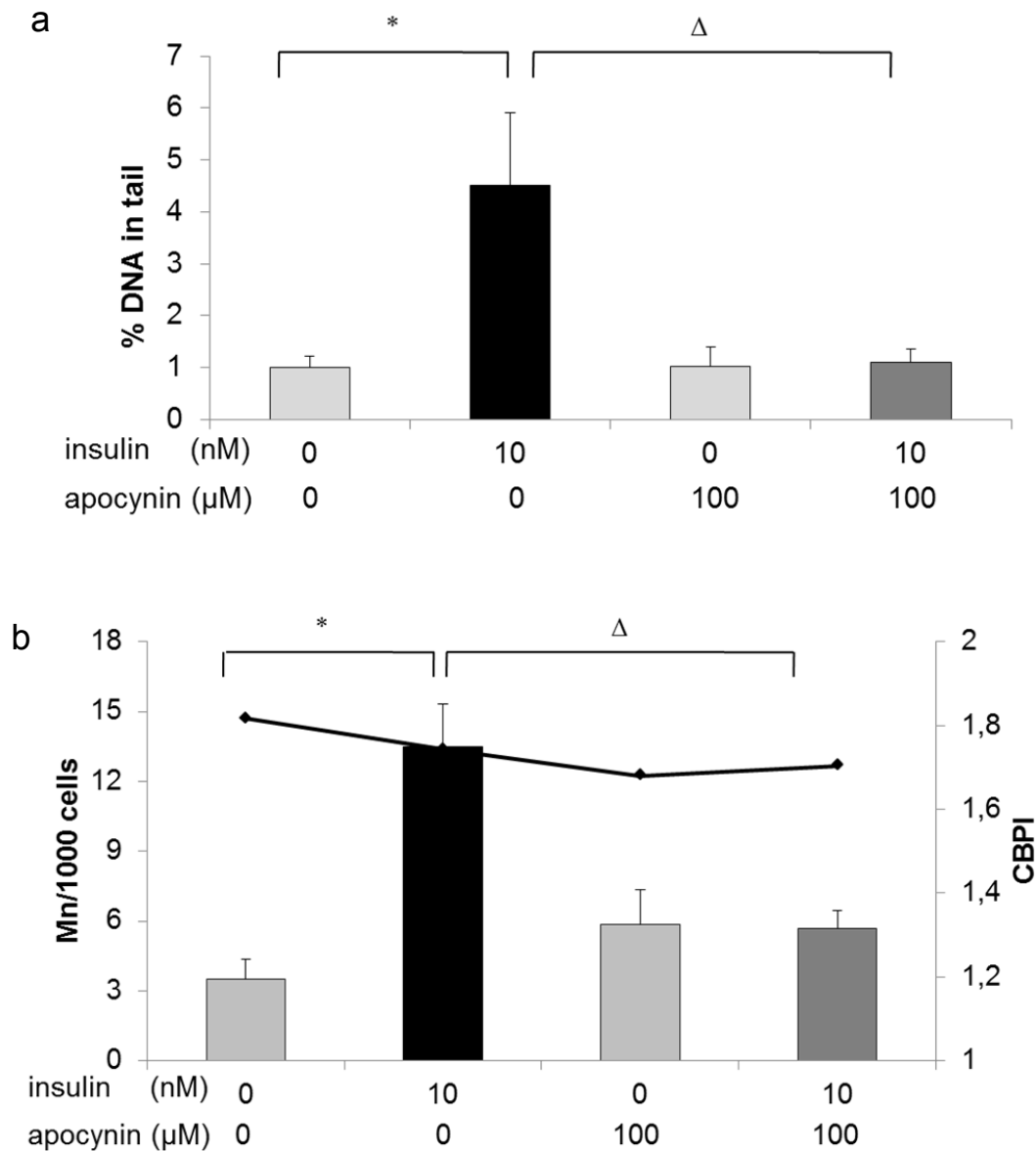


Figure 18: Influence of apocynin on insulin-induced alterations in HT29 cells; a) DNA damage (% DNA in tail) in the comet assay and after a 2 hr treatment with 10 nM insulin, 100 μM apocynin and the combination, and b) micronucleus frequency after 4 hr treatment (plus 22 hr expression time) with 10 nM insulin, 100 μM apocynin and the combination, (* = significantly different from control, Δ = significantly different from insulin).

Results

To test the effect of tempol and apocynin on insulin-stimulated superoxide production, cells were incubated for 30 minutes with insulin, antioxidants and the combination in the presence of 10 μM DHE. The results showed clearly that the combination with tempol and apocynin resulted in a reduction of superoxide production (fig. 19).

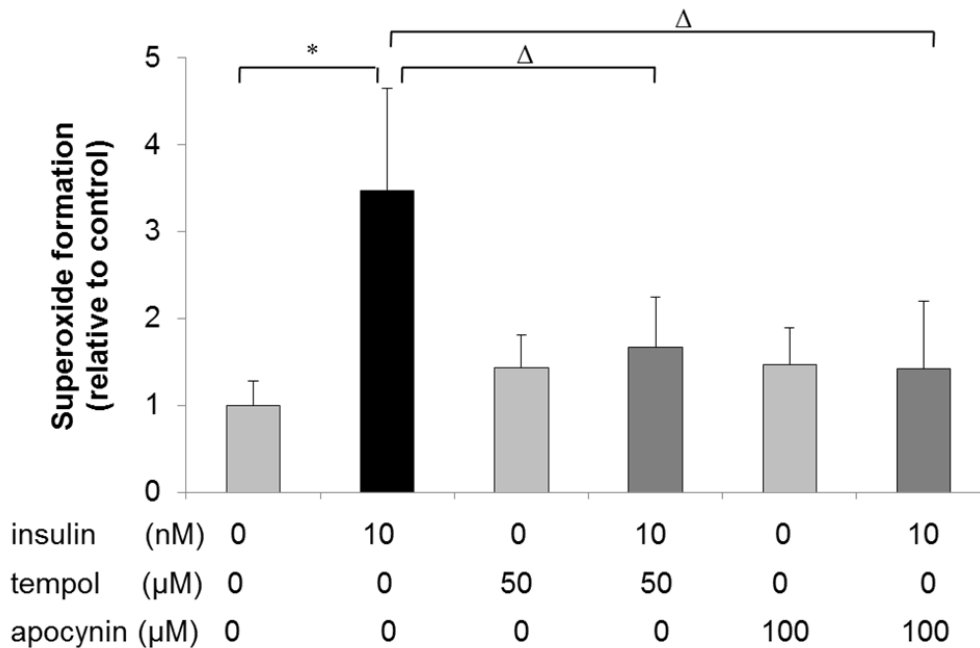


Figure 19: Influence of tempol and apocynin on insulin-induced superoxide after 30 min of treatment with 10 nM insulin, 50 μM tempol, 100 μM apocynin and the combination of insulin with tempol and apocynin, (* = significantly different from control, Δ = significantly different from insulin).

4.1.4 Signaling pathway of insulin-mediates oxidative stress and DNA damage in colon cells

As a first investigation of the mechanistic pathway, the expression of the insulin receptor (IR) and the insulin-like growth factor 1 receptor (IGF-1R) as main targets for insulin binding were confirmed with RT-PCR (fig. 20). The obtained sequences were compared with the Genbank data base, yielding 99 % sequence similarity with IR from homo sapiens insulin receptor mRNA, partial cds with accession number NM 000208.2 and 96 % sequence similarity with IGF-1R from homo sapiens insulin-like growth factor 1 receptor precursor (IGF-1R) mRNA complete cds with accession number BC143721.1.

Results

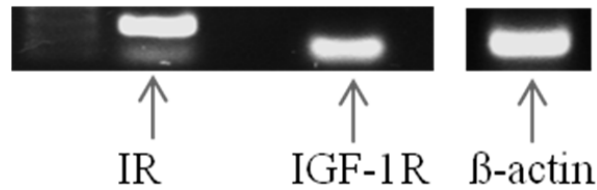


Figure 20: Expression of insulin receptor (IR) and insulin-like growth factor (IGF-1R) in HT29 cells.

To analyze the activation of both receptors, western blot detecting phosphorylated insulin receptor was performed for HT29 cells treated for different times (5 minutes to 4 hours) with 10 nM insulin, and with different insulin concentrations (0.5 – 100 nM) for 2 hours (figs. 21, 22). The amount of the phosphorylated insulin receptor increased after cell stimulation for 2 hours with 0.5 nM insulin and higher (fig. 21).

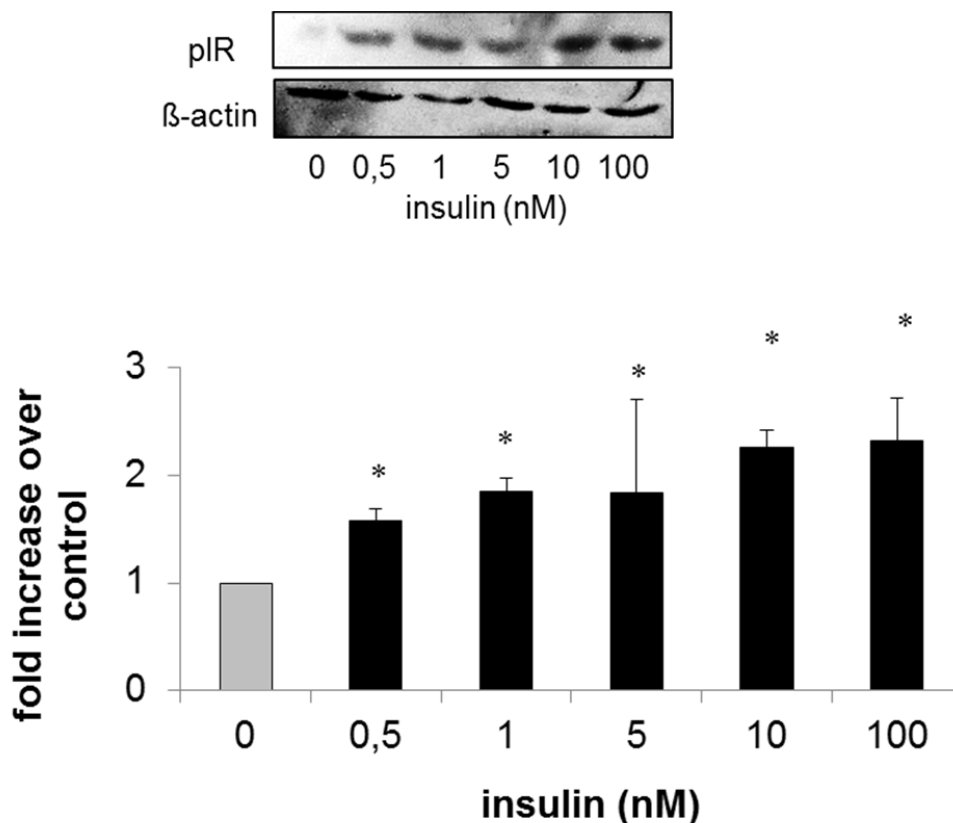


Figure 21: pIR level in HT29 cells treated with different insulin concentrations (0.5 to 100 nM) for 2 hr and measured by Western blot analysis, (* = significantly different from control).

Results

Cells exposed for 5 minutes and longer to 10 nM insulin showed significant increase in insulin receptor phosphorylation (fig. 22).

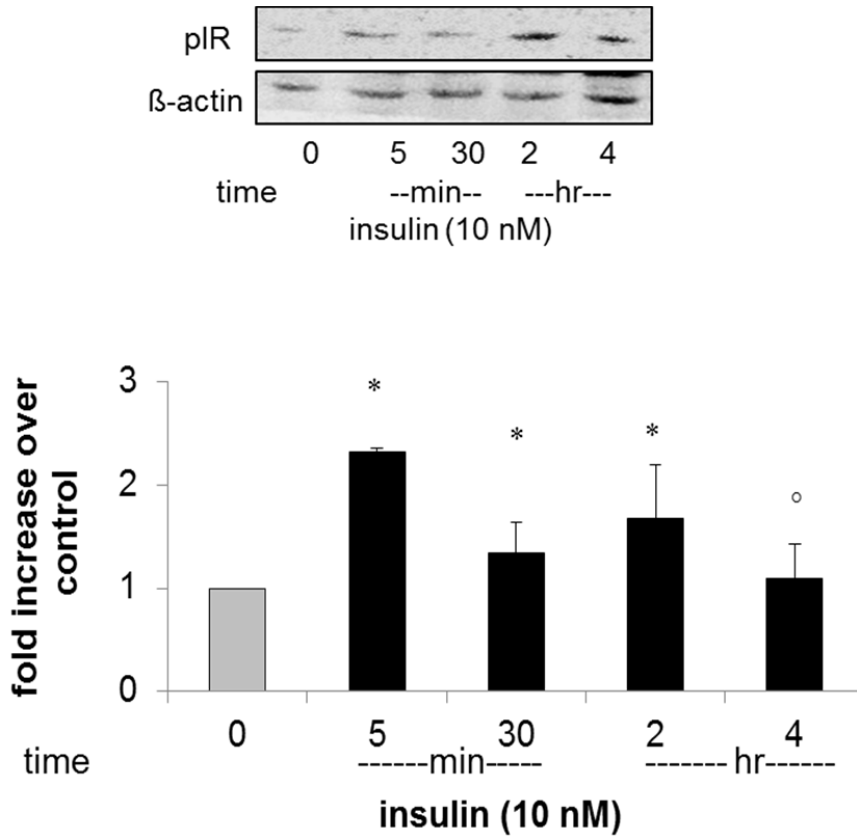


Figure 22: pIR level in HT29 cells treated with 10 nM insulin for different times (5 min to 4 hr) and measured by Western blot analysis (* = significantly different from control, ° = not significantly different from control).

To examine the involvement of the insulin receptor in the insulin genotoxicity pathway, the insulin receptor blocker HNMPA(AM)₃ (50 μ M) was combined with insulin in the cell treatment. The DNA damage that was produced by insulin was reduced, which indicates the involvement of the receptor in the signaling pathway (fig. 23).

Results

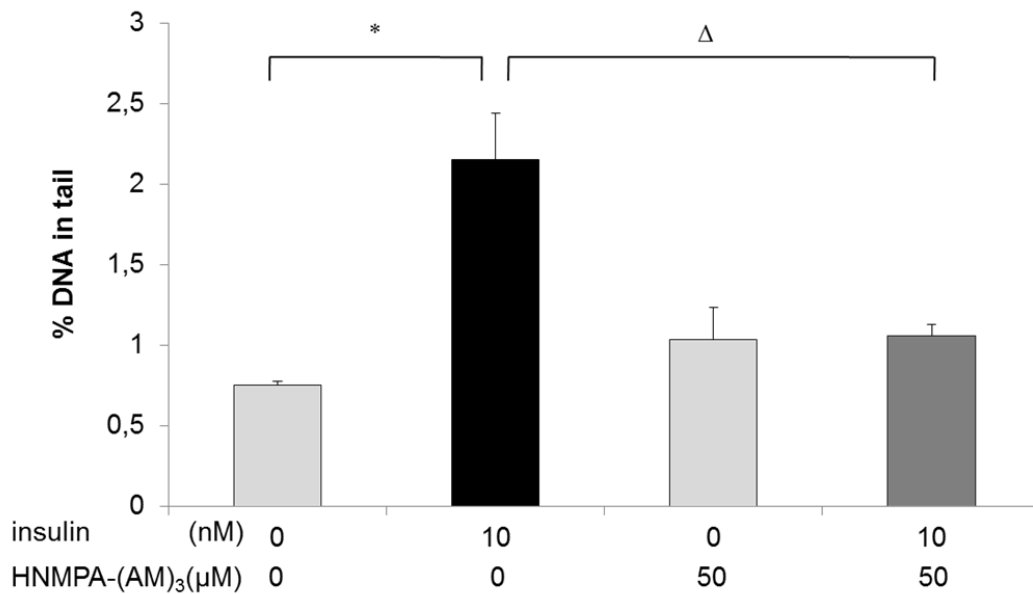


Figure 23: Influence of insulin receptor (IR) blocker on insulin-induced alterations measured as DNA damage (% DNA in tail) in the comet assay for HT29 cells after a 2hr treatment with a) 10 nM insulin and 50 µM HNMP(AM)₃ and the combination (* = significantly different from control, Δ = significantly different from insulin).

At high insulin level, insulin can bind to insulin-like growth factor 1 receptor (IGF-1R). To investigate this; phosphorylated IGF-1R was examined in HT29 treated with insulin under different conditions (figs. 24, 25). In the cells treated with different insulin concentrations (0.5 to 100 nM) for 2 hours, insulin at concentration of 1 nM and higher bound to the IGF-1R and led to its phosphorylation (fig. 24).

Results

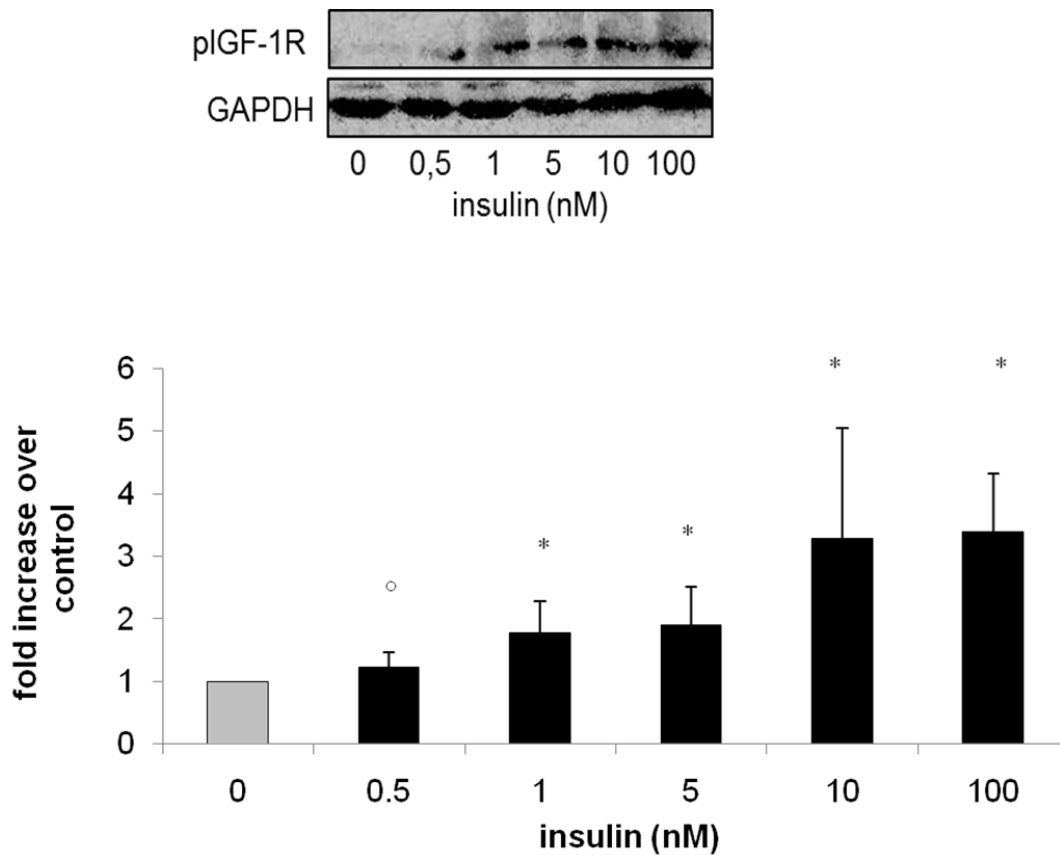


Figure 24: pIGF-1R level in HT29 cells treated with different insulin concentrations (0.5 to 100 nM) for 2 hr and measured by Western blot analysis, (* = significantly different from control).

Cells were treated with 10 nM insulin for different time (5 minutes to 4 hours), where the influence appeared even with short time exposure (5 minutes) (fig. 25), and to connect the activation of IGF-1R with the genomic damage induced by insulin, the specific IGF-1R blocker (PPP) was used in combination with insulin and the effect of this treatment was evaluated by comet assay. Insulin combined with PPP in cell treatment caused less damage than alone (fig. 26).

Results

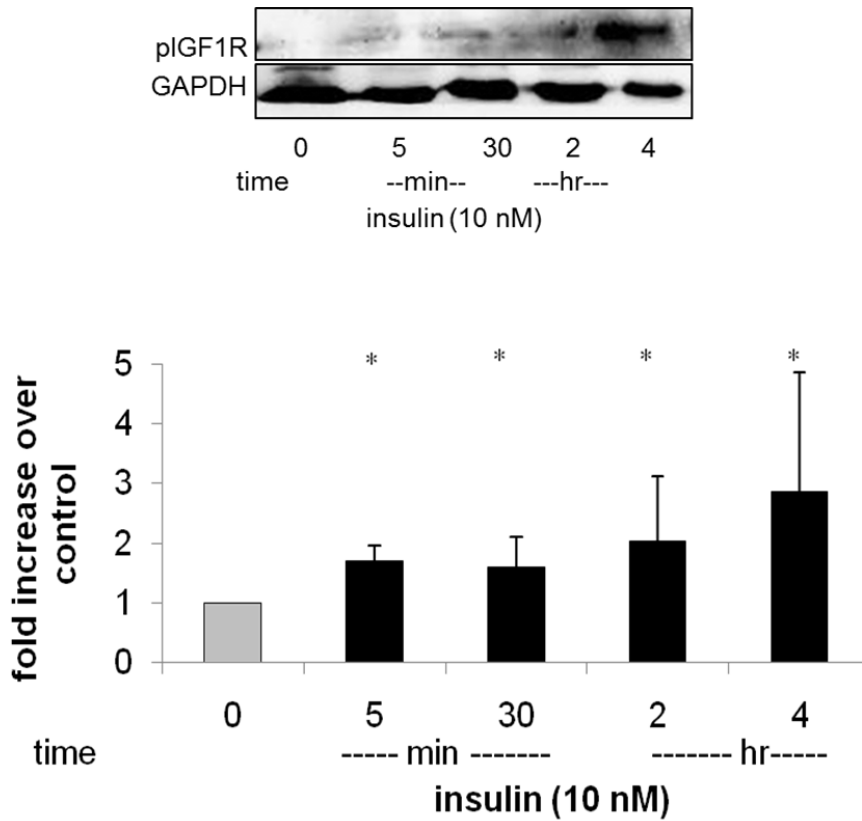


Figure 25: pIGF-1R level in HT29 cells treated with 10 nM insulin for different times (5 min to 4 hr) and measured by Western blot analysis, (* = significantly different from control).

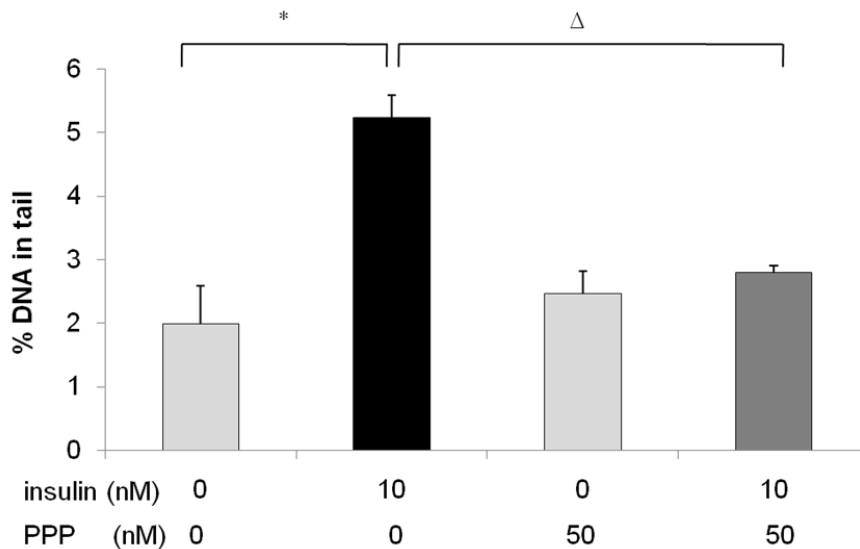


Figure 26: Influence of insulin-like growth factor receptor (IGF-1R) blocker (PPP) on insulin-induced alterations measured as DNA damage (% DNA in tail) in the comet assay for HT29 cells after a 2hr treatment with 10 nM insulin, 50 nM PPP and the combination, (* = significantly different from control, Δ = significantly different from insulin).

Results

The binding of insulin to the insulin receptor and IGF-1R is followed by phosphorylation of insulin substrates, in which the latter activate PI3K, the key enzyme in the insulin signaling pathway. To examine the activation of PI3K under our conditions of treatment, phosphorylation of p85 protein, the regulatory subunit of PI3K, was investigated in cells treated with 10 nM insulin between 5 minutes and 4 hours (fig. 27). HT29 cells showed significant increase in PI3K phosphorylation after the exposure to 10 nM insulin for 30 minutes, this increased more through the first 2 hours while at 4 hours the activation became lower but did not return to control level (fig. 27).

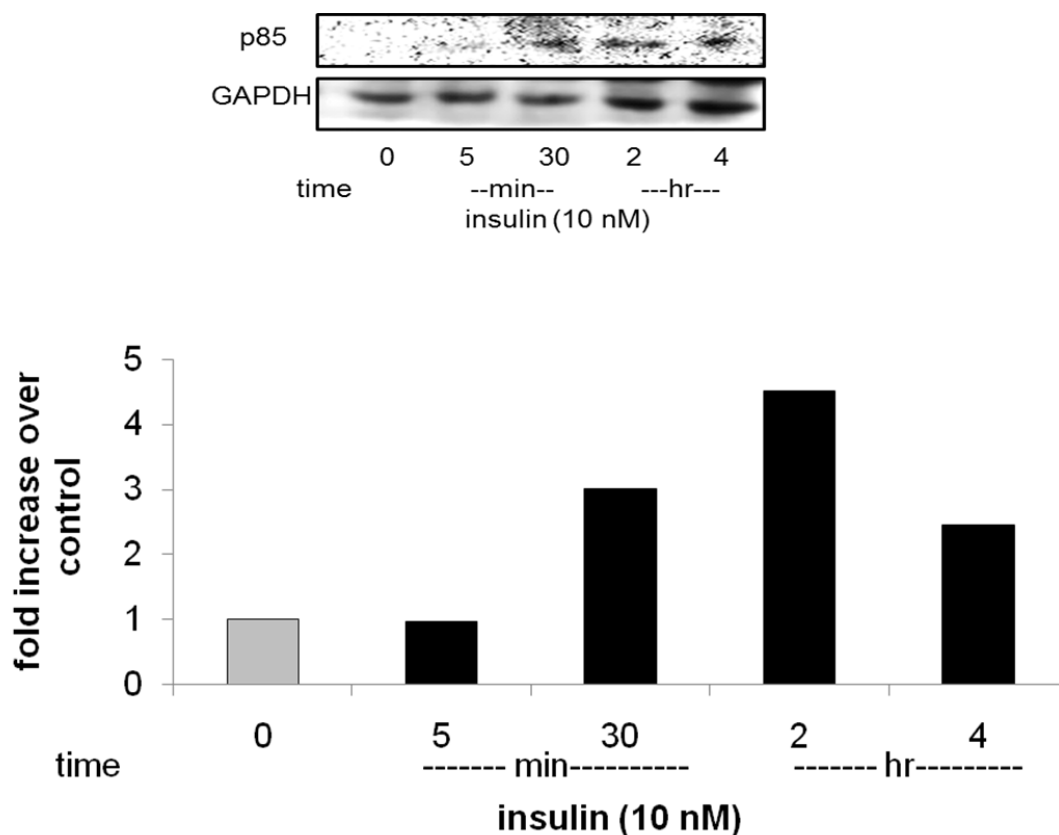


Figure 27: Activated PI3K (p85) level in HT29 cells treated with 10 nM insulin for different times (5 min to 4 hr) and measured by Western blot analysis, (1 experiment).

To link the activation of PI3K to the signaling pathway, the pharmacological PI3K inhibitor, wortmannin (100 nM) was used. Cells treated with the combination of wortmannin and insulin exhibited less DNA damage in comparison with cells treated with insulin alone (fig. 28).

Results

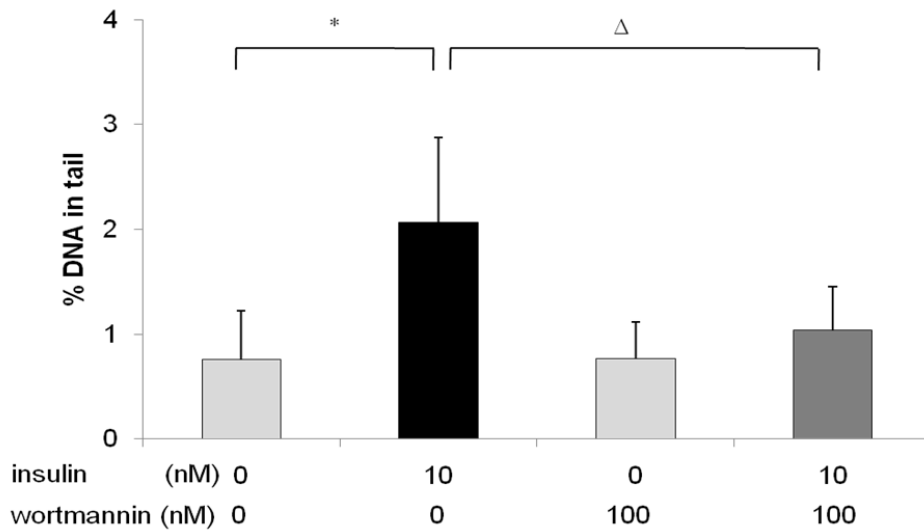


Figure 28: Influence of PI3K inhibitor (wortmannin) on insulin-induced alterations measured as DNA damage (% DNA in tail) in the comet assay for HT29 cells after 2hr treatment with 10 nM insulin, 100 nM wortmannin and the combination (* = significantly different from control, Δ = significantly different from insulin).

The three inhibitors (HNMPA(AM)₃, PPP and wortmannin) offered protection against insulin-induced micronucleus formation (fig. 29).

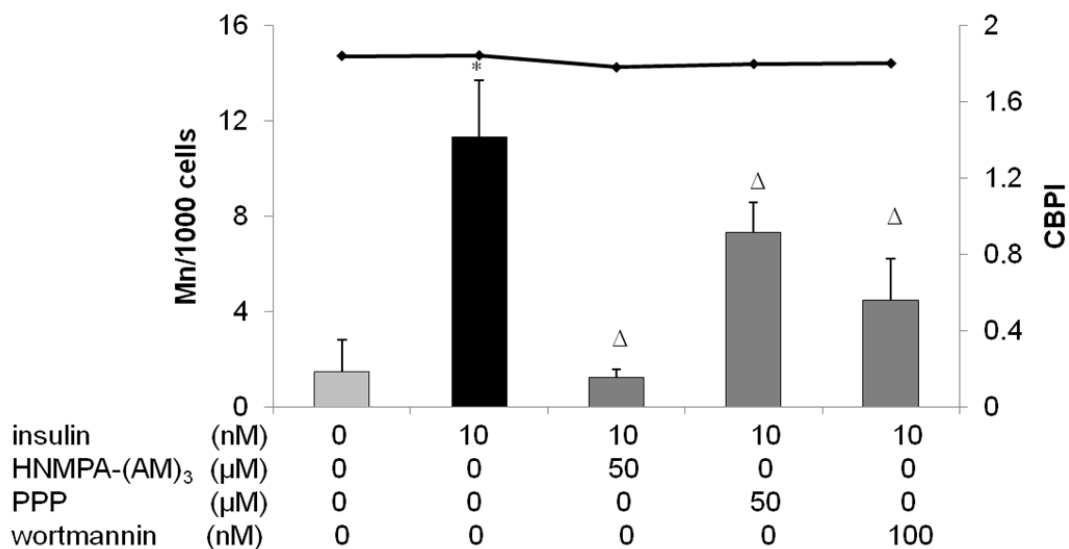


Figure 29: Influence of different receptor blockers and enzyme inhibitor on chromatin damage (Mn/1000 cells) measured as micronucleus frequency in the HT29 cell line treated with 10 nM insulin and insulin in combination with HNMP(AM)₃, PPP and wortmannin (with cytochalasine B addition) plus an expression time of 20-22 hours after treatment. Cell proliferation (CBPI) (straight line) is shown on the second y-axis, (* = significantly different from control, Δ = significantly different from insulin).

Results

Phosphorylation of PI3K leads to activation of AKT via phosphorylation. PAKT level was determined after treatment of the cells for 2 hours with different concentrations of insulin (0.5 to 100 nM) (fig. 30), as well as, after treatment of cells with 10 nM insulin for different times (fig 31). Cells showed significant increase in AKT phosphorylation after stimulation with 1 nM insulin and higher for 2 hours while 30 minutes exposure to 10 nM insulin was enough to activate AKT significantly in comparison to control (figs. 30, 31).

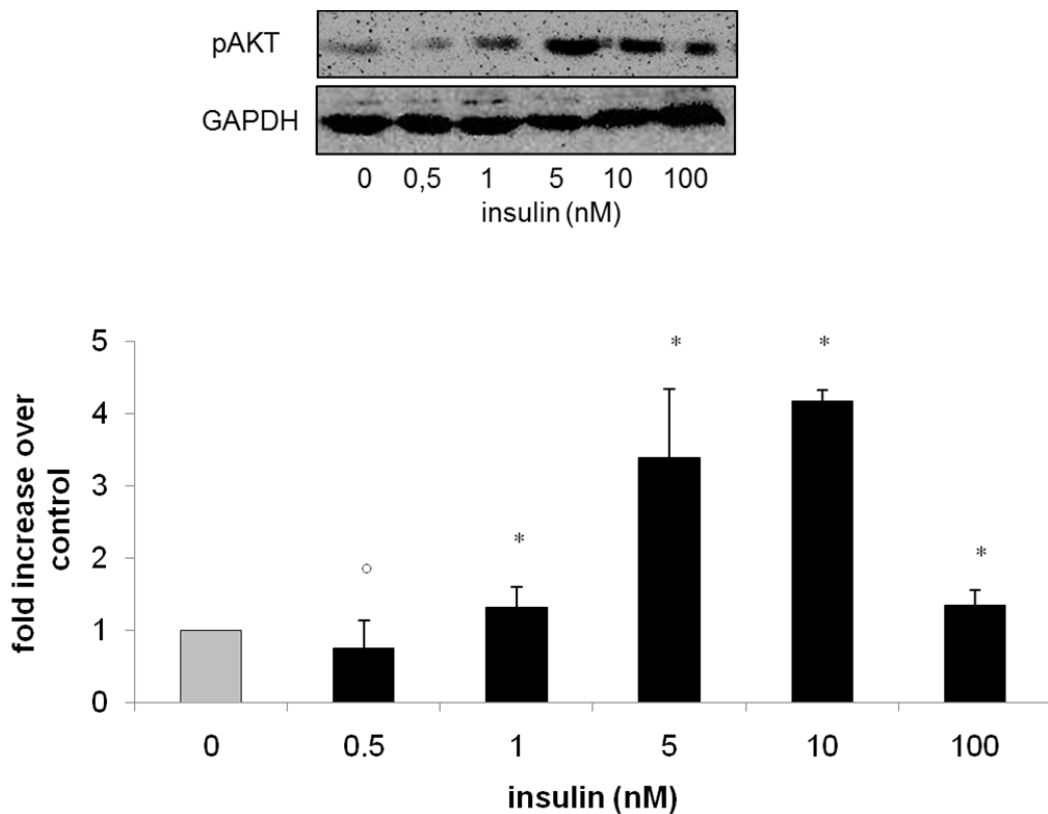


Figure 30: AKT phosphorylation in HT29 cells treated with different concentrations of insulin (0.5 to 100 nM) for 2 hr and measured by Western blot analysis, (* = significantly different from control, ° = not significantly different from control).

Results

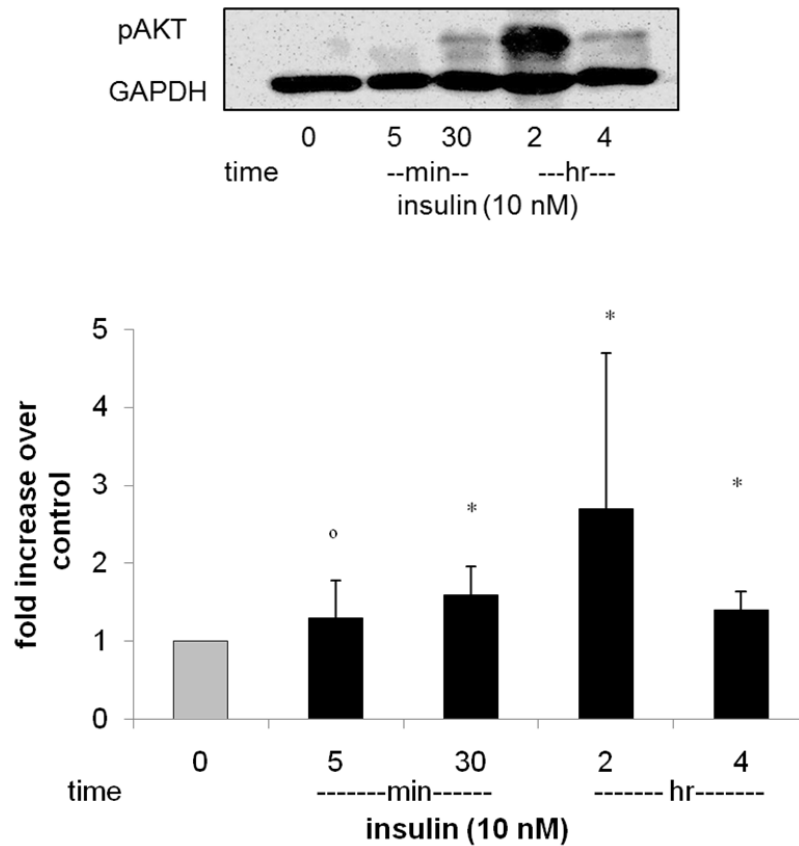


Figure 31: AKT phosphorylation HT29 cells treated with 10 nM insulin for different time points and measured by Western blot analysis. (* = significantly different from control, ° = not significantly different from control).

To investigate the sequence of the receptor and protein activations in the signaling pathway, HT29 cells were treated with insulin, receptor blockers (HNMPA(AM)₃ and PPP) and PI3K inhibitor (wortmannin) and the previously activated receptors (IR and IGF-1R) and proteins (p53 and AKT) levels were measured by western blot analysis (fig. 32).

Results

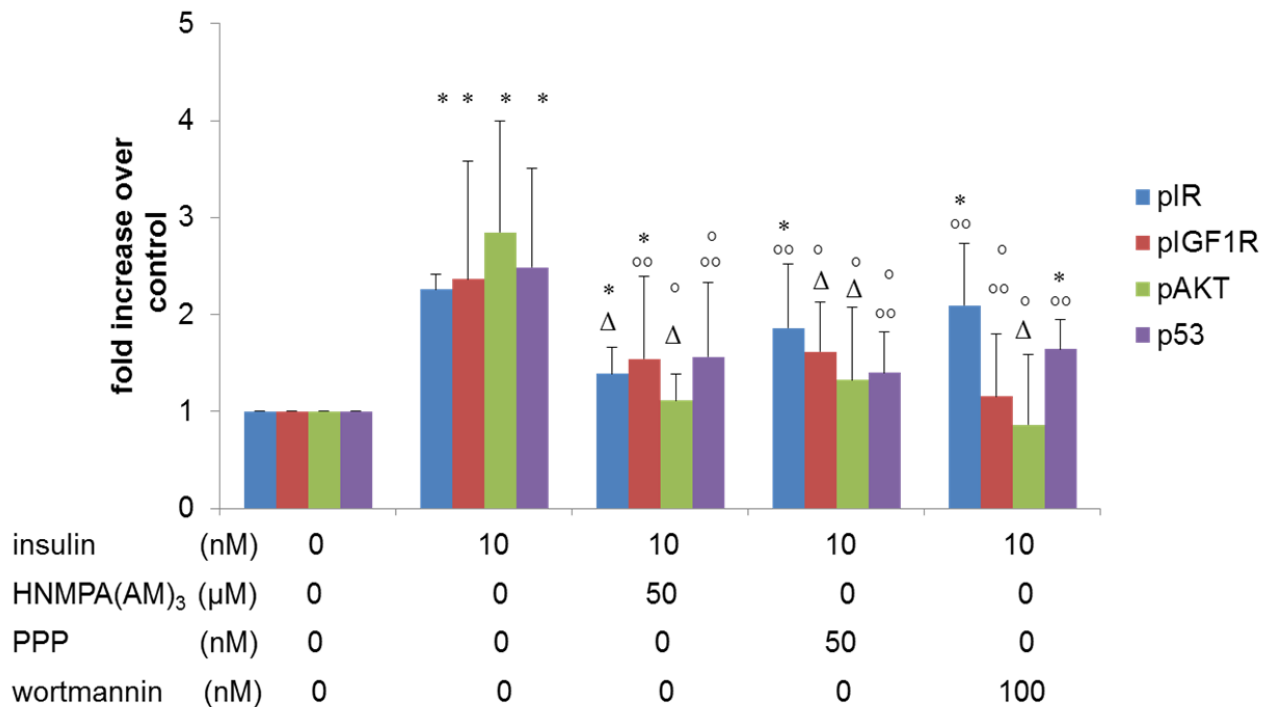


Figure 32: Influence of different receptor blockers and enzyme inhibitor on activation of IR, IGF1R, AKT and accumulation of p53 in HT29 cells treated for 2 hr with 10 nM insulin and with insulin in combination with HNMP(AM)₃(50 μM), PPP (50 nM) or wortmannin (100 nM) and measured with Western blot analyses, (* = significantly different from control, ° = not significantly different from control, Δ = significantly different from insulin, °° = not significantly different from insulin).

To evaluate the role of PKC in the signaling mechanism, cells were treated with 10 nM sphingosine (PKC inhibitor) in combination with the insulin. The DNA damage which measured by the comet assay was not affected by the presence of the sphingosine, thus the results exclude the PCK from the signaling pathway in colon (fig. 33).

Results

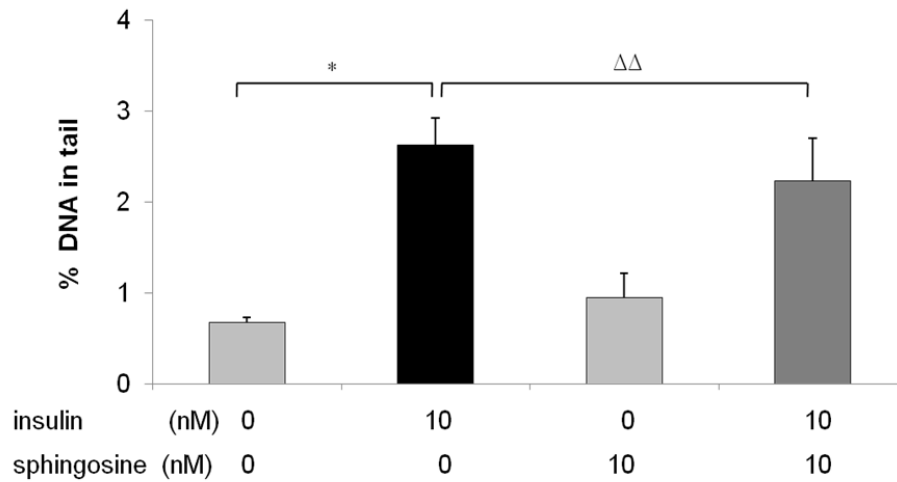


Figure 33: DNA damage (% DNA in tail) measured by the comet assay in HT29 treated with 10 nM insulin, 10 nM sphingosine and the combination for 2 hr, (* = significantly different from control, ΔΔ = not significantly different from insulin).

To specify the source of ROS, the mitochondrial inhibitor rotenone (10 nM) was used in combination with insulin in cell treatment and the result showed the contribution of mitochondria in insulin mediated oxidative stress and genomic damage (fig. 34).

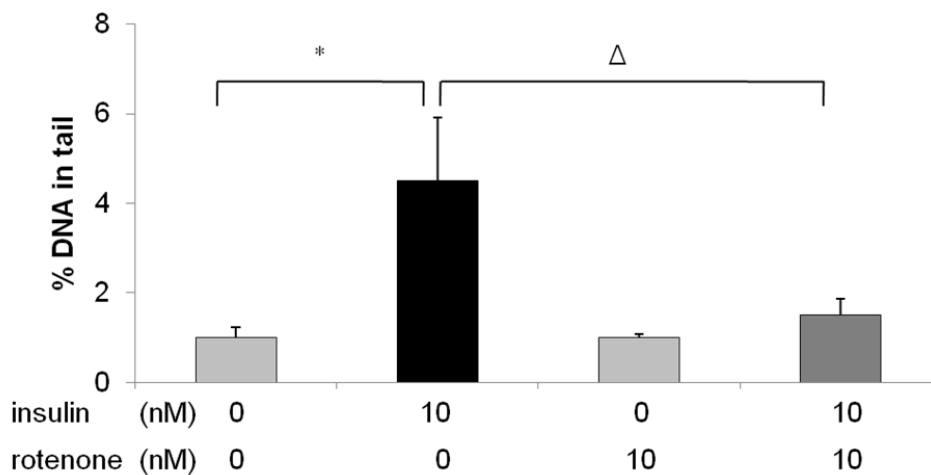


Figure 34: Influence of rotenone on insulin-induced alterations in HT29 cells, DNA damage (% DNA in tail) in the comet assay after a 2hr treatment with 10 nM insulin, 10 nM rotenone and the combination (* = significantly different from control, Δ = significantly different from insulin).

Results

To confirm the role of mitochondria in insulin genotoxicity, HT29 rho0 cells were used. In this regard, mitochondria were depleted by culturing the cells in the presence of ethidium bromide and depletion of the mitochondria was examined by comparing presence of the mitochondrial DNA between rho0 cells and normal control HT29 cells using RT-PCR (fig.35), 10 and 100 nM insulin were applied to the cells for 2 hours, The application of insulin resulted in lower DNA damage in comparison to normal cells (fig. 36).

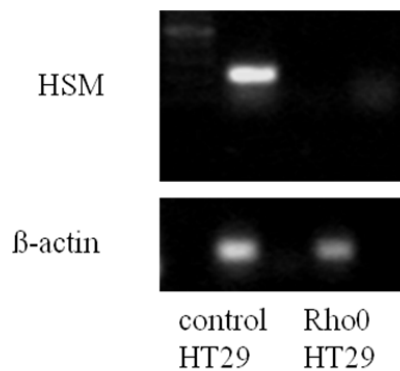


Figure 35. RT- PCR confirmation of mtDNA depletion in HT29 rho0 cells (HSM= human small mitoDNA).

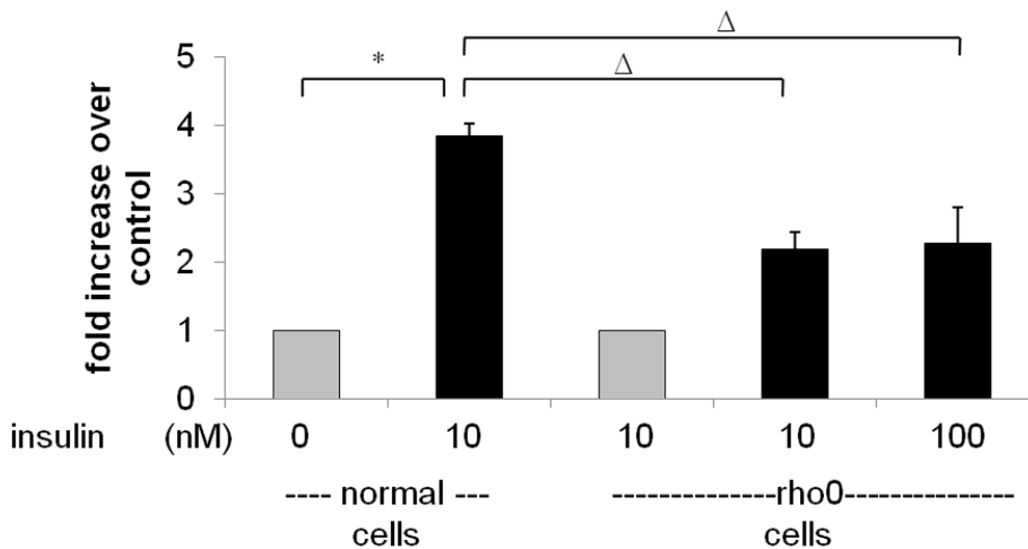


Figure 36: Influence of mitochondria depletion on insulin-induced alterations in HT29 (normal and rho0) cells, DNA damage in the comet assay after a 2 hr treatment with 10 and 100 nM insulin (* = significantly different from control, Δ = significantly different from insulin).

Results

The contribution of NADPH oxidase enzyme complex as a main source of ROS production in the cells was also examined by using the specific NADPH oxidase inhibitor VAS2870 (1 μ M) in combination with insulin. This provided significant protection from the genomic damage induced by insulin in the comet assay (fig. 37).

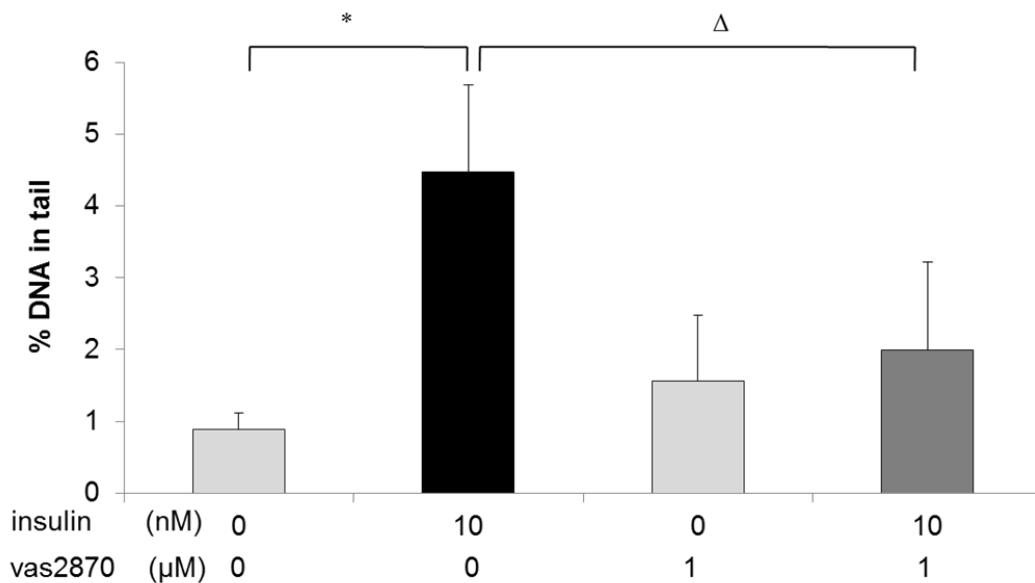


Figure 37: Influence of VAS2870 on insulin-induced alterations in HT29 cells; DNA damage (% DNA in tail) in the comet assay after a 2 hr treatment with 10 μ M insulin, 1 μ M VAS2870 and the combination, (* = significantly different from control, Δ = significantly different from insulin).

To confirm the involvement of both sources in the oxidative stress and DNA damage induced by insulin. DHE staining and micronucleus test were performed using both inhibitors (rotenone and VAS2870), in which both inhibitors reduced the ROS production in the cells treated with 10 nM insulin and inhibitors for 30 minutes (fig 38), and lowered the micronucleus formation in the same cells after treatment for 4 hours (fig. 39).

Results

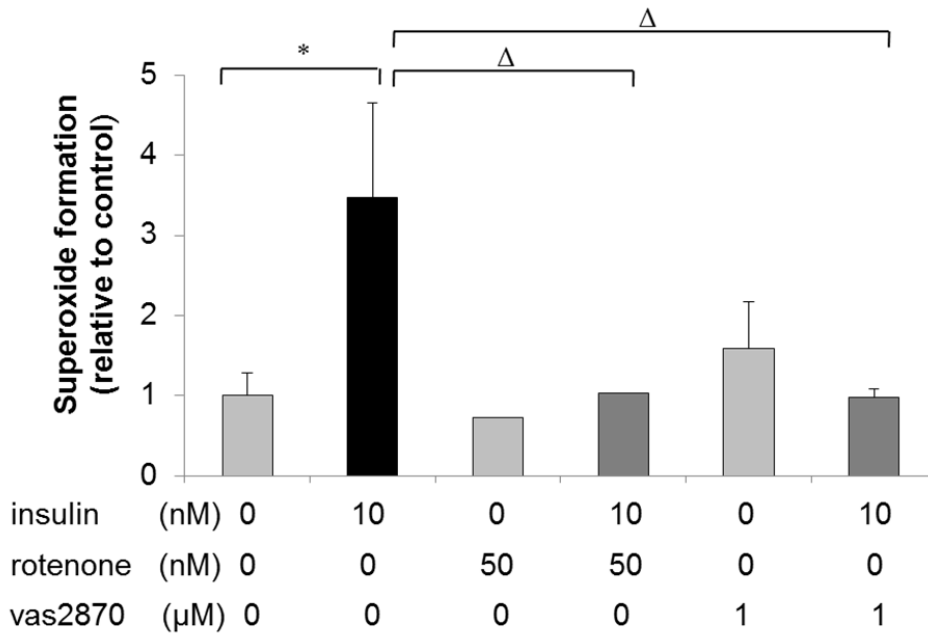


Figure 38: Influence of rotenone and VAS2870 on insulin-induced superoxide in HT29 after 30 min of treatment with 10 nM insulin, 50 nM rotenone, 1 μM VAS2870 and the combinations, (* = significantly different from control, Δ = significantly different from insulin).

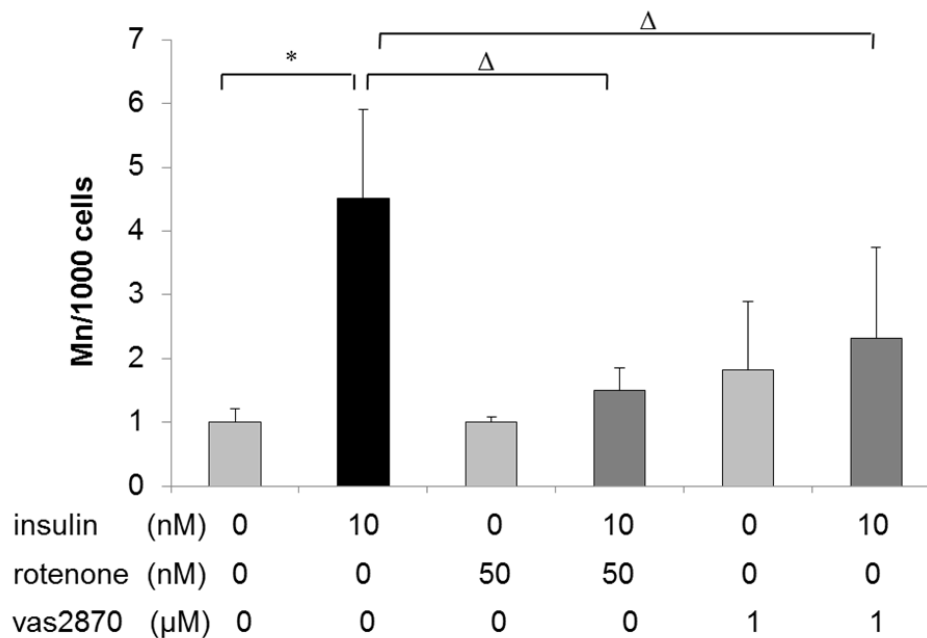


Figure 39: Influence of rotenone and VAS2870 on insulin-induced alterations in HT29 cells; micronucleus frequency after 4 hr treatment (plus 22 hours expression time) with 10 nM insulin, 10 nM rotenone, 1 μM VAS2870 and the combinations, (* = significantly different from control, Δ = significantly different from insulin).

Results

The NADPH oxidase enzyme complex is expressed as seven isoforms with different tissue distribution (Nox1-5 and Duox1 and 2). In the present HT29 cells, both Nox1 and Nox2 are highly expressed as observed by RT-PCR (fig. 40), while the kidney cell line HK2 express Nox2 and Nox4.

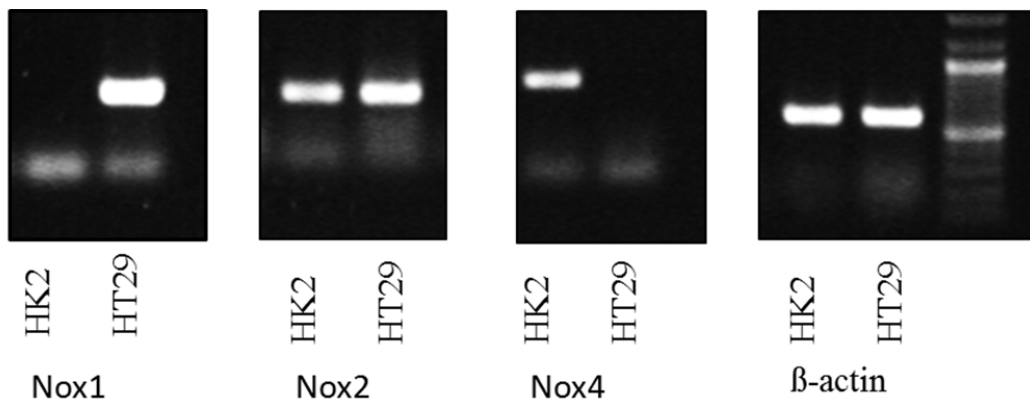


Figure 40: Expression of Nox1, Nox2 and Nox4 NADPH oxidase isoforms in kidney HK2 and colon HT29 cells.

To elucidate which Nox isoform is responsible for ROS production after insulin stimulation, Nox1 and Nox2 were knocked down with siRNA and the levels of the Nox1 and Nox2 were analyzed by western blot, the transfected cells were treated with 10 nM insulin for 2 hours. Cells with knocked down Nox1 showed significant reduction in DNA damage examined by comet assay (fig.41), as well as superoxide production (fig. 42) compared to transfection medium and control siRNA treated cells, while cells with knocked down Nox2 did not show reduction in the DNA damage as evaluated by comet assay (fig.43).

To confirm the previous results, the micronucleus frequency test was applied for the cells with knocked down Nox1 and Nox2, treated with 10 nM insulin for 4 hours (figs. 44). The same pattern of results was observed confirming the involvement of Nox1 in our signaling mechanism and excluding Nox2 from the insulin mediated genotoxicity in colon.

Results

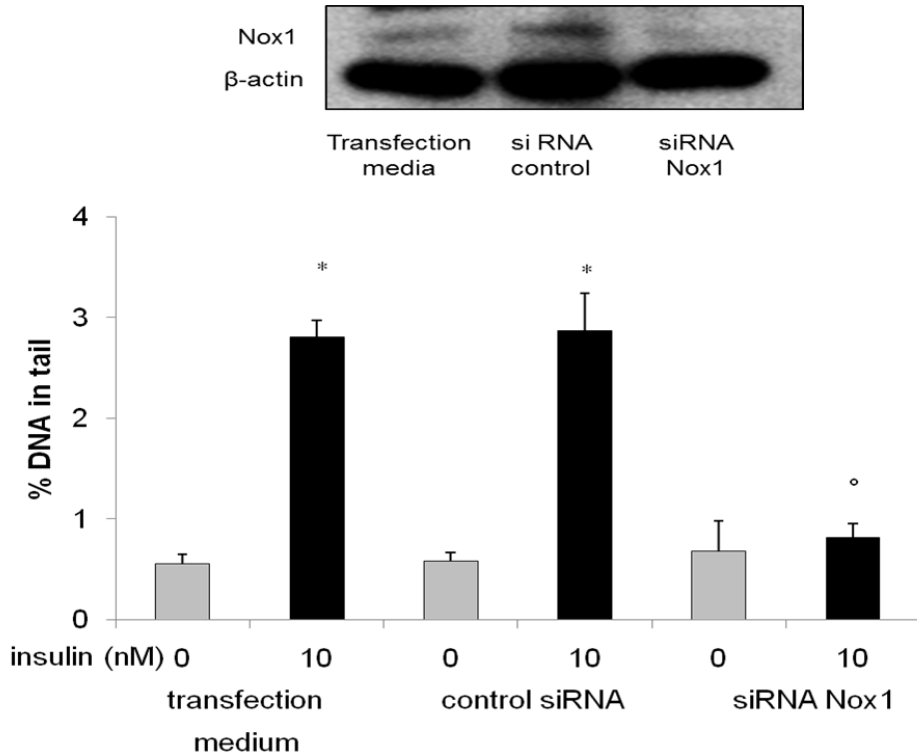


Figure 41: DNA damage measured by the comet assay after 10 nM insulin treatment for 2 hr in HT29 cells transfected with transfection buffer, control-siRNA and Nox1-siRNA, (* = significantly different from control, ° = not significantly different from control).

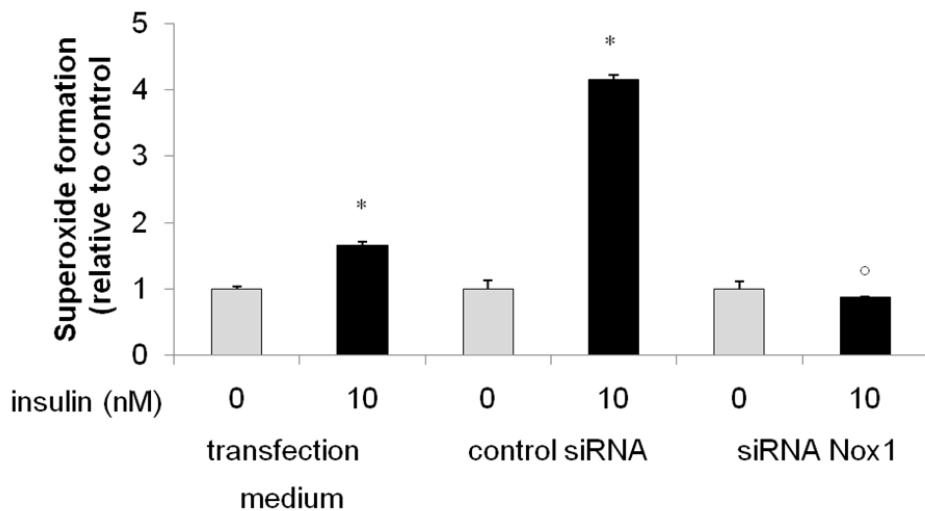


Figure 42: Superoxide production after 30 min of treatment with 10 nM insulin in HT29 cells transfected with transfection buffer, control-siRNA and Nox1-siRNA, (* = significantly different from control, ° = not significantly different from control).

Results

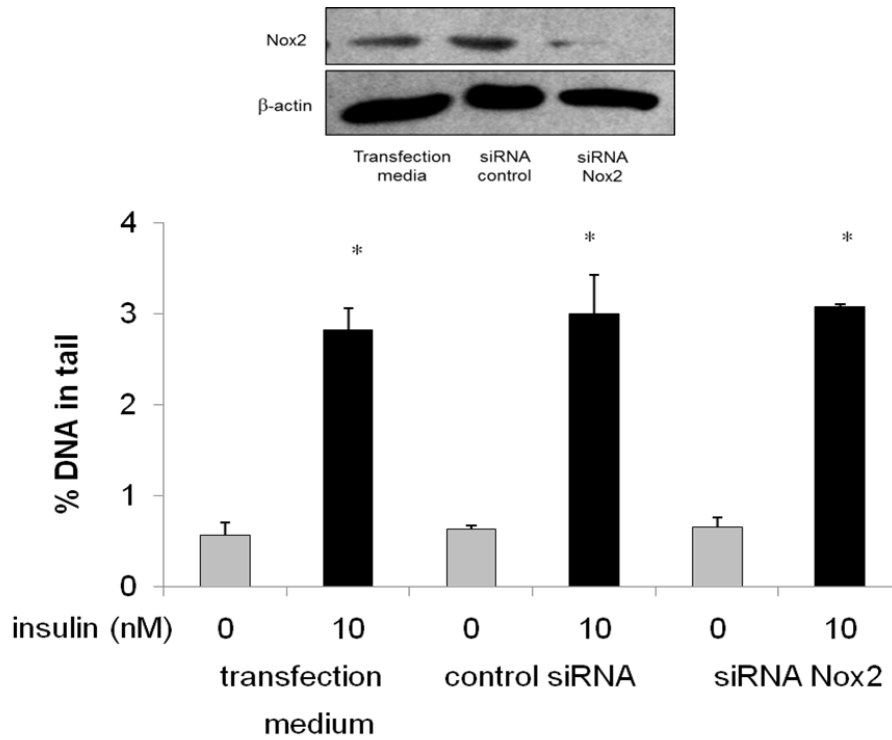


Figure 43: DNA damage measured by the comet assay after 10 nM insulin treatment for 2 hr in HT29 cells transfected with transfection buffer, control-siRNA and Nox2-siRNA, (* = significantly different from control).

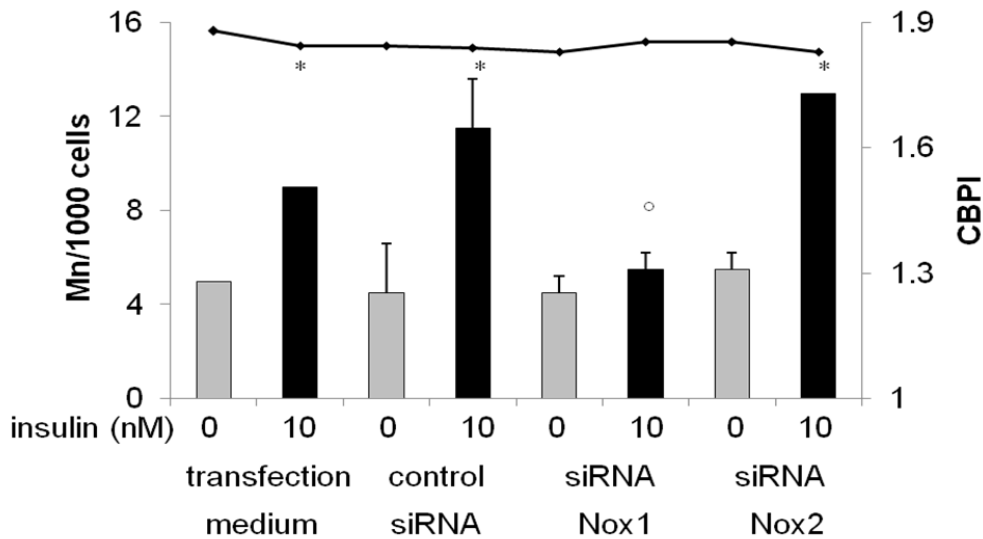


Figure 44 : Chromatin damage (Mn/1000 cells) measured as micronucleus frequency after 10 nM insulin treatment for 4 hr in HT29 cells transfected with transfection buffer, control-siRNA, Nox1-siRNA and Nox2-siRNA, with cytochalasin B addition for the last 20-22 , cell proliferation (CBPI) (straight line) is shown on the second y-axis, (* = significantly different from control, ^o = not significantly different from control).

Results

To elucidate the effect of Nox1 down regulation on AKT activation, the HT29 cells with knocked down Nox1 were treated with insulin and the level of pAKT was measured by western blot analysis, where the treated cells did not show difference in pAKT compared to cells transfected with the transfection buffer or control-siRNA (fig. 45).

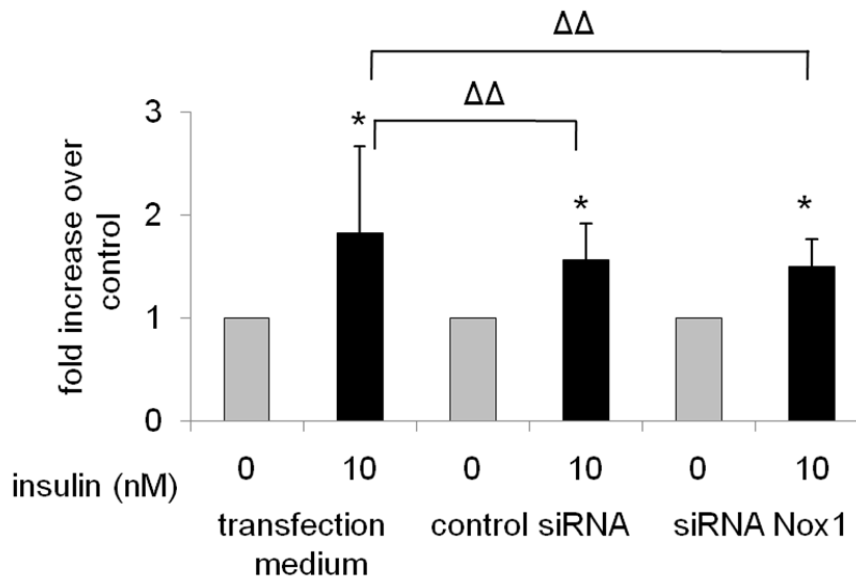


Figure 45: pAKT level after 10 nM insulin treatment for 2 hr in HT29 cells transfected with transfection buffer, control-siRNA and Nox1-siRNA, (* = significantly different from control, ΔΔ= not significantly different from insulin-treated cells with transfection buffer).

Although, no Nox4 had been detected by RT-PCR in HT29 cells, the Nox4 inhibitor plumbagin (100 nM) was applied as additional control in combination with insulin to treat the cells; no reduction in the DNA damage was observed (fig.46).

Results

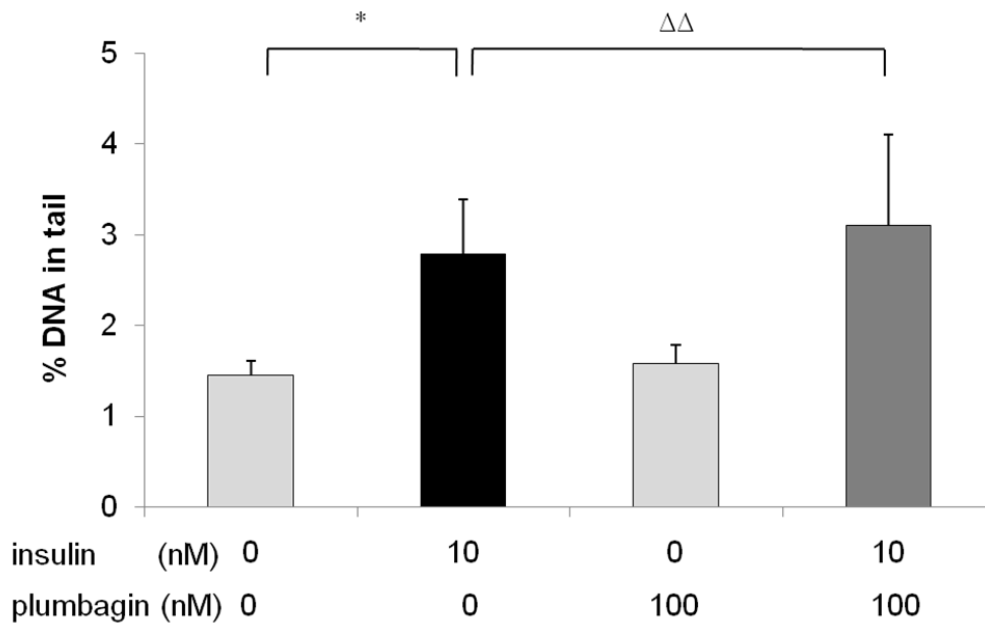


Figure 46: DNA damage (% DNA in tail) measured by the comet assay in HT29 treated with 10 nM insulin, 100 nM plumbagin and the combination for 2 hr, (* = significantly different from control, $\Delta\Delta$ = not significantly different from insulin).

4.1.5 Insulin mediated genotoxicity in Caco-2 cells and primary rat colon cells

To confirm the effect of insulin on the colon further, Caco-2 cells as another model of a colon derived cell line were examined. For the exposure conditions applied, 5 to 100 nM insulin for 2 hours, these cells exhibited a significant increase in DNA damage as measured by comet assay (fig.47).

Results

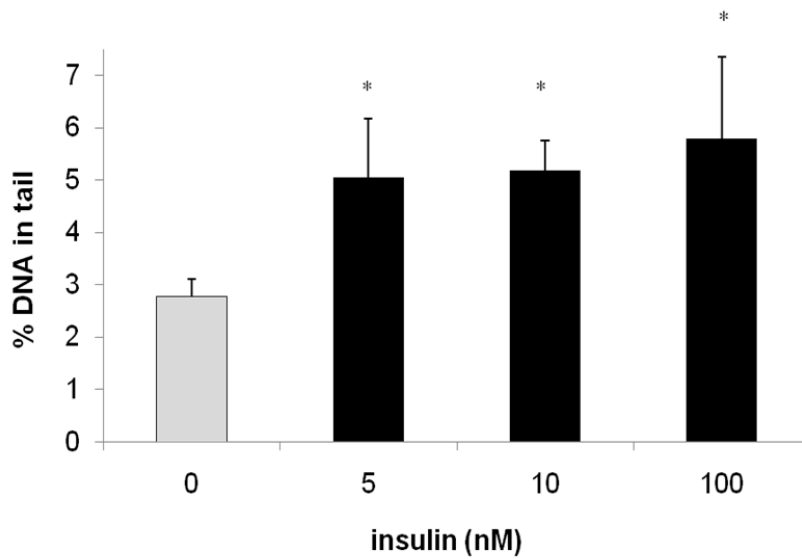


Figure 47: Caco-2 cells treated with different insulin concentrations for 2 hr and examined by comet assay, (* = significantly different from control).

To ascertain that the insulin effects were not only limited to permanent cell lines, primary cells from rat colon were treated with different concentrations of insulin (0.01, 0.1 and 2 μ M) for 30 minutes and comet assay analysis revealed an increase in DNA damage in comparison to the control which was treated with solvent (fig.48).

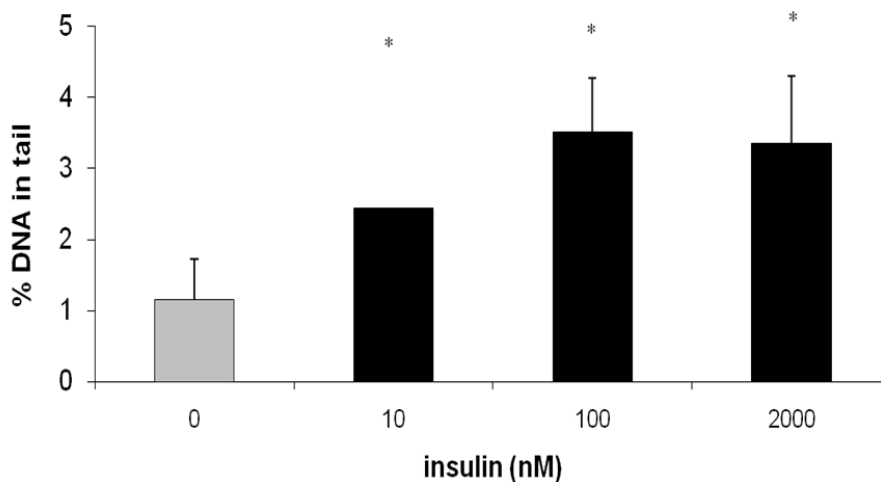


Figure 48: Primary rat colon cells treated with different insulin concentrations for 30 min and examined by comet assay, (* = significantly different from control).

Results

4.2 Insulin mediated oxidative stress and genomic damage in mammalian kidney cells

4.2.1 Insulin induces genotoxicity in kidney cells

To confirm the effect of a high insulin level on different tissues instead of being limited to colon cells, other cells originating from different organs were examined. First LLC-PK1, a pig kidney cell line with many properties of proximal tubular cells, was used.

Comet assay characterization of insulin induced DNA damage in LLC-PK1 cells was evaluated in an insulin concentration ranging from 0.005 μM to 2 μM for 4 hours incubation time (fig 49).

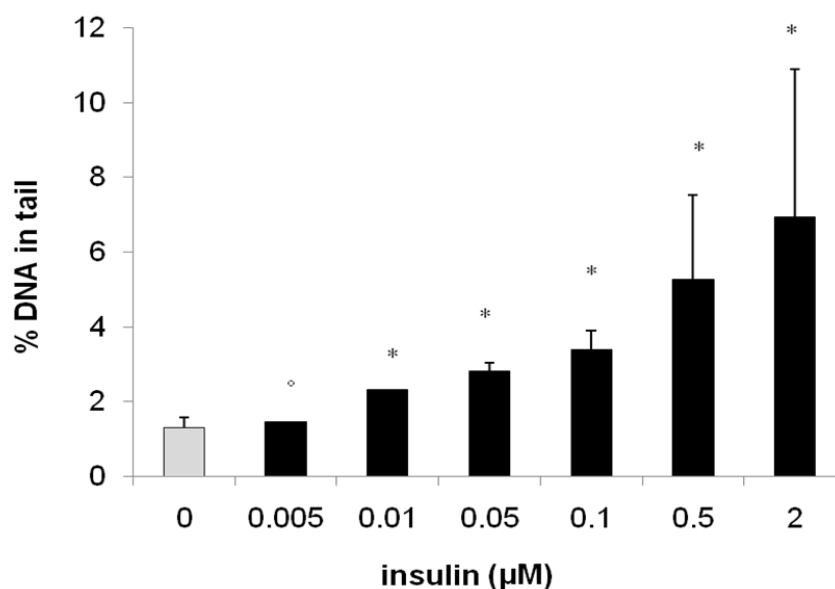


Figure 49: DNA damage (% DNA in tail) measured by comet assay analysis in the LLC-PK1 cell line treated with different insulin concentrations for 4 hr (* = significantly different from control, ° = not significantly different from control).

With 0.1 nM insulin, treatment durations from 5 minutes to 4 hours were applied to the cells to evaluate the shortest time needed for the induction of DNA damage and to see if the damage is constant over time for several hours of treatment (fig 50). The cells reacted with significant induction of DNA damage starting at 0.01 μM and 5 minutes of insulin treatment (fig 50).

For all further comet assay experiments with LLC-PK1 cells, 0.1 μM and 2 hours were used. In parallel to all comet assay experiments, vitality tests and cell number counting

Results

were used as markers for cell proliferation and the applied treatments did not result in significant reduction in vitality or alteration of proliferation.

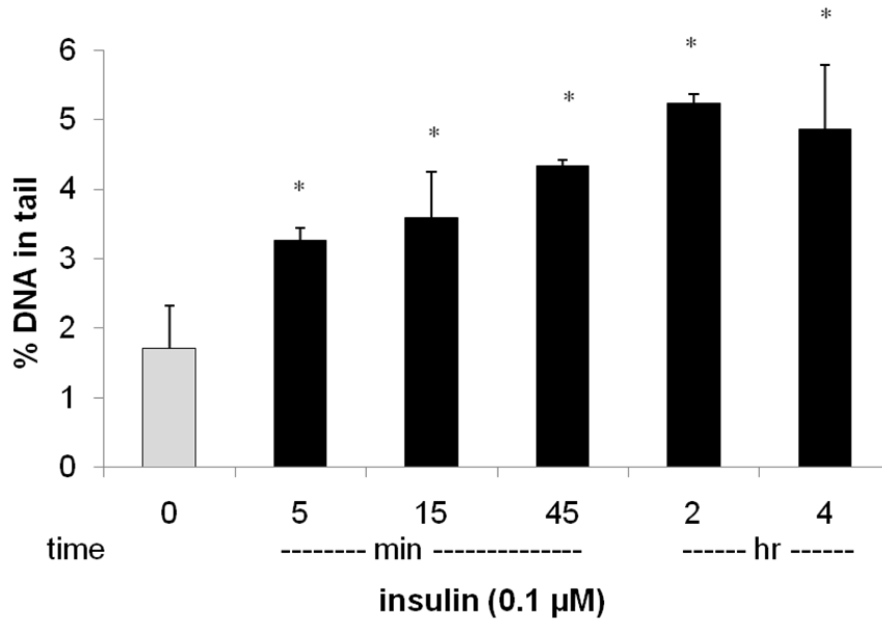


Figure 50: DNA damage (% DNA in tail) measured by comet assay analysis in the LLCPK1 cell line treated with 0.1 μM insulin for different times, (* = significantly different from control).

Formation of micronuclei by DNA strand breaks was evaluated in LLC-PK1 treated with 2 μM insulin for different incubation times (5 minutes to 4 hours) where the first significant increase in micronucleus formation was observed after 30 minutes treatments (fig.51).

Results

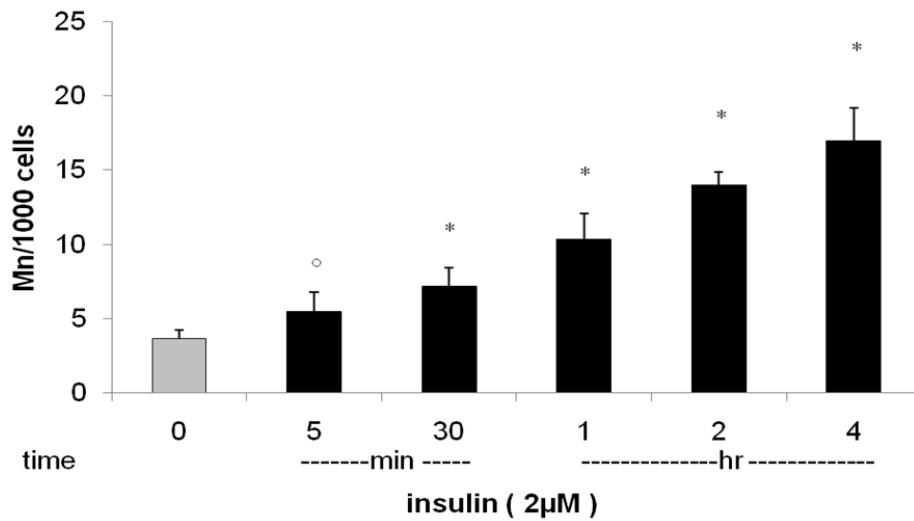


Figure 51: Micronucleus frequency in LLC-PK1 treated with 0.1 μM insulin for different time and harvested after an additional 22 hr expression time, (* = significantly different from control, ° = not significantly different from control).

Formation of micronuclei by DNA strand breaks was evaluated for an insulin concentration range from 0.005 to 2 μM in LLC-PK1 cells and the treatment duration was 4 hours (fig. 52). A concentration dependent increase in micronucleus formation was observed with significant difference to the control at 10 nM and higher.

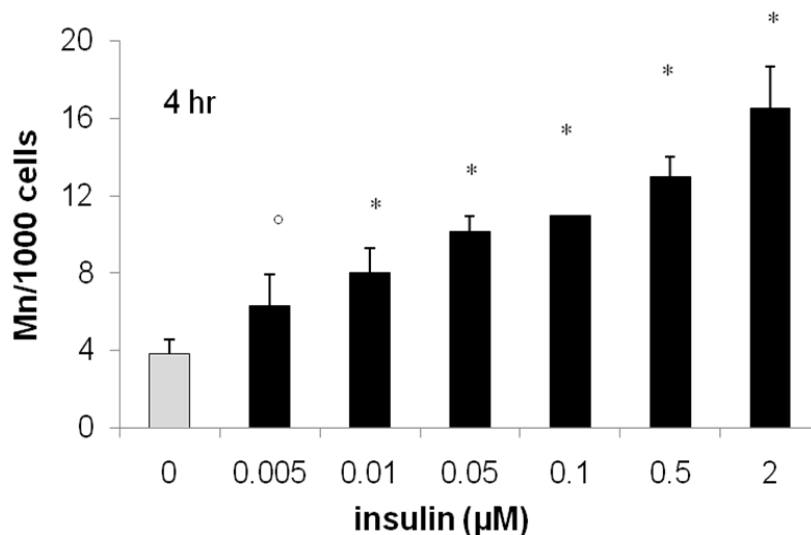


Figure 52: Micronucleus frequency in LLC-PK1 treated with different concentrations of insulin for 4 hr and harvested after an additional 22 hr expression time, (Mn-cell = cell containing one or more micronucleus/i) (* = significantly different from control, ° = not significantly different from control).

Results

An increased formation of micronuclei was achieved by extension of the treatment duration to 48 hours where 5 nM insulin showed significant increase in micronuclei formation (fig. 53).

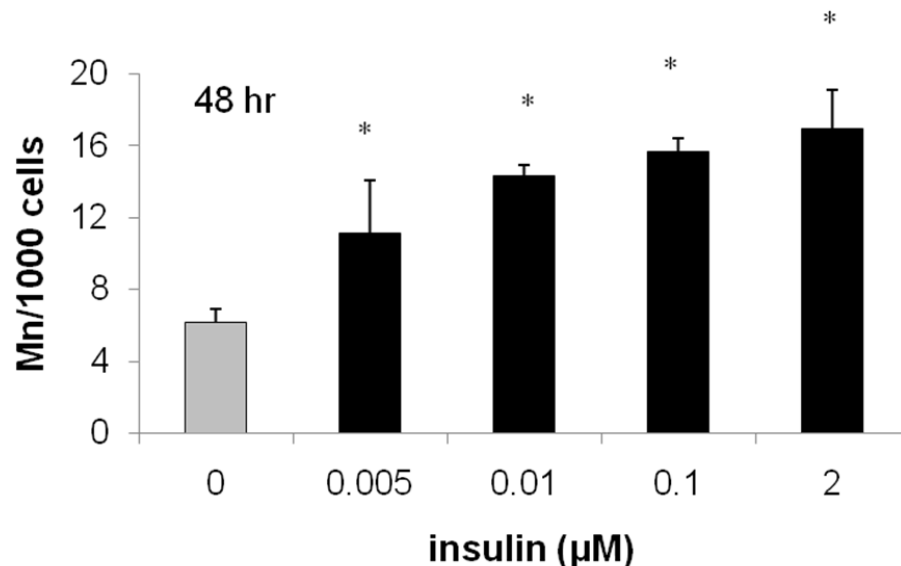


Figure 53: Micronucleus frequency in LLC-PK1 treated with different concentrations of insulin for 48 hr and harvested after an additional 22 hr expression time (Mn-cell = cell containing one or more micronucleus/i) (* = significantly different from control).

For all further micronucleus experiments with LLC-PK1 cells, 2 μM and 4 hours were used. In the micronucleus test, apoptotic cells were quantified according to their nuclear morphology and no significant increase was observed after any of the treatments. For confirmation, flow cytometric analysis of annexin V positive and propidium iodide negative early apoptotic cells was performed after treatment with 100 nM insulin. No significant increase compared to the control ($1.85 \pm 0.50\%$) was observed after 8 hours ($2.43 \pm 0.37\%$) and 16 hours ($2.21 \pm 0.66\%$). Proliferation (cell number) was also assessed in parallel with the MN experiments and no alteration was observed under the tested conditions.

To investigate the interference of serum or medium components in the insulin-induced DNA damage, first the cells were treated in normal medium and serum free medium or PBS (fig. 54).

Results

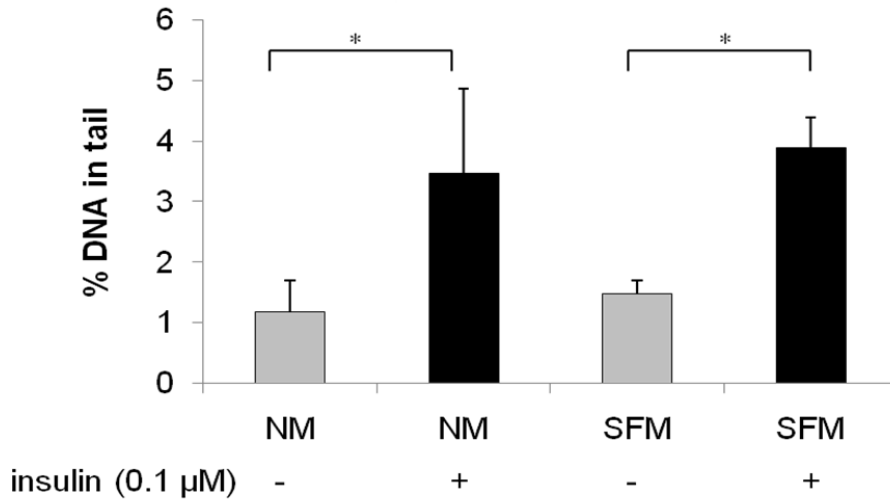


Figure 54: DNA damage (% DNA in tail) measured by comet assay in LLC-PK1 cells treated with 0.1 μM insulin for 2 hr a) in different media, in normal medium (NM) and serum free medium (SFM), (* = significantly different from control).

Second, cells were treated with varying amounts of glucose (0; 5.5 mM; 25 mM) in PBS and in combination with insulin (fig. 55). A significant and comparable induction of genomic damage was observed after all treatments (figs. 54, 55).

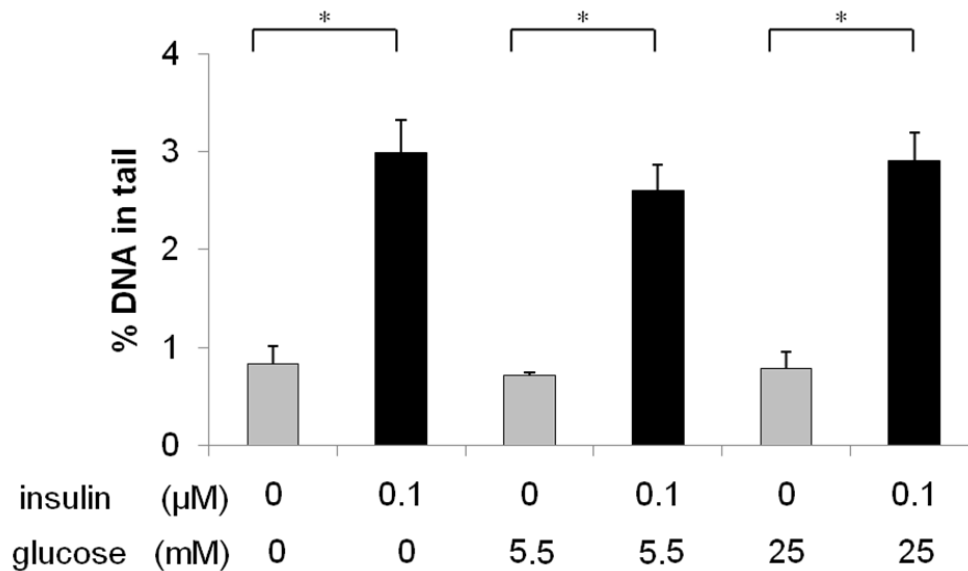


Figure 55: DNA damage (% DNA in tail) measured by comet assay in LLC-PK1 cells treated with 0.1 μM insulin for 2 hr in phosphate buffered saline (PBS, and PBS with different glucose concentrations (5.5 and 25 mM),(* = significantly different from control).

Results

4.2.2 ROS production and antioxidants

Next, ROS production in LLC-PK1 cells was measured and representative pictures were inserted in figure 56. Treatment with 0.1 μM insulin revealed an equal amount of ROS after treatment times between 5 minutes and 2 hours (fig.56).

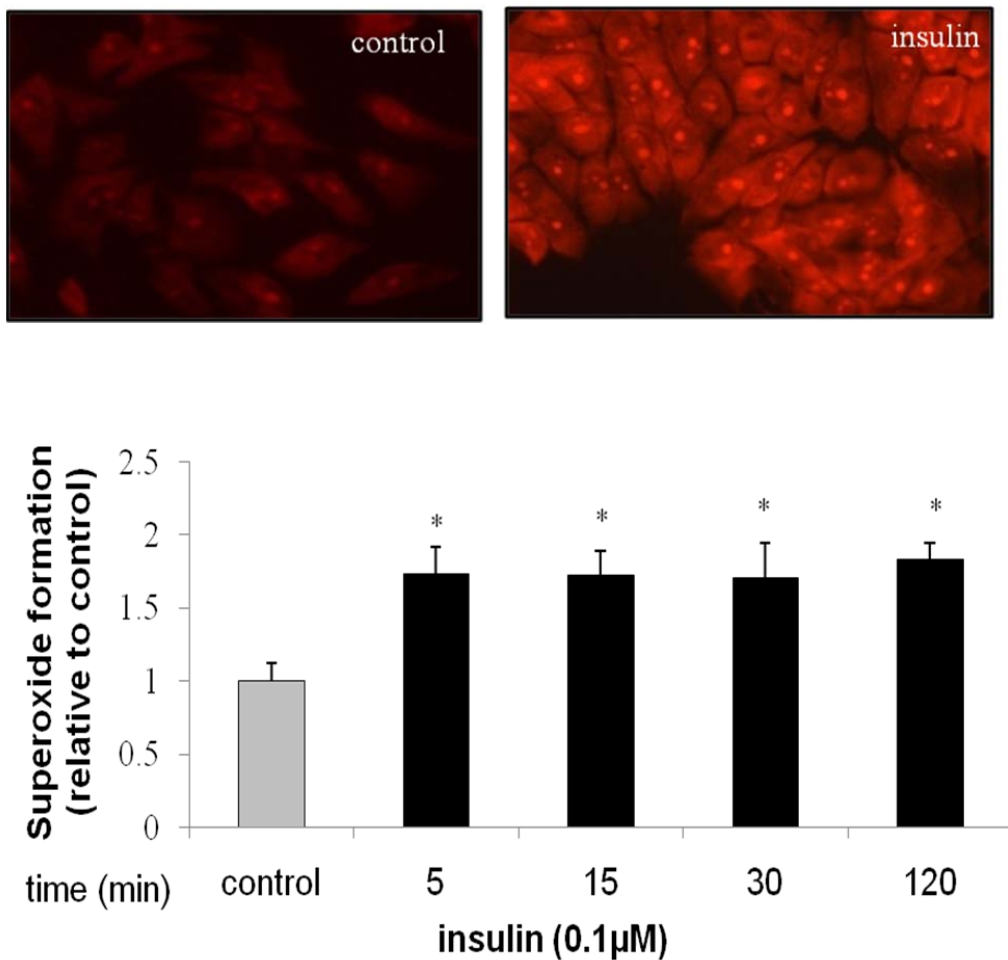


Figure 56: Superoxide production in LLC-PK1 cells incubated with 0.1 μM insulin for different time points and detected with the $\text{O}_2^{\cdot-}$ -reactive probe DHE (10 μM); and quantified by the mean of gray values of DHE fluorescence (* = significantly different from control).

Results

We chose 5 minutes for a dose response experiment (fig. 57), in which significant ROS production was found with all concentrations of insulin (5 nM to 2 μ M).

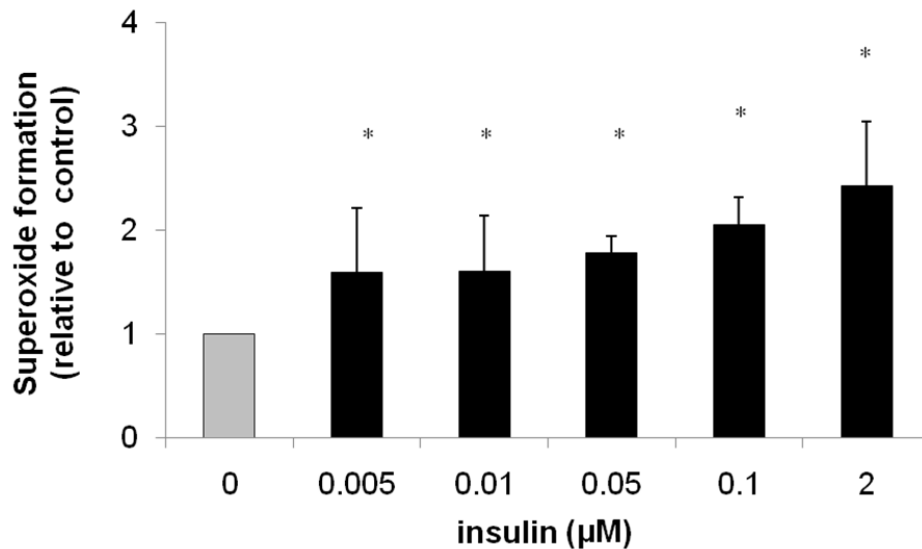


Figure 57: Superoxide production in LLC-PK1 cells incubated with different concentrations of insulin in normal medium for 5 min and detected with the $O_2^{\cdot-}$ -reactive probe DHE (10 μ M); and quantified by the mean of gray values of DHE fluorescence (* = significantly different from control).

For further confirmation of the involvement of ROS in the DNA damage, 50 μ M of the radical scavenger tempol was combined with insulin and the effect was detected by comet assay and micronucleus frequency test, (fig.58 a and b).

Results

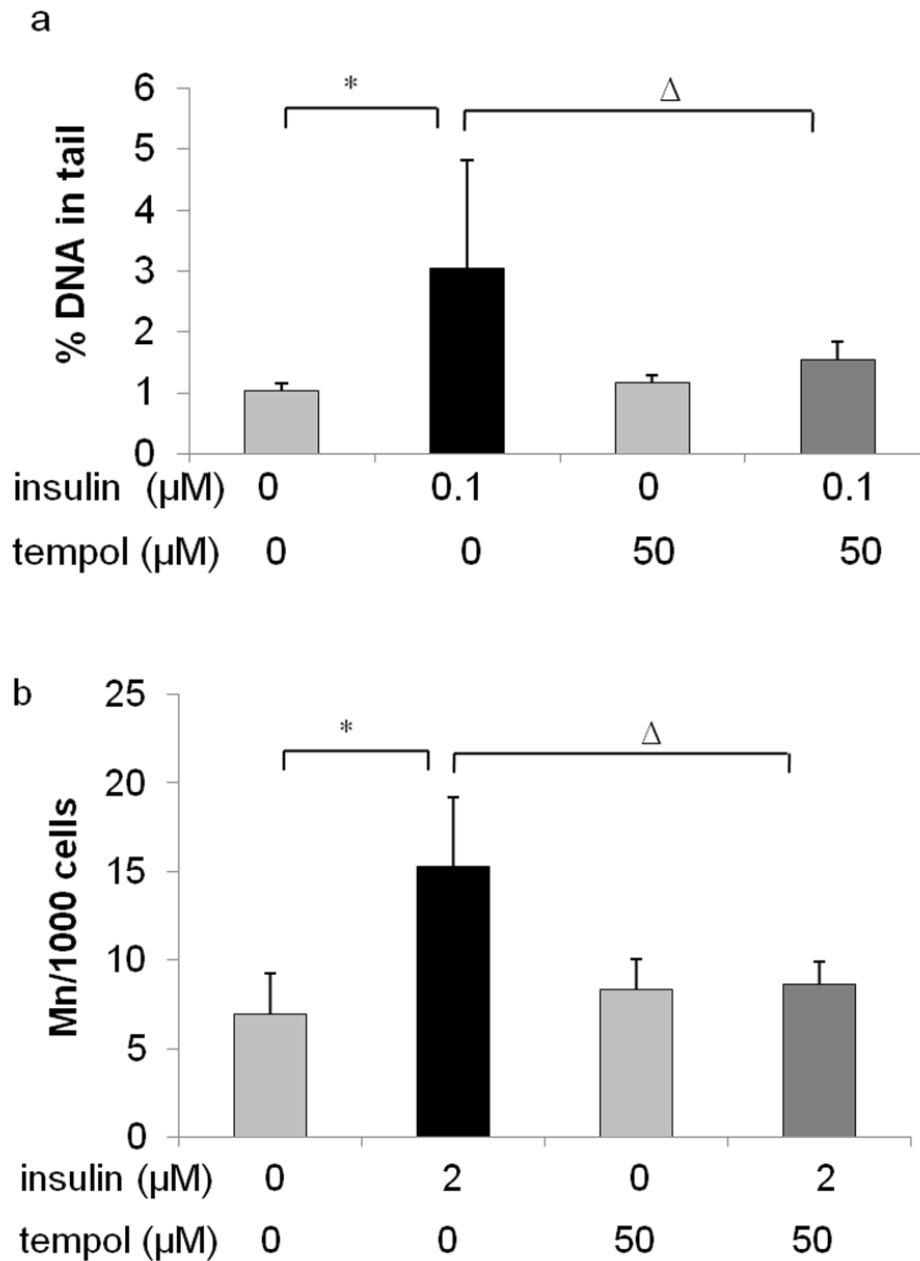


Figure 58: Influence of tempol on insulin-induced alterations in LLC-PK1 cells; a) DNA damage (% DNA in tail) in the comet assay after a 2 hr treatment with 0.1 μM insulin, 50 μM tempol and the combination, and b) micronucleus frequency after 4 hr treatment (plus 22 hours expression time) with 2 μM insulin, 50 μM tempol and the combination (Mn-cell = cell containing one or more micronucleus/i) (* = significantly different from control, Δ = significantly different from insulin).

Results

The antioxidant and flavoenzyme inhibitor apocynin (100 μM) was combined with insulin in both genotoxicity tests (fig.59 a and b).

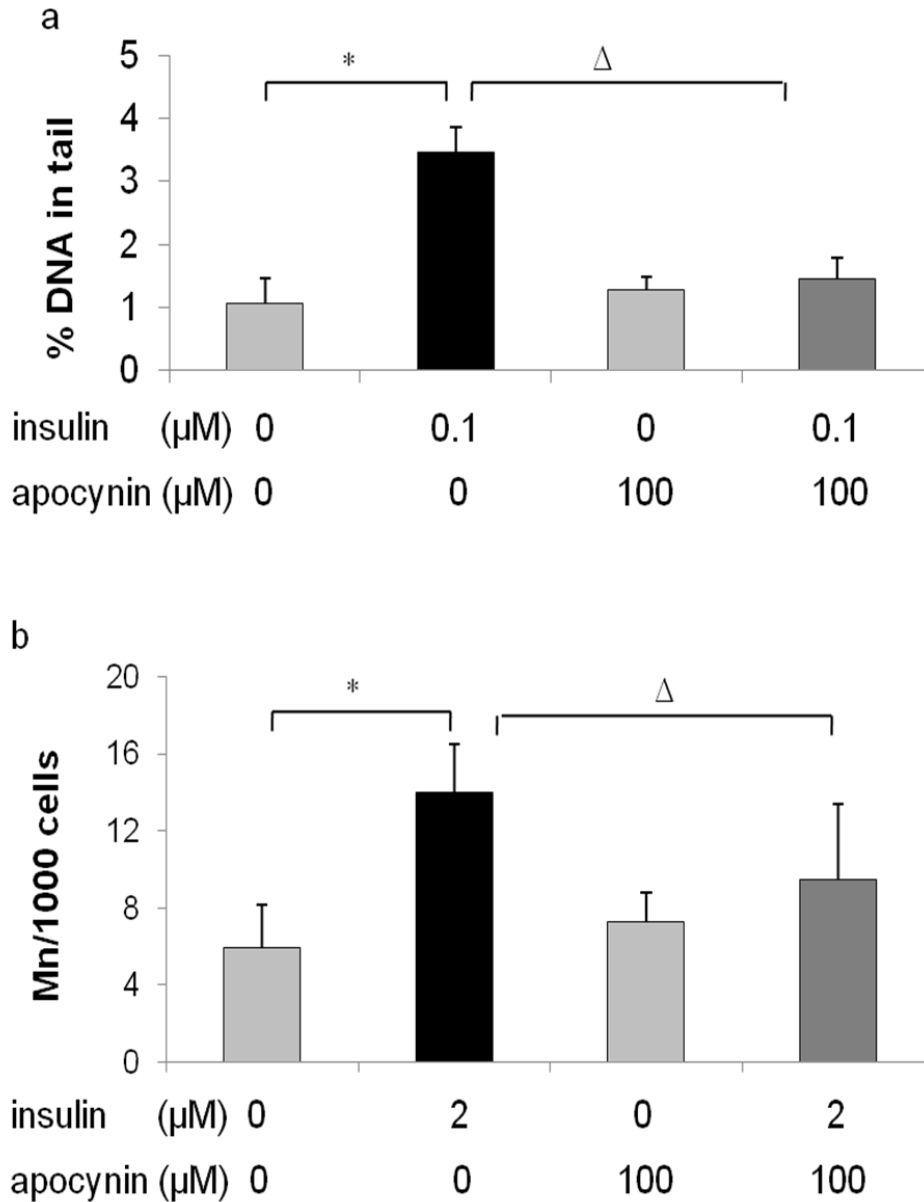


Figure 59: Influence of apocynin on insulin-induced alterations in LLC-PK1 cells; a) DNA damage (% DNA in tail) in the comet assay after a 2 hr treatment with 0.1 μM insulin, 100 μM apocynin and the combination, and b) micronucleus frequency after 4 hr treatment (plus 22 hours expression time) with 2 μM insulin, 100 μM apocynin and the combination (Mn-cell = cell containing one or more micronucleus/i) (* = significantly different from control, Δ = significantly different from insulin).

Results

Both chemicals (tempol and apocynin) reduced the insulin induced genomic damage in the comet assay (figs.58a, 59a) and the micronucleus frequency test (figs. 58b, 59b) as well as the ROS production (fig. 60).

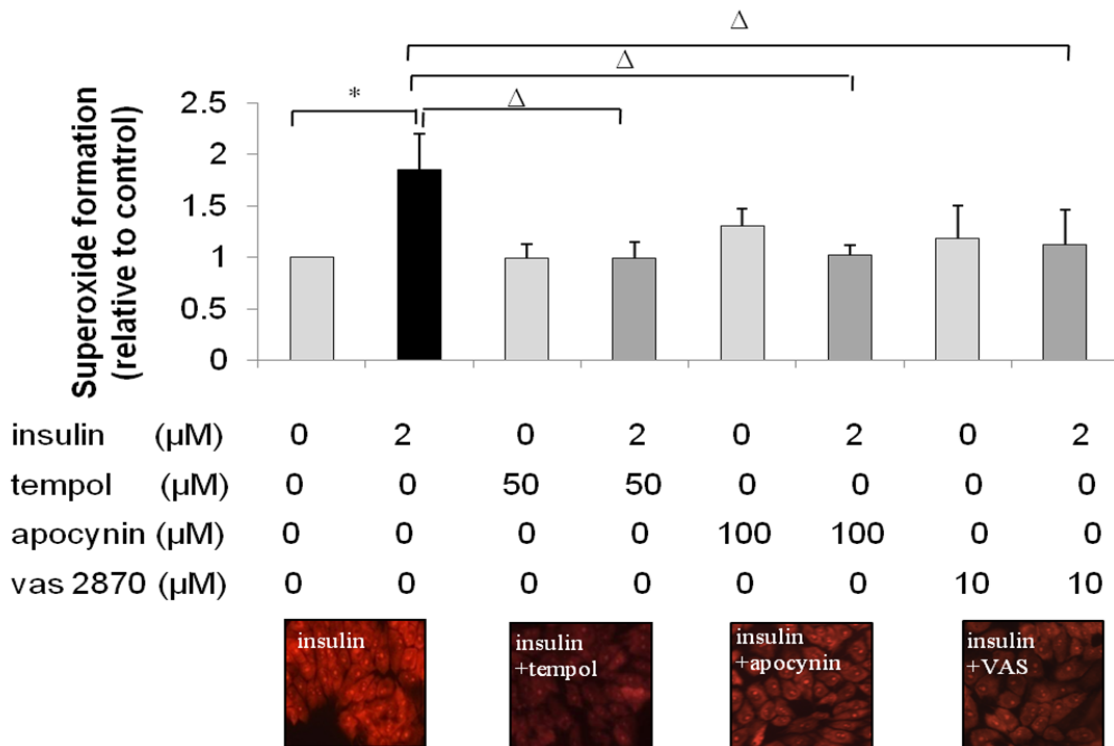


Figure 60: Superoxide analysis after 5 min of treatment with 2 μM insulin, 50 μM tempol, 100 μM apocynin, 10 μM VAS2870 and the combination of insulin with the inhibitors (* = significantly different from control, Δ = significantly different from insulin).

4.2.3 Role of insulin receptor (IR) and insulin-like growth factor (IGF-1R) receptor in insulin genotoxicity

The expression of insulin receptor (IR) and insulin-like growth factor 1 receptor (IGF-1R) as main targets for insulin binding in LLC-PK1 was confirmed with RT-PCR. The obtained sequences were compared with the Genbank data base, yielding 99 % Identity for both with *Sus scrofa* insulin receptor mRNA, partial cds with accession number AF102858.1 and *Sus scrofa* insulin-like growth factor 1 receptor precursor (IGF-1R) mRNA complete cds with accession number HQ322390.1 (fig. 61).

Results

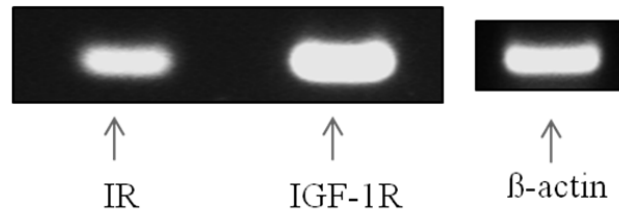


Figure 61: Expression of insulin receptor (IR) and insulin-like growth factor (IGF1R) in LLCPK1 cells.

Next, cells were incubated with a combination of insulin and several antagonists or inhibitors. Specifically, the insulin receptor antagonist HNMPA(AM)₃ (100 μM) and the specific IGF-1 receptor antagonist PPP (50 nM) were applied (fig.62,63), both of which reduced the damage induction.

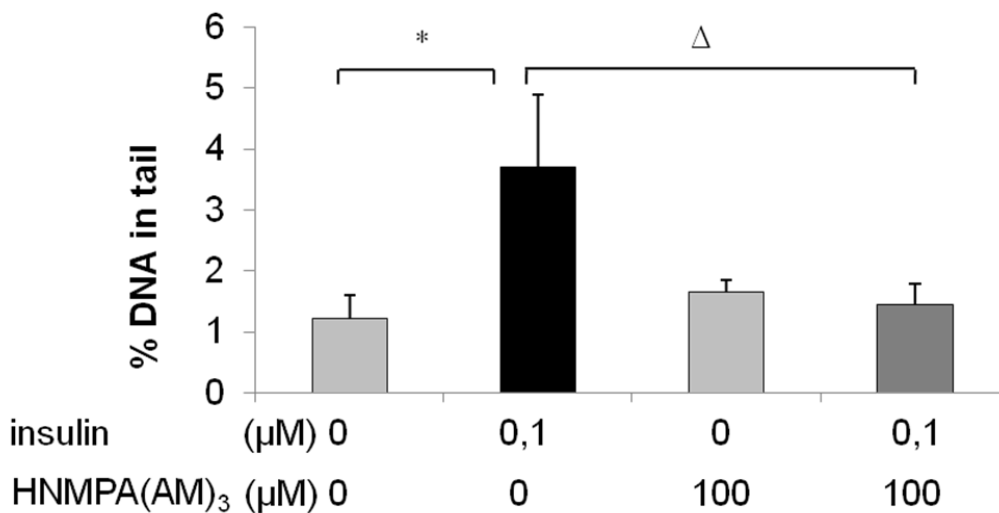


Figure 62: Influence of HNMPA(AM)₃ on insulin-induced alterations in LLC-PK1 cells; DNA damage (% DNA in tail) in the comet assay after a 2 hr treatment with 0.1 μM insulin, 100 μM HNMPA(AM)₃ and the combination (* = significantly different from control, Δ = significantly different from insulin).

Results

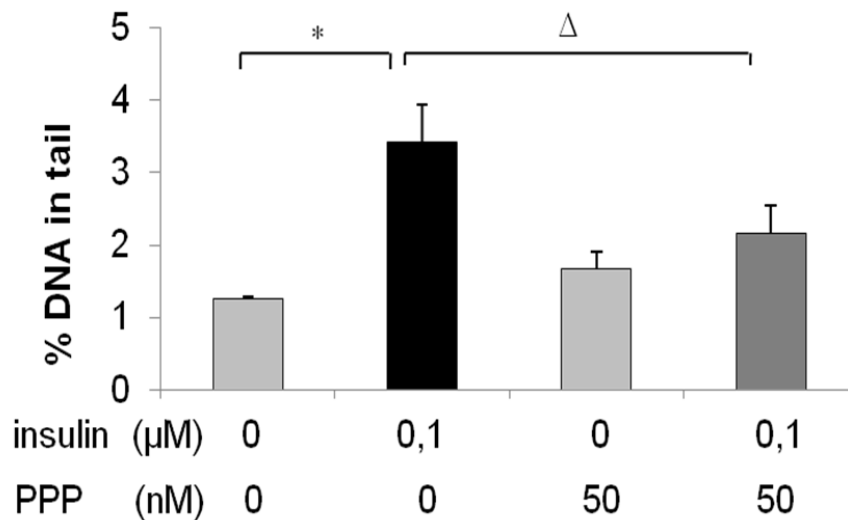


Figure 63: Influence of PPP on insulin-induced alterations in LLC-PK1 cells; DNA damage (% DNA in tail) in the comet assay after a 2 hr treatment with 0.1 μM insulin, 50 nM PPP and the combination (* = significantly different from control, Δ = significantly different from insulin).

4.2.4 Activation of PI3 kinase and AKT

In the normal signaling pathway, activation of PI3K is following the activation of the two receptors. To investigate the contribution of PI3K in insulin genotoxicity, the PI3K inhibitor wortmannin was used in combination with insulin to treat the cells. The treated cells showed reduction in the DNA damage (figs. 64,65) as well as in p53 accumulation (fig. 66).

Results

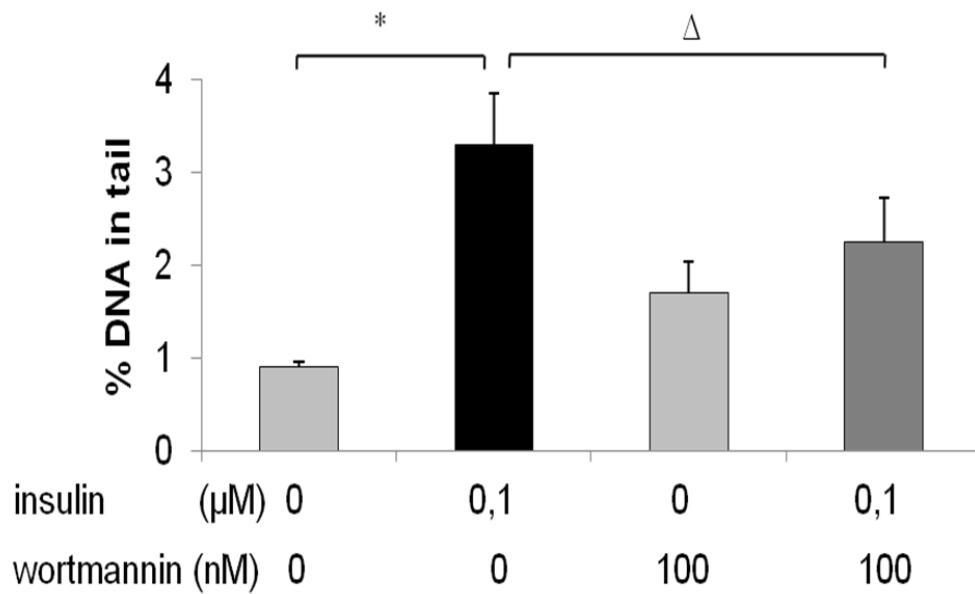


Figure 64: Influence of wortmannin on insulin-induced alterations in LLC-PK1 cells; DNA damage (% DNA in tail) in the comet assay after a 2 hr treatment with 0.1 μM insulin, 100 nM wortmannin and the combination (* = significantly different from control, Δ = significantly different from insulin).

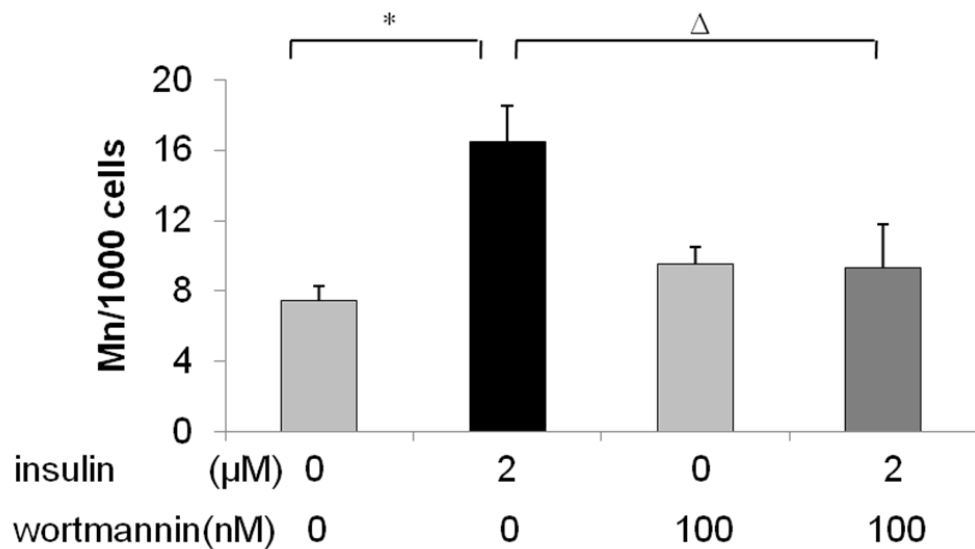


Figure 65: Influence of wortmannin on insulin-induced alterations in LLC-PK1 cells; chromatin damage (Mn/1000 cells) measured as micronucleus frequency in cells treated for 4 hr with 2 μM insulin, 100 nM wortmannin and the combination plus an expression time of 20-22 hr after treatment (* = significantly different from control, Δ = significantly different from insulin).

Results

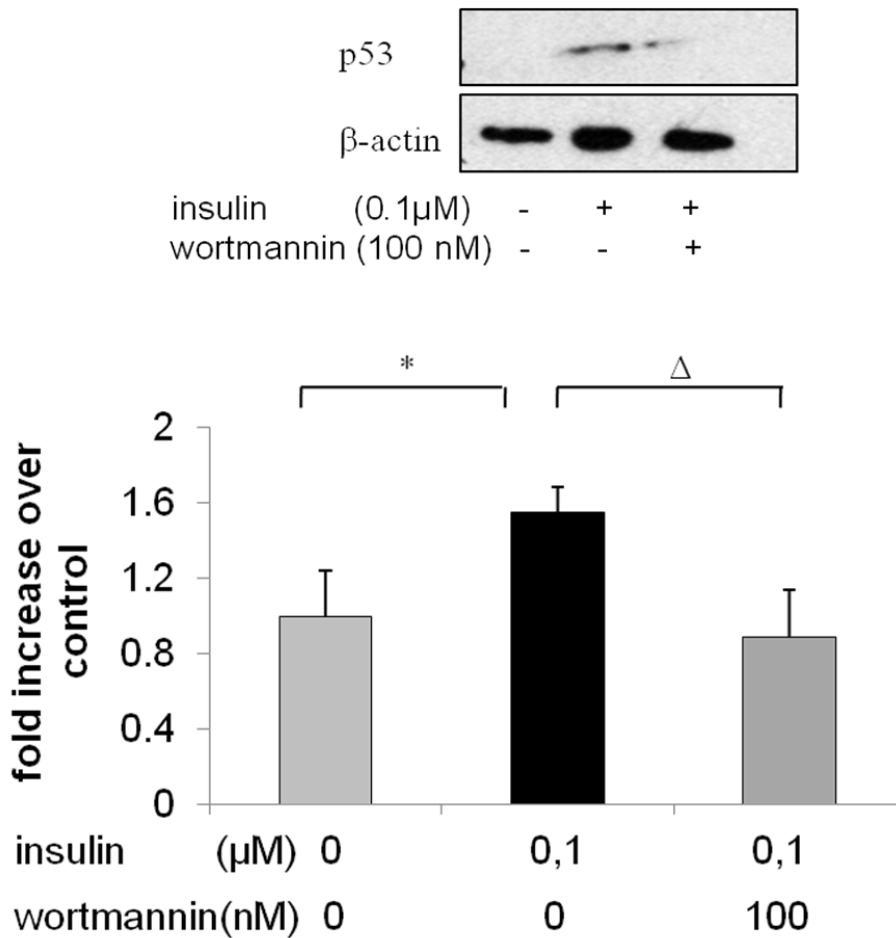


Figure 66: p53 levels in LLC-PK treated for 30 min with 0.1 μ M insulin, 100 nM wortmannin and the combination and measured by Western blot analysis (* = significantly different from control, Δ = significantly different from insulin).

AKT activation was investigated in the LLC-PK cells treated with insulin and insulin in combination with wortmannin (fig. 67), treatment of the cells with insulin increased the pAKT level while addition of wortmannin inhibited the effect of insulin on AKT activation.

Results

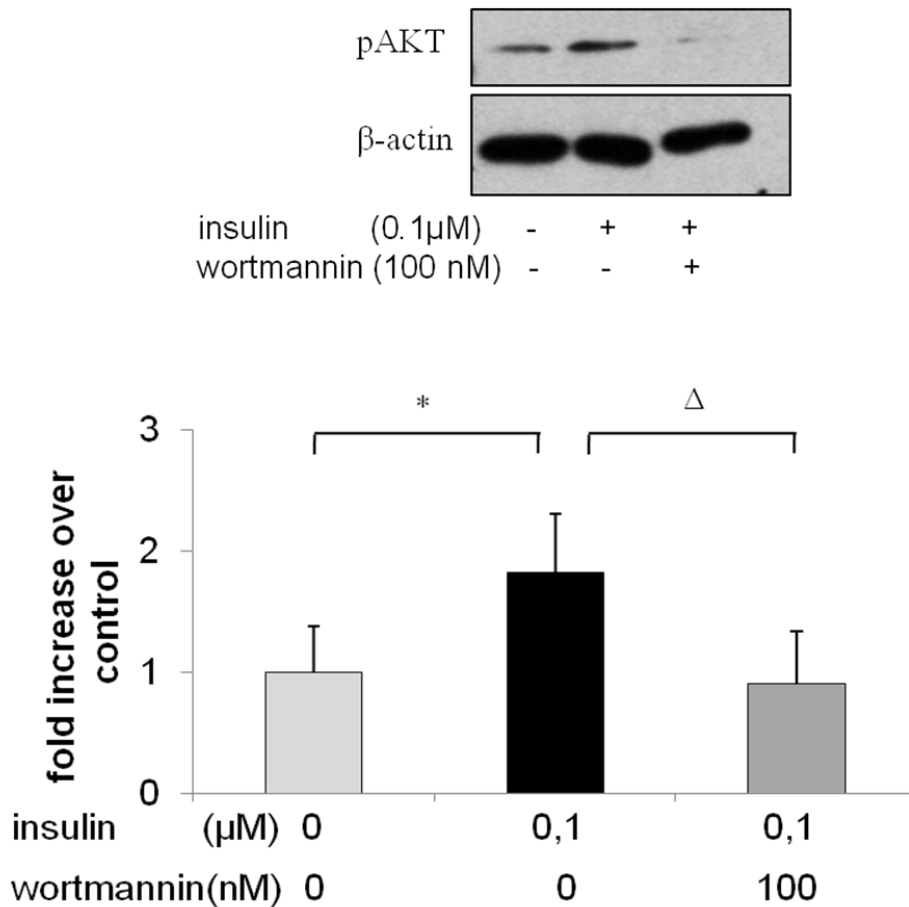


Figure 67: pAKT level in LLC-PK treated for 30 min with 0.1 μ M insulin , 100 nM wortmannin and the combination and measured by Western blot analysis, (* = significantly different from control, Δ = significantly different from insulin).

4.2.5 ROS sources

For investigation of the involvement of the two major ROS sources, the mitochondrial inhibitor rotenone (10 nM) and the NADPH oxidase inhibitor VAS2870 (10 μ M) were used (fig.68 a and b). Again, the DNA damage was reduced by the two inhibitors, and in figure 60, VAS2870 showed reduction of ROS production in the LLC-PK1 cells.

Results

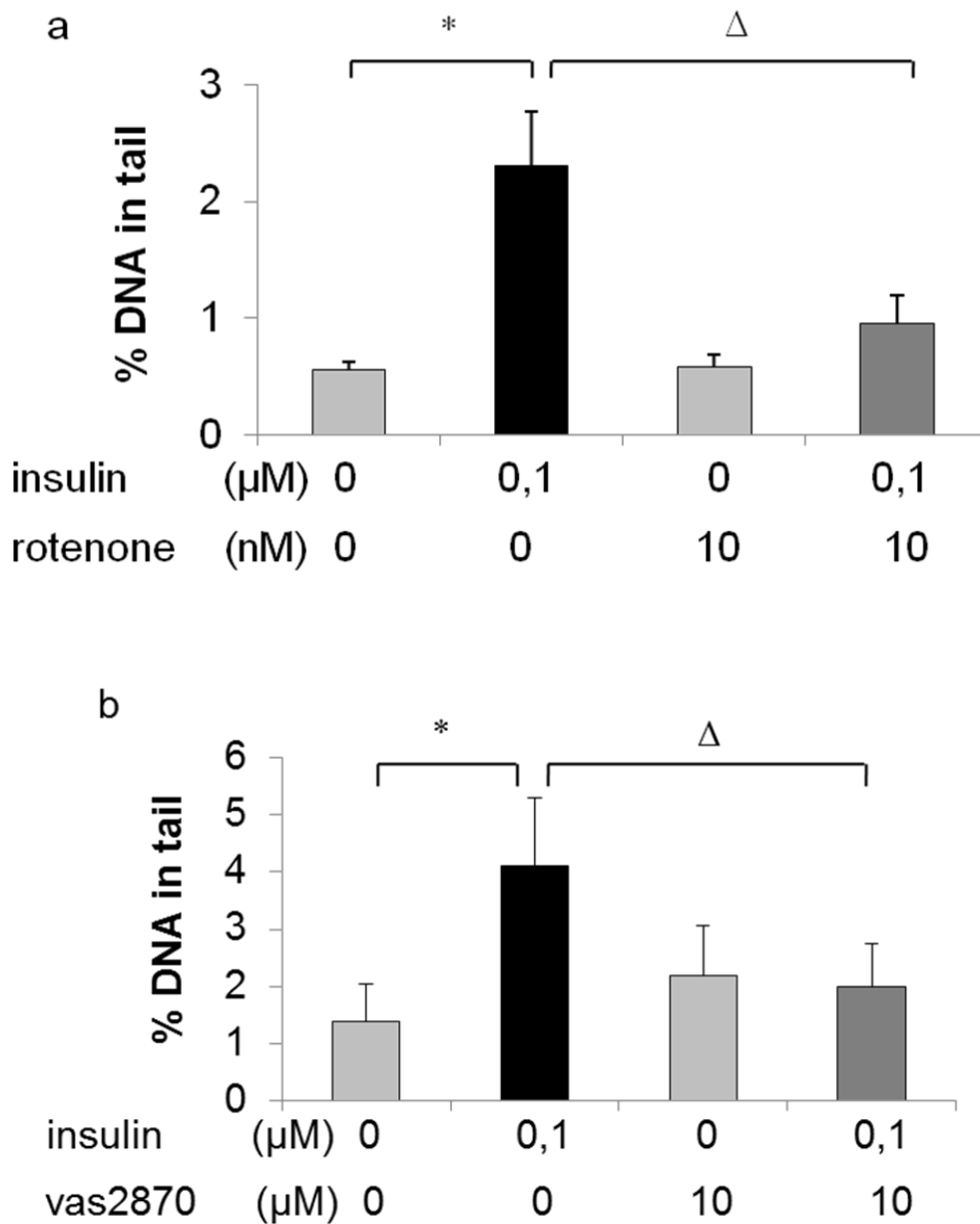


Figure 68: Influence of rotenone and VAS2870 on insulin-induced alterations in LLC-PK1 cells; DNA damage (% DNA in tail) in the comet assay after a 2hr treatment with 0.1 μM insulin a) 10 nM rotenone and the combination, b) 10 μM VAS2870 and the combination, (* = significantly different from control, Δ = significantly different from insulin).

Results

4.2.6 Effect of insulin in primary rat kidney cells

Primary rat kidney cells were treated with three different concentrations of insulin (0.01, 0.1 and 2 μM) for 30 minutes and comet assay analysis revealed an increase in DNA damage in comparison to the solvent control for kidney cells (fig.69).

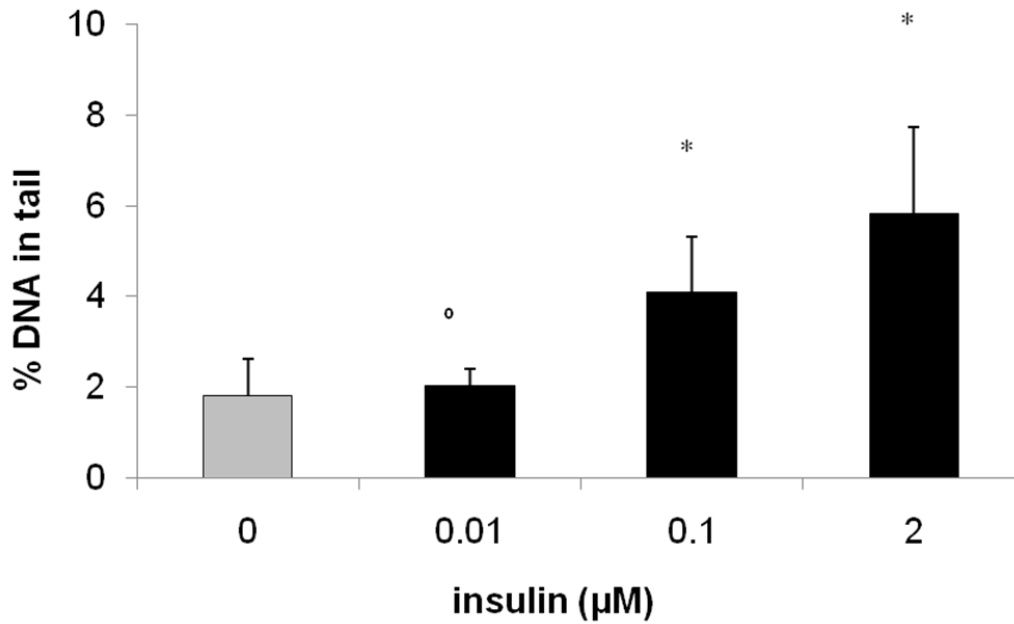


Figure 69: Primary rat kidney cells treated with different insulin concentrations for 30 min and examined by comet assay (* = significantly different from control, ° = not significantly different from control).

Results

4.2.7 Signaling pathway of the insulin mediated genotoxicity in kidney cells using the human kidney cell line HK2.

To investigate the signaling pathway of insulin mediated genotoxicity in kidney. HK2 cells were used as a model for human kidney cells. First the effect of insulin was confirmed by comet assay and micronucleus frequency test (figs. 70, 71) where HK2 cells showed significant increase in DNA damage after 2 hours treatment.

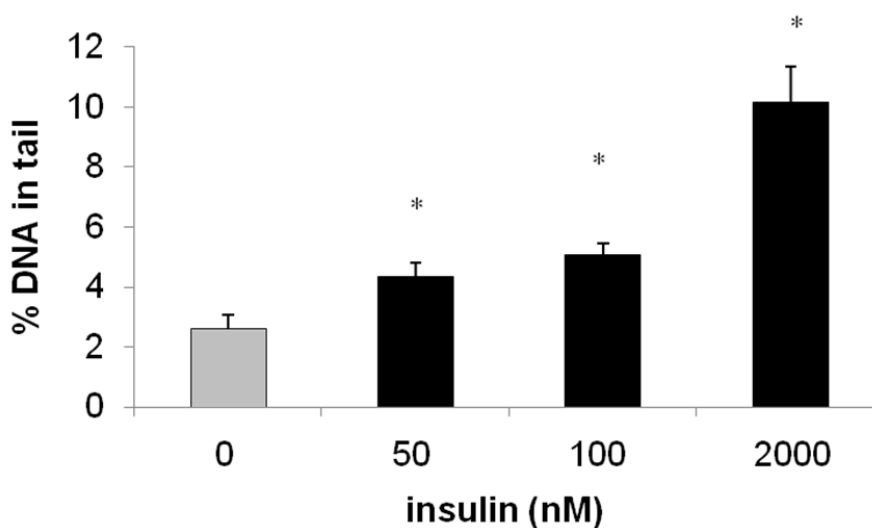


Figure 70: DNA damage (% DNA in tail) measured by comet assay analysis in the HK2 cells treated with different insulin concentrations for 2 hr (* = significantly different from control).

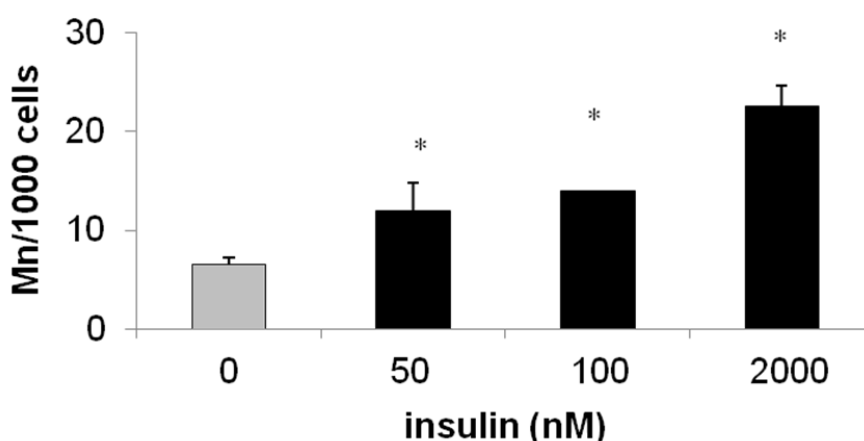


Figure 71: Micronucleus frequency in HK2 cells treated with different insulin concentrations for 2 hr and harvested after an additional 22 hr expression time, (* = significantly different from control).

Results

p53 level was used as an indicator for the DNA damage induced in HK2 cells treated with insulin. Different insulin concentrations (0.5-100 nM) were applied to the cells for 2 hours (fig.72). Upon treatment of the cells with insulin, p53 accumulated at 0.5 nM insulin and higher.

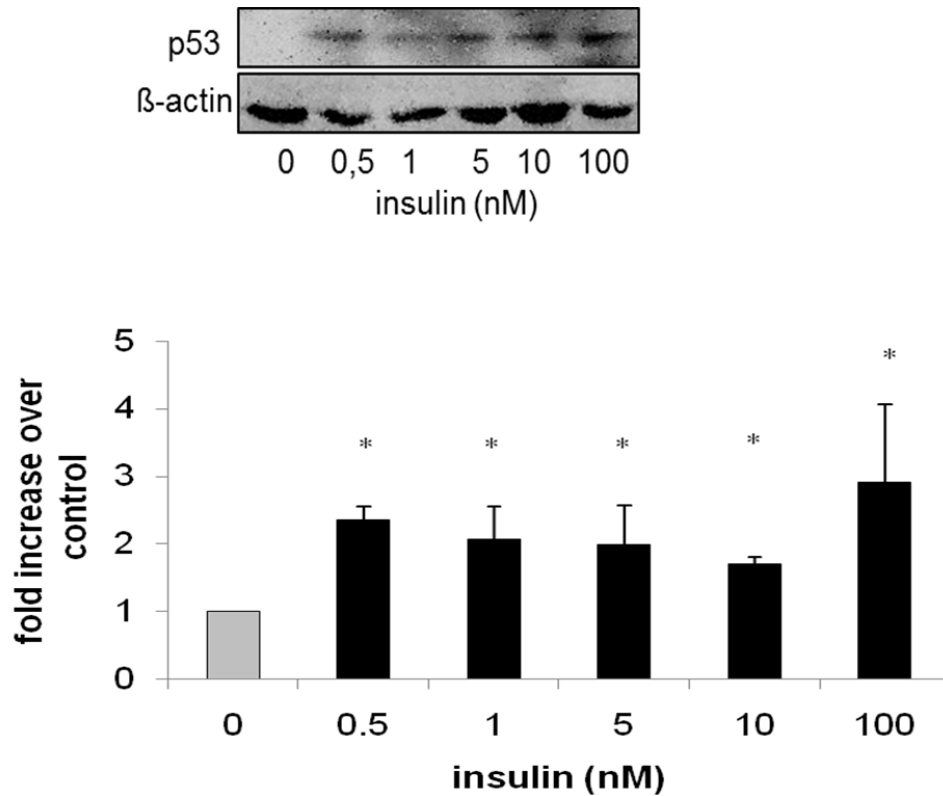


Figure 72: p53 levels in HK2 cells treated for 2 hr with different insulin concentrations (0.5 to 100 nM) and measured by Western blot analysis (* = significantly different from control, ° = not significantly different from control).

The signaling pathway usually starts when the ligand binds to its receptor. In this case, insulin is able to bind to both insulin receptor and insulin-like growth factor 1 receptor. In our study, we detected the expression of both receptors in HK2 cells using RT-PCR, where the cells showed the expression of both receptors (fig. 73).

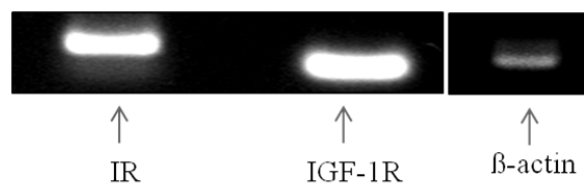


Figure 73: Expression of insulin receptor (IR) and insulin-like growth factor (IGF-1R) in HK2 cells.

Results

Insulin receptors and IGF-1 receptors are phosphorylated upon binding of insulin to them. The binding process was detected by analyzing the phosphorylated insulin and IGF-1 receptors levels in the cells treated with 10 nM insulin for different times and for 2 hours treatment with different insulin concentrations (figs. 74, 75).

HK2 cells showed an increased level of insulin receptor phosphorylation at 0.5 nM concentration and higher, applying a 2 hours treatment (fig.74).

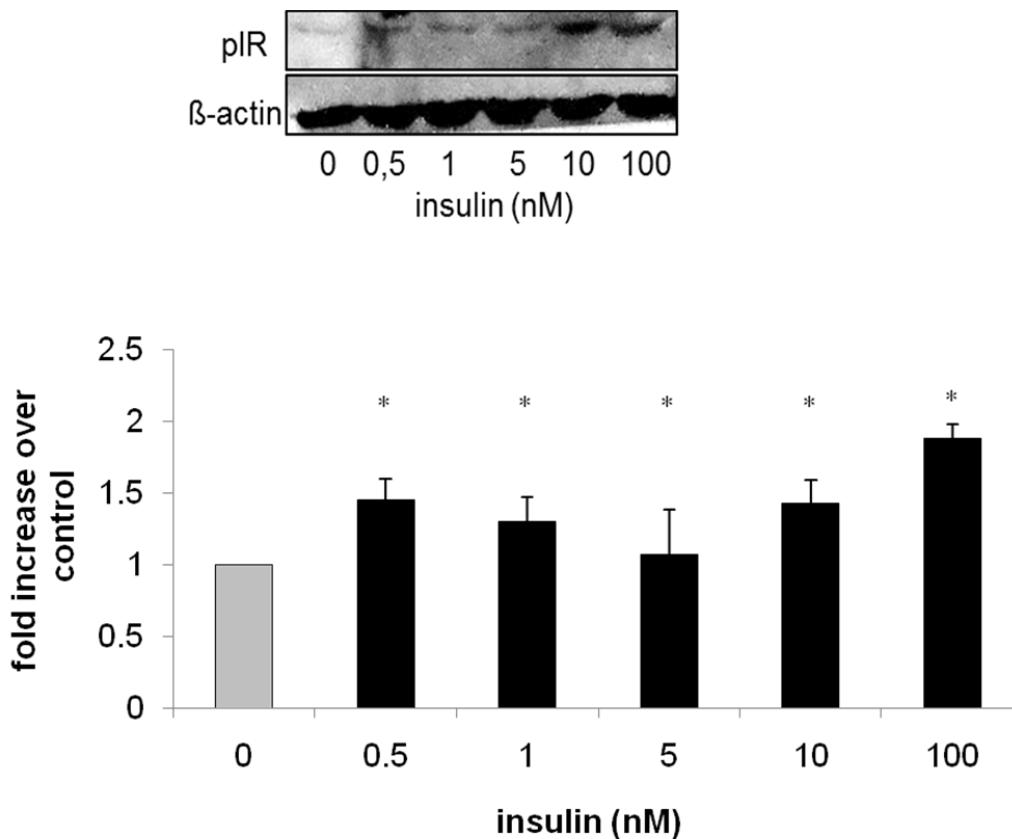


Figure 74: Insulin receptor phosphorylation in HK2 cells treated for 2 hr with different insulin concentrations (0.5 to 100 nM) and measured by Western blot analysis, (* = significantly different from control).

Investigating the time dependence, our results showed that 30 minutes treatment with 10 nM insulin was sufficient to stimulate the insulin receptor phosphorylation to be significantly higher than the control (fig. 75).

Results

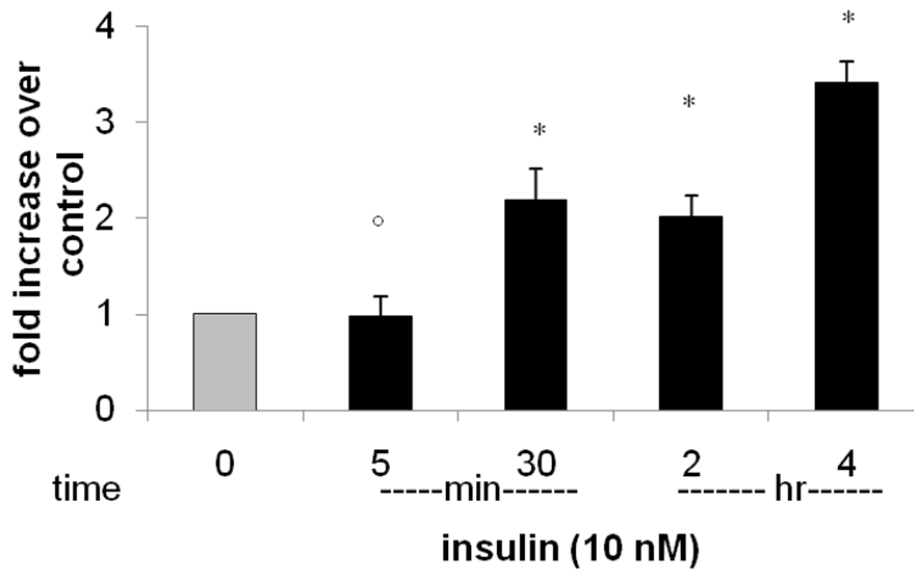


Figure 75: Insulin receptor phosphorylation (pIR) in HK2 cells treated with 10 nM insulin for different time (5 min- 4 hr) and measured by Western blot analysis (* = significantly different from control, ° = not significantly different from control).

IGF-1 receptor, the second target for insulin was, examined for its phosphorylation in HK2 cells, in which 0,5 nM insulin treatment induced significant increase in IGF-1 receptor phosphorylation (fig.76). The activation of the receptor was significantly increased after 5 minutes of treatment with 10 nM insulin (fig. 77)

Results

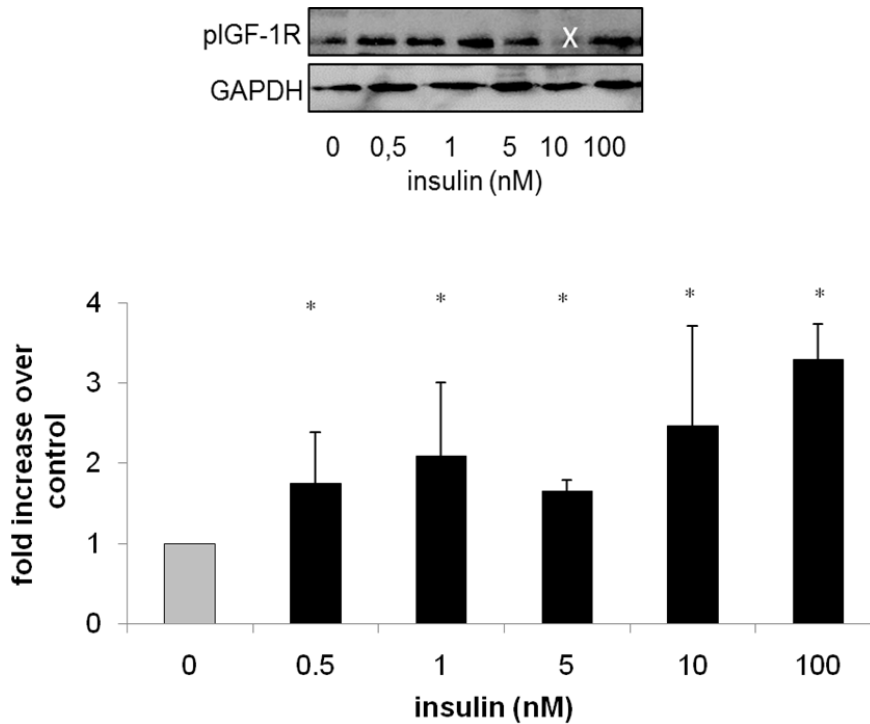


Figure 76: IGF-1R phosphorylation (pIGF1R) in HK2 cells treated with different insulin concentrations (0.5 -100 nM) and measured by Western blot analysis, (* = significantly different from control, x= empty lan).

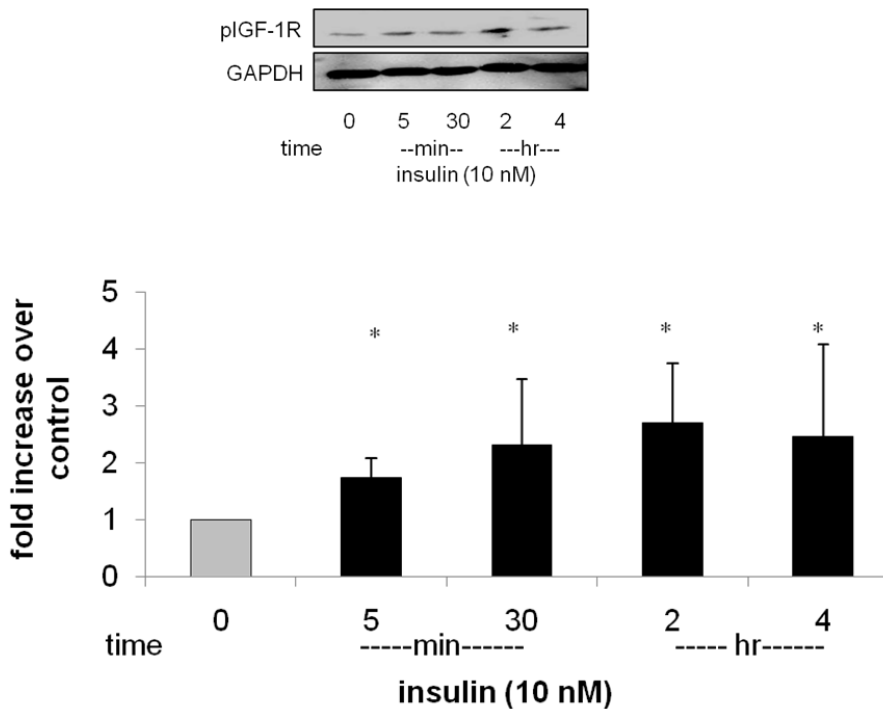


Figure 77: IGF-1R phosphorylation (pIGF-1R) in HK2 cells treated with 10 nM insulin for different time points (5 min to 4 hr), (* = significantly different from control).

Results

All the previous observations indicate that insulin can bind to the insulin receptor as well as the IGF-1 receptor.

In LLC-PK1 cells, we showed that inhibition of both receptors by HNMPA(AM)₃ and PPP inhibitors reduced the DNA damage significantly (figs. 62,63). To confirm the same effect in HK2, cells were treated with both inhibitors and the inhibition of DNA damage was observed in the comet assay (fig.78), which allows the conclusion that both receptors are involved in the insulin genotoxicity signaling pathway in kidney cells. In LLC-PK1 cells, wortmannin, the PI3K inhibitor, reduced the DNA damage in both genotoxicity tests, comet assay and micronucleus frequency test (figs. 64, 65). In addition, p53 level was decreased in cells treated with insulin in combination with wortmannin (fig. 67). In HK2 cells, wortmannin played the same role in DNA damage reduction (fig.78), thus the results from LLC-PK1 and HK2 cells showed the involvement of PI3K in the signaling pathway.

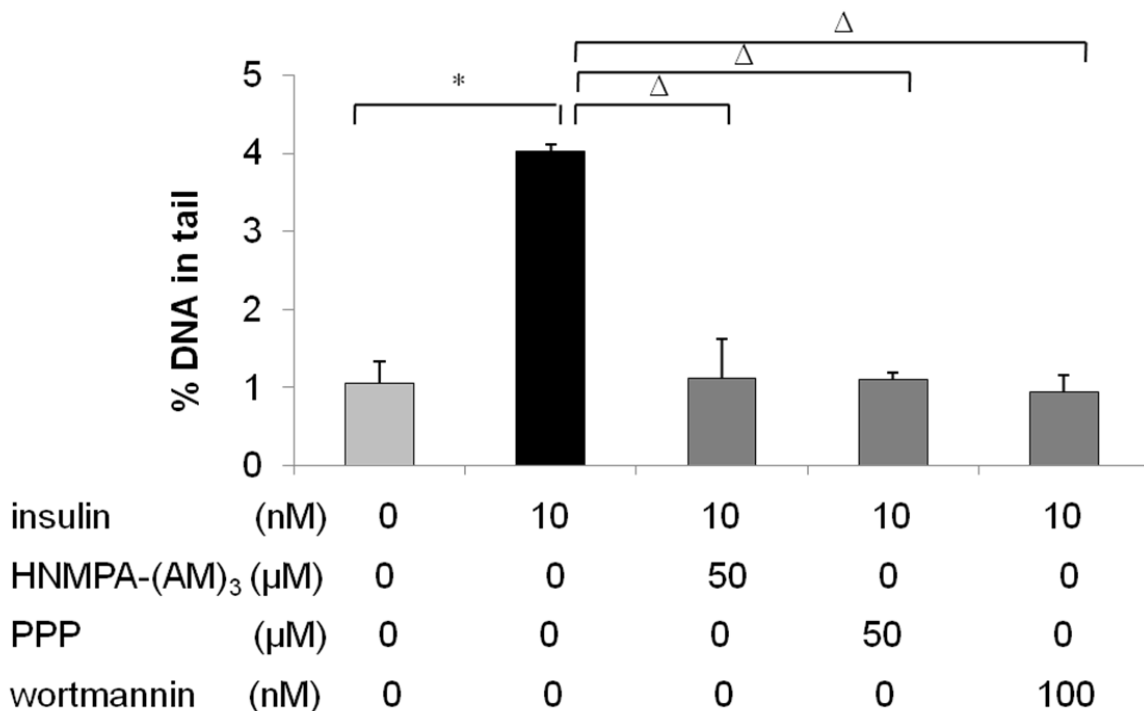


Figure 78: Influence of HNMPA(AM)₃, PPP and wortmannin on insulin-induced alterations in HK2 cells; DNA damage (% DNA in tail) in the comet assay after a 2 hr treatment with 10 nM insulin, and the combinations of insulin with 50 μM HNMPA(AM)₃, 50 nM PPP and 100 nM wortmannin (* = significantly different from control, Δ = significantly different from insulin).

Results

LLCPK1 showed an activation of AKT upon treatment with insulin (fig.66). In HK2 cells the phosphorylation of AKT was examined under different conditions, where phosphorylation of AKT increased significantly at 0.5 nM insulin and higher treatment (fig.79) as well as with 5 minutes and longer treatment with 10 nM insulin (fig.80).

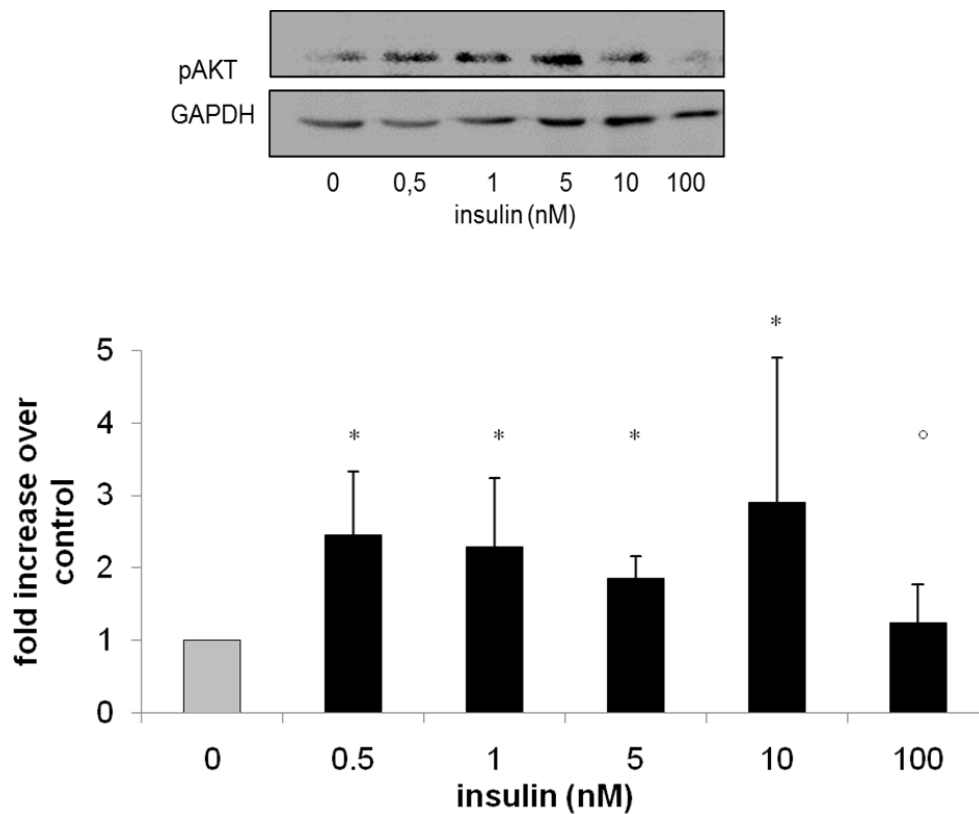


Figure 79: AKT phosphorylation in HK2 cells treated with different concentrations of insulin (0.5 to 100 nM) for 2 hr and measured by western blot analysis, (* = significantly different from control, ° = not significantly different from control).

Results

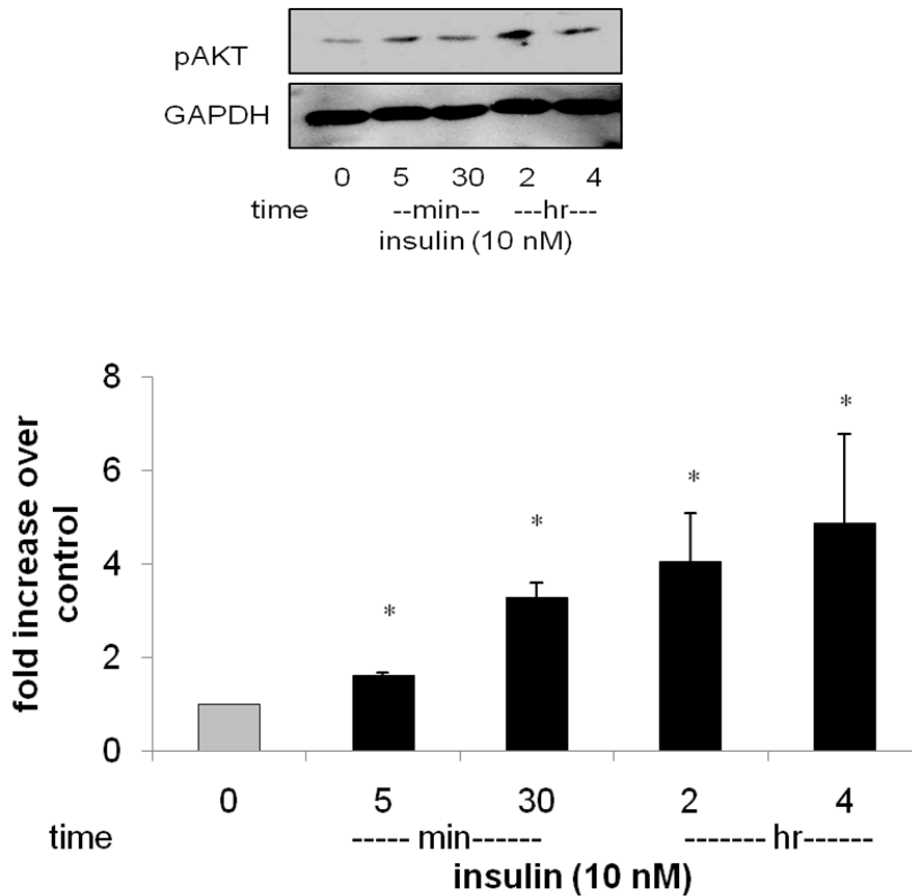


Figure 80: AKT phosphorylation in HK2 cells treated with 10 nM insulin for different time point (5 min to 4 hr) and measured by western blot analysis, (* = significantly different from control, ° = not significantly different from control).

To confirm the order of AKT activation in the signaling pathway, pAKT level was measured in cells treated with insulin and the three previous inhibitors (HNMPA(AM)₃, PPP and wortmannin) (fig.81), where all inhibitors decreased pAKT level in the treated cells, which confirm that activation of AKT follows the activation of insulin and IGF-1 receptors as well as PI3K activation.

Results

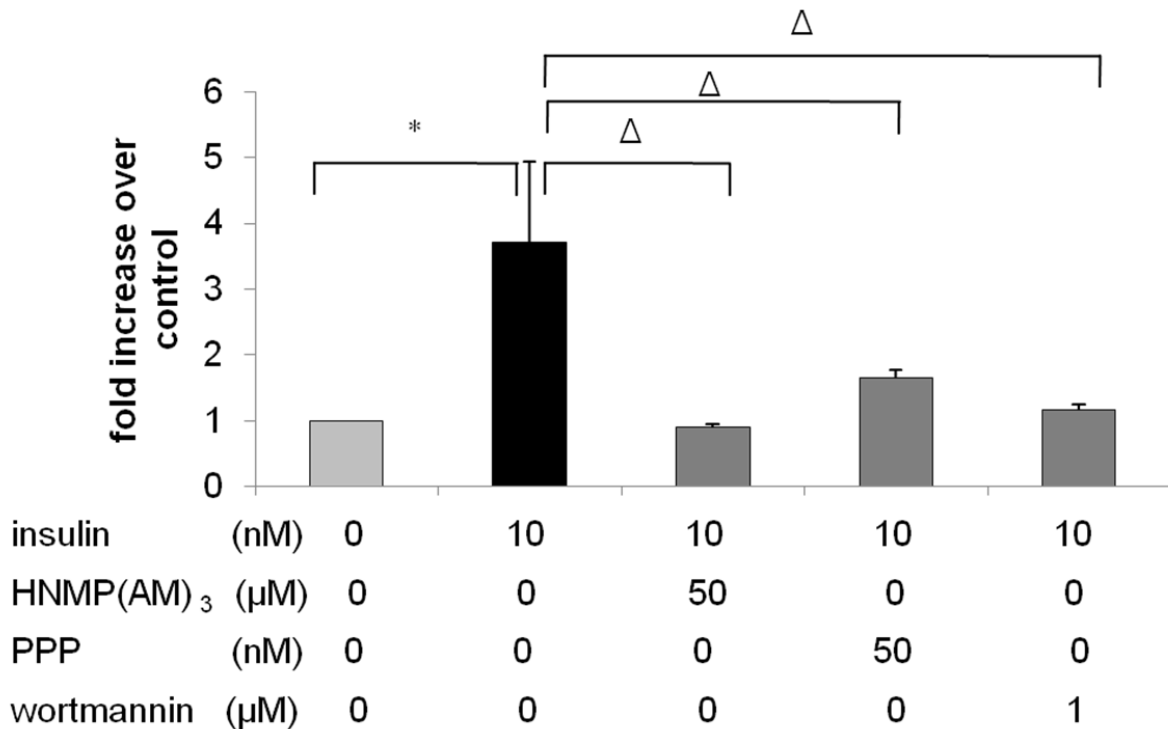


Figure 81: Influence of HNMPA(AM)₃, PPP and wortmannin on pAKT level in HK2 cells; after a 2hr treatment with 10 nM insulin, and the combinations of insulin with 50 μM HNMPA(AM)₃, 50 nM PPP and 100 nM wortmannin and measured by Western blot analysis (* = significantly different from control, Δ = significantly different from insulin).

Next, the involvement of mitochondria was investigated by treatment of the LLC-PK1 cells with rotenone (fig. 68) which caused reduction in the DNA damage. For further confirmation, HK2 rho0 cells (depleted from mtDNA, fig.82) were treated with insulin, in which the cells did not exhibit the same DNA damage in comparison to the normal HK2 cells treated with the same insulin concentration and for the same time of incubation (fig.83). From these results, we can conclude the significant role of mitochondria in insulin stimulate ROS production and DNA damage.

Results

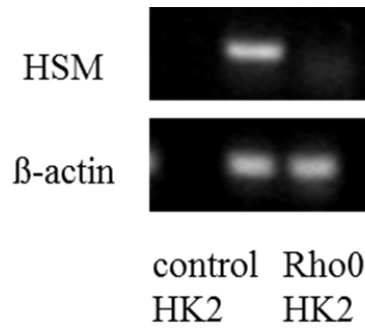


Figure 82: PCR confirmation of mtDNA depletion in HK2 rho0 cells.

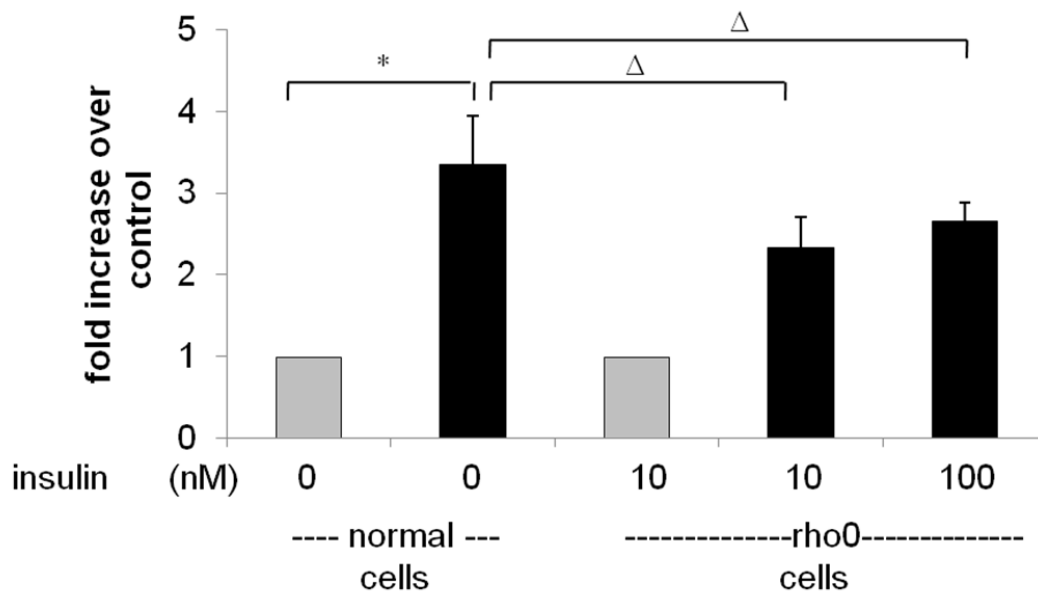


Figure 83: Influence of mitochondria depletion on insulin-induced alterations in HK2 (normal and rho0) cells, DNA damage in the comet assay after a 2 hr treatment with 10 and 100 nM insulin (* = significant vs control, Δ = significant decrease vs insulin).

VAS2870, the NADPH oxidase inhibitor reduced the insulin-induced alterations in LLC-PK1 cells (fig.68), which indicates the involvement of NADPH oxidase as a ROS source in our investigation. To specify the responsible Nox isoform for ROS production, HK2 cells were examined for the expression of different Nox isoforms by RT-PCR, where the cells showed high expression of Nox2 and Nox4 (fig.84).

Results

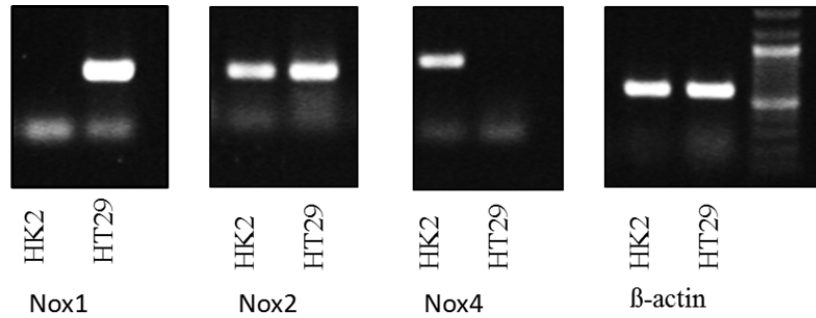


Figure 84: Expression of NADPH oxidase isoforms in HK2 and HT29 cells, the same photographs are shown as figure 40 in the context of HT29 cells investigations and are shown again here in the context of Hk2 cells investigations for easier reading.

To differentiate between the two isoforms, Nox2 and Nox4 were knocked down with siRNA and the levels of the Nox2 and Nox4 were analyzed by western blot and the transfected cells were treated with 10 nM insulin for 2 hours. Cells with knocked down Nox4 showed significant reduction in DNA damage examined by comet assay (fig.85), and micronucleus frequency test (fig.86).

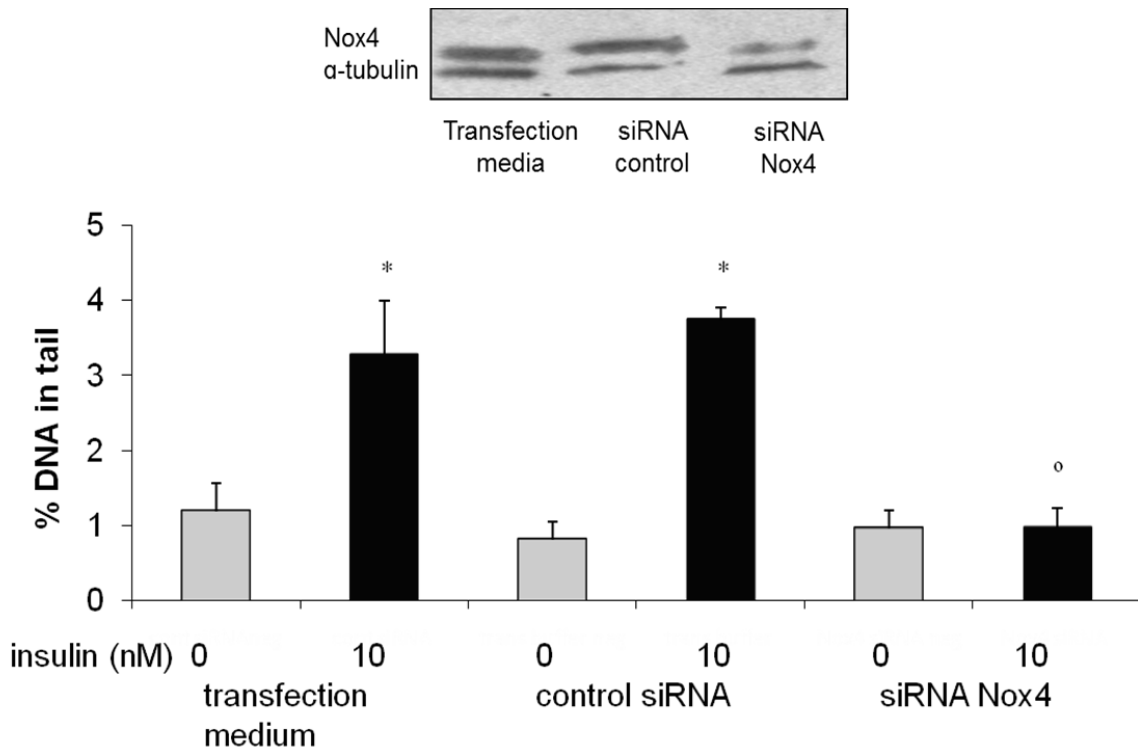


Figure 85: DNA damage measured by the comet assay after 10 nM insulin treatment for 2 hr in HK2 cells transfected with transfection buffer, control-siRNA and Nox4-siRNA (* = significantly different from control, ° = not significantly different from control).

Results

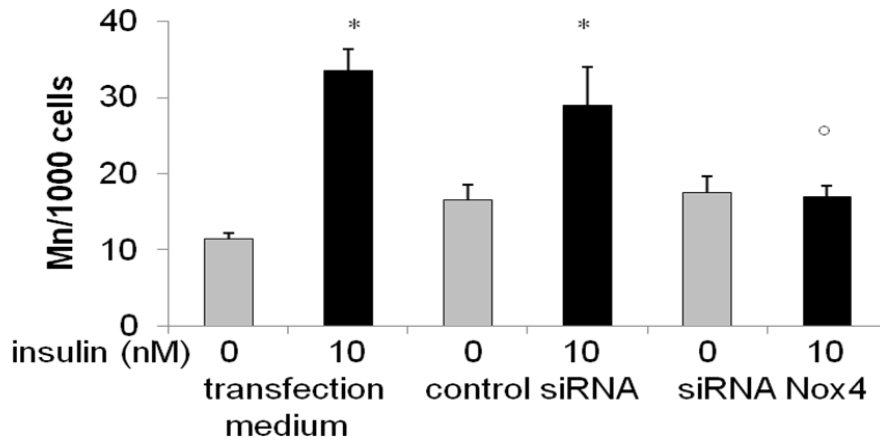


Figure 86: Chromatin damage (Mn/1000 cells) measured as micronucleus frequency after 10 nM insulin treatment for 4 hr in HK2 cells transfected with transfection buffer, control-siRNA, Nox1-siRNA and Nox2-siRNA, and harvested after 20-22 hr, (* = significantly different from control, ° = not significantly different from control).

HK2 cells with knocked down Nox2 did not show reduction in the DNA damage (fig.87).

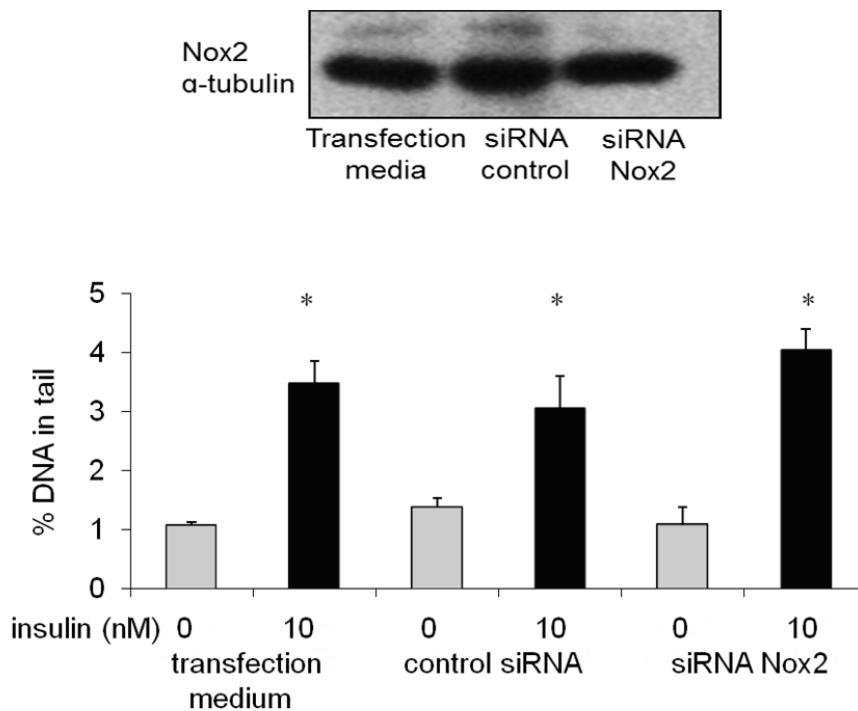


Figure 87: DNA damage measured by the comet assay after 10 nM insulin treatment for 2 hr in HK2 cells transfected with transfection buffer, control-siRNA and Nox2-siRNA (* = significantly different from control, ° = not significantly different from control).

Results

As a result for the stimulation of ROS production through mitochondria and Nox4 activation, oxidation of the DNA can occur. This is demonstrated in HK2 cells by detection of oxidized bases in the FPG assay modification of the comet assay (fig.88).

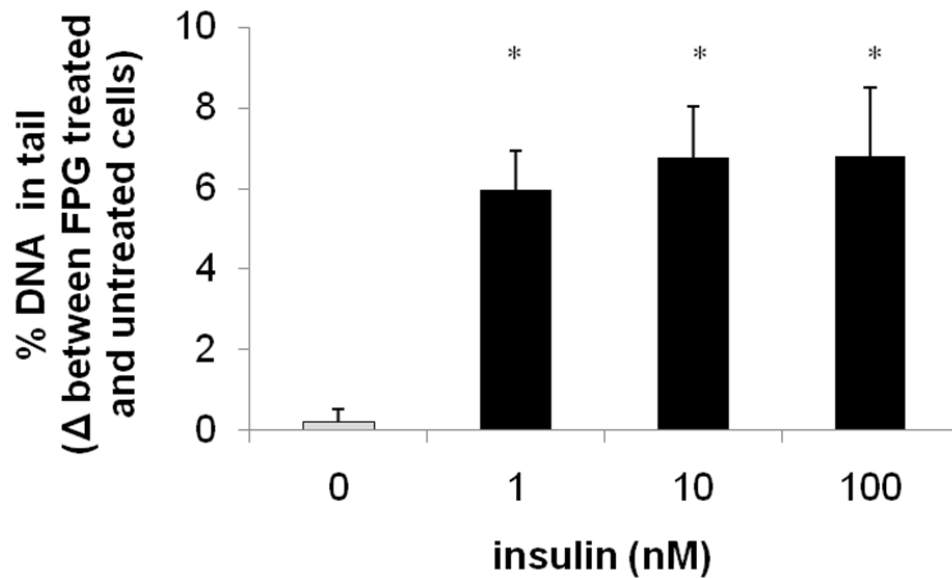


Figure 88: Effect of FPG post treatment on insulin-induced DNA damage in the comet assay in HK2 cells treated with different insulin concentrations for 2 hr (* = significantly different from control).

Results

4.2.8 Zucker Diabetic fatty rats (ZDF)

As an animal model for elevated insulin, lean healthy ZDF rats were subjected to a hyperinsulinemic euglycemic clamp (table 3, lines 1 and 2). In this regard, insulin was infused and glucose was added to prevent hypoglycemia. Blood glucose levels were adjusted to an equal and normal range in all animals, but insulin infusion was designed to result in normal postprandial levels in the control group and to pathophysiological levels in the high insulin group (table 3). ROS were analyzed with DHE staining of kidney slices and ROS production was significantly elevated in the high insulin group. Representing genomic damage, the amount of p53 was elevated in the high insulin group. As a model for diabetes type II, in which levels of insulin and glucose can be elevated, fatty diabetic ZDF rats were analyzed (table 3, line 3). Animal treatment and organ preparation were kept the same as in the lean rats, but glucose as well as insulin were elevated in these animals. In these diabetic rats, oxidative stress and amount of p53 were also elevated compared with the lean normal insulin animals.

Group	Glucose in plasma (mM)		Insulin in plasma (nM)		DHE staining (fold increase over control)	p53 protein
	Fasting	After clamp	Fasting	After clamp		
ZDF lean (normal insulin)	4.22 ± 0.24	4.40 ± 0.53	0.046 ± 0.047	0.28 ± 0.179	1.00 ± 0.15	1.00 ± 0.21
ZDF lean (high insulin)	3.93 ± 0.63 ≠	4.99 ± 0.56 ≠	0.031 ± 0.033 ≠	1.67 ± 0.67 *	1.94 ± 0.56 *	1.50 ± 0.25 *
ZDF fa/fa (diabetic)	7.80 ± 1.39 *	6.16 ± 2.12 ≠	0.363 ± 0.328 *	2.19 ± 1.23 *	2.14 ± 0.48 *	1.62 ± 0.47 *

Table 3: Glucose and insulin concentrations measured in plasma before and after hyperinsulinemic euglycemic clamp, superoxide production in ZDF kidney cryosections incubated for 30 min with the O^{2•-}-reactive probe DHE (10 μM); and quantified by the mean of gray values of DHE fluorescence, and p53 level measured by western blot in ZDF rat kidneys (* = significantly different from low insulin group, ≠ = not significantly different from low insulin group).

Results

To evaluate the influence of treatment with insulin sensitizing medication on the oxidative stress and DNA oxidization in the ZDF rat, we investigated the ROS production and DNA oxidization in the kidney of lean ZDF, ZDF placebo and metformin treated ZDF rats (table 4). Before the clamp procedure, the plasma fasting glucose and insulin levels of the untreated placebo group and the metformin treated group were higher than those of the lean control group (table 4). The ROS production (DHE on cryosections) and the DNA oxidization (8oxdG; LC-MS/MS analysis) were also higher in the placebo and (to a lesser extend) in the metformin group than in the lean control. Due to the infusion of insulin during the hyperinsulinemic clamp procedure that these animals received immediately before sacrifice, the plasma insulin levels were increased in all three groups, but to a lesser extend in the lean group than in the two diabetic (fa/fa) groups (table 4). The concentration of insulin found in the kidney of the animals was higher in the diabetic rats than in the lean controls and the increase was more limited in the metformin group than in the placebo group (table 4).

Group	Glucose in plasma mM		Insulin in plasma (nM)		Insulin in kidney (pg/μg protein)	DHE staining (Fold increase over control)	8-oxodG/10 ⁶ dG
	Fasting	After clamp	Fasting	After clamp			
ZDF lean	3.74 ± 0.74	7.81 ± 2.54	0.027 ± 0.02	1.50 ± 1.03	3.54 ± 1.94	1	2.14 ± 0.09
ZDF fa/fa	7.78 ± 1.38 *	8.07 ± 0.98 °	0.36 ± 0.33 *	2.06 ± 1.41 °	7.62 ± 6.18 °	2.23 ± 0.51 *	9.95 ± 3.50 *
ZDF fa/fa +metformin	10.00 ± 2.01*	7.73 ± 1.60 °	0.26 ± 0.06 ΔΔ	2.04 ± 0.46 ΔΔ	5.92 ± 6.00 ΔΔ	1.40 ± 0.59 Δ	5.13 ± 1.86 Δ

Table 4: Glucose and insulin concentrations measured in plasma before and after hyperinsulinemic euglycemic clamp, HPLC analysis for insulin concentrations in kidney tissue, superoxide production in ZDF kidney cryosections incubated for 30 min with the O^{2•-}-reactive probe DHE (10 μM); and quantified by the mean of gray values of DHE fluorescence, and 8-oxodG level measured by LC-MS/MS in ZDF rat kidneys (* = significantly different from Lean group, ° = not significantly different from Lean group, Δ = significantly different from placebo group, ΔΔ = not significantly different from placebo group).

Results

4.3 Insulin mediated oxidative stress and genomic damage in cells of the hematopoietic system

4.3.1 Insulin-induces oxidative stress and DNA damage in HL60 cells

HL60 the human premyelocytic cells were treated with different concentrations of insulin (0.5 to 10 nM) for 2 hours. A significant increase in the % DNA in tail and the micronucleus frequency was achieved in the comet assay and micronucleus frequency test at ≥ 1 nM insulin treatment (fig.89).

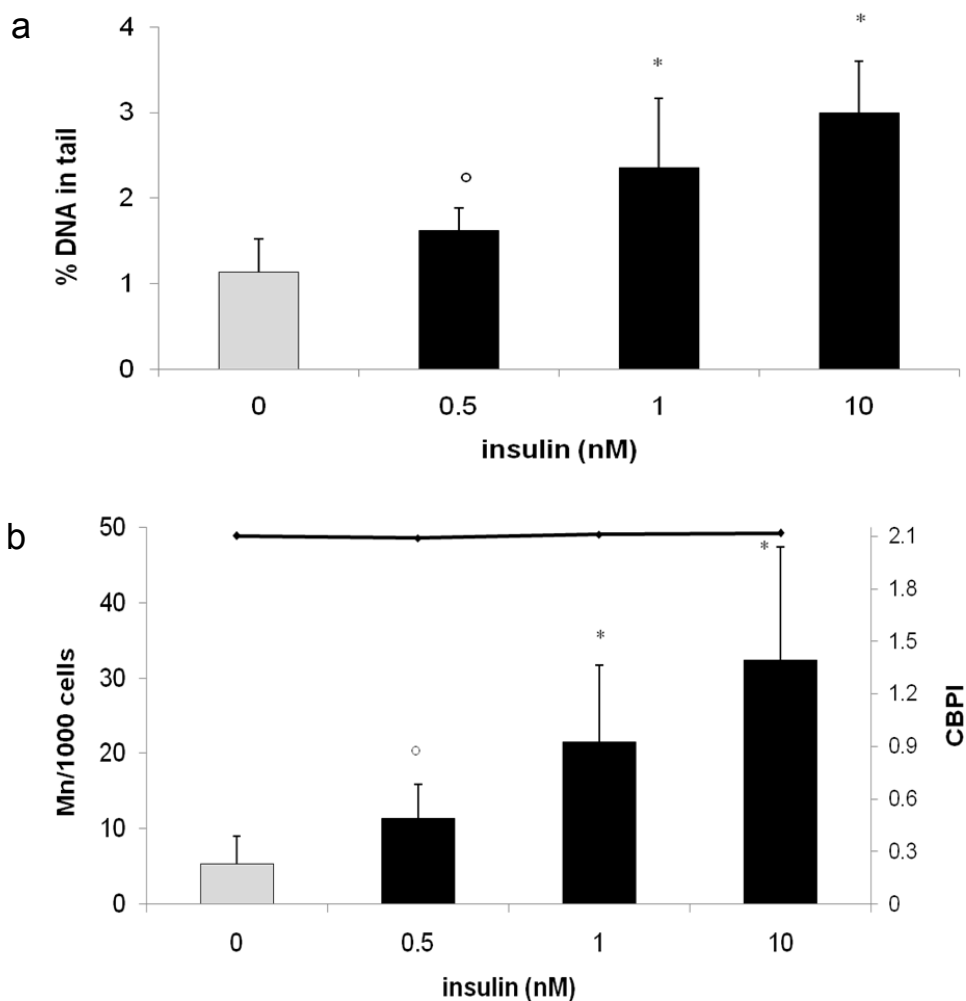


Figure 89: Influence of insulin on insulin-induced alterations in HL60 cells; a) DNA damage (% DNA in tail) in the comet assay after 2hr treatment with different insulin concentrations, and b) micronucleus frequency after 4 hr treatment (plus 22 hours expression time) with different insulin concentrations (Mn-cell = cell containing one or more micronucleus/i) (* = significantly different from control, ° = not-significantly different from control).

Results

The HL60 cell line was found to express mainly the Nox2 isoform of the NADPH oxidase as detected by RT-PCR (fig.90).

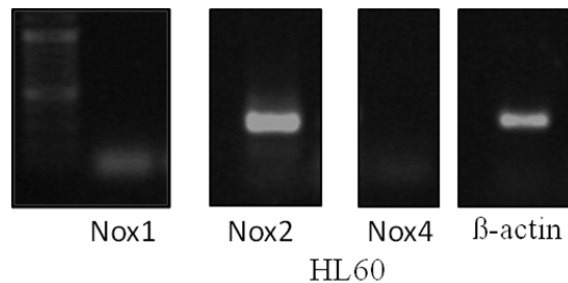


Figure 90: Expression of NADPH oxidase isoforms in HL60 cells.

Using the scavengers and inhibitors; tempol (ROS scavenger), apocynin (NADPH oxidase inhibitor and antioxidant) and wortmannin (PI3K inhibitor) in combination with insulin in the HL60 cell treatment led to the reduction of the observed insulin-mediated DNA damage (fig.91).

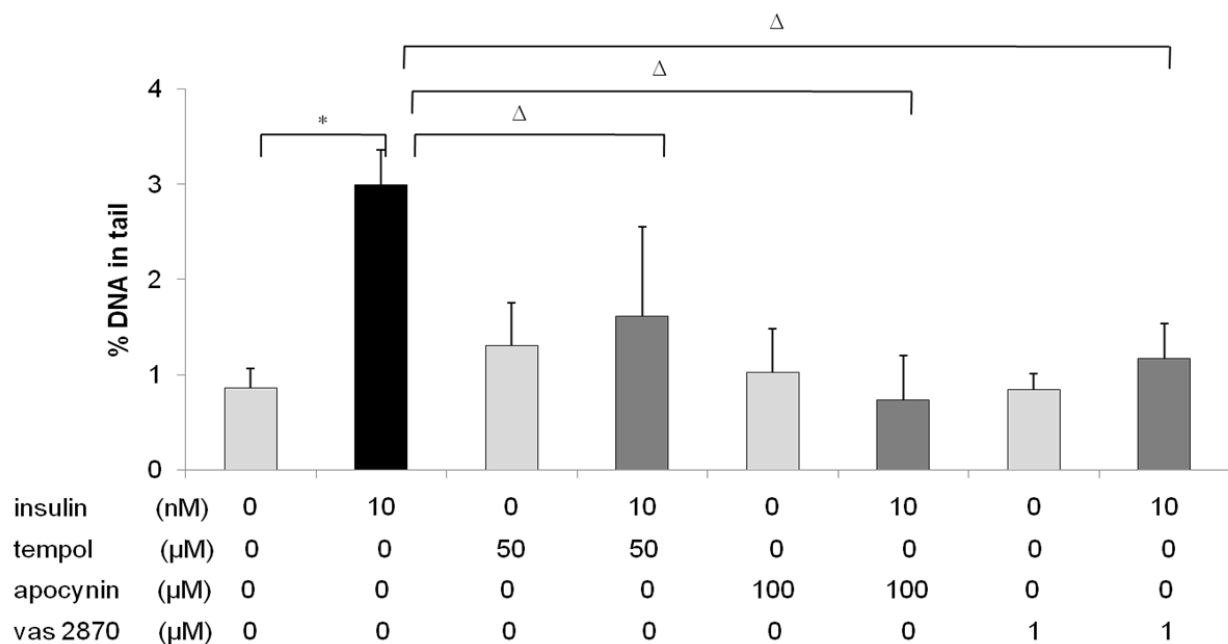


Figure 91: Influence of tempol, apocynin and VAS2870 on insulin-induced alterations in HL60 cells; DNA damage (% DNA in tail) in the comet assay after a 2hr treatment with 10 nM insulin , 50 μ M tempol and the combination, 100 μ M apocynin and the combination , 1 μ M VAS2870 and the combination (* = significantly different from control, Δ = significantly different from insulin).

Results

4.3.2 Insulin-induces DNA damage in peripheral lymphocytes

To further confirm the activity on primary cells, peripheral human lymphocytes were treated with 10 and 100 nM insulin for 24 hours in vitro after stimulation of proliferation with PHA and examined by the two endpoints comet assay and micronucleus frequency test (fig.92). In both endpoints, the cells showed significant induction of DNA damage over control. There was no reduction of the proliferation index (fig.92).

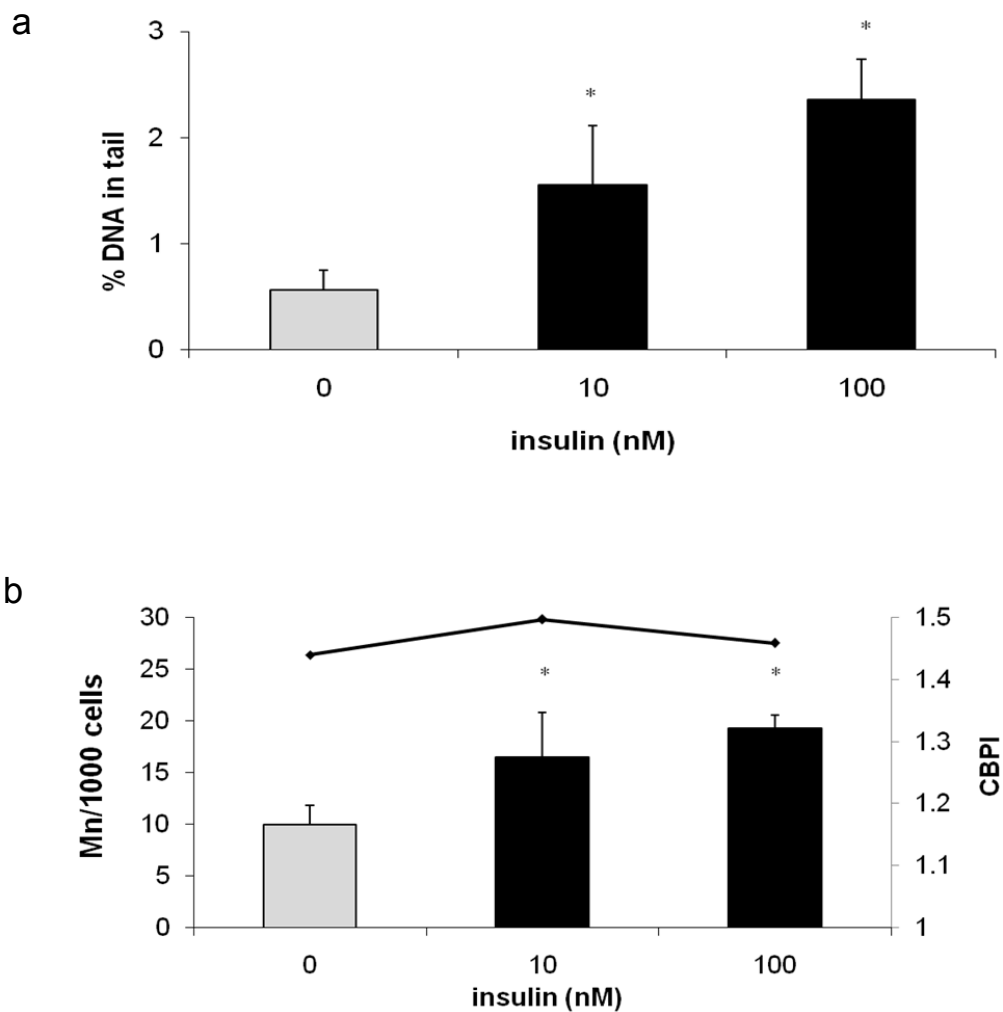


Figure 92: Human peripheral lymphocytes treated in vitro with insulin for 24 hr and examined by comet assay (a) and treated with insulin plus cytochalasin B for 24 hr, analyzed in the micronucleus test (b). In (b), cell proliferation (CBPI) (straight line) is shown on the second y-axis (* = significantly different from control).

Results

4.3.3 Micronucleus frequency elevation in type II diabetes mellitus patients

To evaluate the biological relevance of the in vitro results in the cultured lymphocytes, peripheral lymphocytes from type II diabetes mellitus patients were isolated and examined for the micronucleus formation and compared with the results obtained from healthy individuals' lymphocytes. The diabetic patients showed significant increase in micronucleus formation over the control group (fig.93).

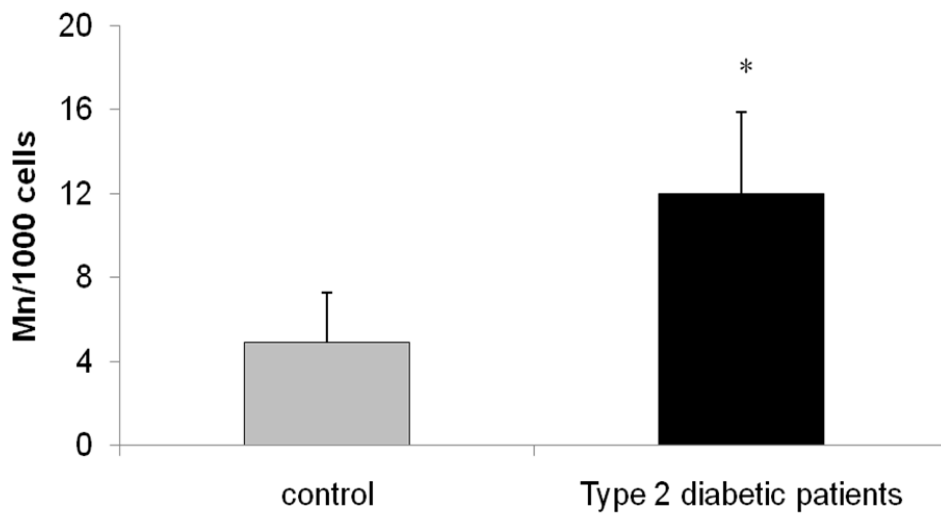


Figure 93: Micronucleus frequency in peripheral blood lymphocytes of healthy control individuals (n=15) and type II diabetic patients (n=35) (* = significantly different from control).

Results

4.4 Insulin-mediated genomic damage in different mammalian cells

Primary rat cells (hepatocytes and fatty tissues) were treated with three different concentrations of insulin (0.01, 0.1 and 2 μ M) for 30 minutes and comet assay analysis revealed an increase in DNA damage in comparison to the solvent control for hepatocytes and fatty tissue cells (table 5). In addition, two human breast cancer cell lines (MCF-7 and BT-474 cells) were treated with different insulin concentrations (0.5 - 100 nM) for 2 hours and they also showed an induction of DNA damage in comet assay (table 5).

Cell type	Insulin concentration					
	0	0.5 nM	1 nM	10 nM	0.1 μ M	2 μ M
	% DNA in tail					
Primary hepatocytes	0.76 \pm 0.01	ND	ND	1.53 \pm 0.00*	4.09 \pm 1.24 *	4.35 \pm 1.27 *
Primary fatty tissues	1.14 \pm 0.20	ND	ND	3.15 \pm 0.00 *	3.20 \pm 0.72 *	3.78 \pm 1.02 *
MCF-7	0.57 \pm 0.14	1.38 \pm 0.18*	1.42 \pm 0.11*	1.59 \pm 0.20*	1.83 \pm 0.11*	ND
BT-474	0.89 \pm 0.40	1.92 \pm 0.03*	2.31 \pm 0.42*	2.37 \pm 0.43*	2.67 \pm 0.52*	ND

Table 5: DNA damage (% DNA in tail) measured with the comet assay after treatment of SD rat primary cells (hepatocytes and fatty tissues)(n=3) with different concentrations of insulin for 30 min. and MCF-7 and BT-474 cell lines after treatment of the cells for 2 hr with different concentrations of insulin, (ND = non determined), (* = significantly different from control).

Discussion

5. Discussion

Oxidative stress reflects an imbalance between the systemic oxidants expressed as reactive species (RS) and a biological system's ability to readily detoxify the reactive intermediates or to repair the resulting damage. Reactive species can affect the macro and micro molecules in the cells such as lipids, protein and DNA. Reaction of the reactive species with the DNA leads to what is called genotoxicity, the term which describes deleterious properties of a substance, acting on cell's genetic material and affecting its integrity. In recent years, and between many genotoxic compounds, researchers highlighted the genotoxicity of endogenous hormones in high levels [62-63, 128]. One of the most important hormones in the body is insulin, which controls different metabolic pathways and plays a critical role in cell proliferation [66]. The production of a large amount of cellular reactive oxygen species by hematopoietic phagocytic cells is essential for host defenses in bactericidal killing [129]. However, more recently it has been appreciated that low levels of cellular oxidants, including superoxide and H_2O_2 , are produced in a rapid temporal response to cellular growth factor and cytokine stimulation and are integral to the regulation of a variety of intracellular signaling pathways [114]. Cellular reactive oxygen species have been shown to be elevated in response to epidermal growth factor, platelet-derived growth factor, transforming growth factor, and other growth factors [110-114] as well as after insulin stimulation [104-106].

Hyperinsulinemia, meaning high insulin blood levels, was reported as a risk factor in development and promotion of different types of cancer [130-132]. The influence of insulin on cancer growth has been widely studied. Observational human studies have reported increased cancer mortality in patients with obesity and type II diabetes, which might be attributable to hyperinsulinemia, elevated IGF-I, or both factors [132-135].

A role for insulin in promoting cancer growth was first recognized by studies in experimental animals. Rats and mice made diabetic with streptozotocin or alloxan (hyperglycemic and insulin deficient) developed less aggressive tumors compared to control animals [136]. Insulin treatment reversed this observation [137]. This could be due to the well-known mitogenic effect of insulin and/or the described production of reactive oxygen species which might lead to genomic damage formation.

Discussion

5.1 Insulin-mediated oxidative stress and DNA damage in mammalian colon cells

Colon cancer was linked to hyperinsulinemia in a rat model, as early as 1996 [138] when the direct promoting effect of insulin on colon carcinogenesis in F344 rats was tested. After azoxymethane initiation and injections of insulin given 5 times/week for 17 weeks, the fraction of rats with colon tumors was greater in rats receiving insulin than in rats receiving saline and the average number of tumors/ rat was also greater. Human epidemiological data seem to hint in the same direction; men with high levels of C-peptide had a 2.7-fold significantly increased the risk of colorectal cancer [139], while Larsson et al. reported in two different studies that diabetic patients have 1.36 and 1.29 fold higher risk of colorectal cancer compared to controls [140]. In 2004, Yang et al conducted a retrospective cohort study among patients with a diagnosis of type II diabetes mellitus and found that chronic insulin therapy significantly increased the risk of colorectal cancer among these patients [141].

Insulin-induced DNA damage in colon cells

Several mechanisms are likely to contribute to the development of colon cancer. To detect whether a DNA-damaging capacity of insulin signaling derived ROS might be one of them, we investigated whether insulin can induce DNA damage in mammalian colon cells in vitro and ex vivo. In HT29 cells, an insulin concentration of 5 nM significantly induced DNA damage after a 2 hours exposure, and after a chronic exposure for 6 days, 0.5-1 nM insulin was able to induce DNA damage. Increasing the insulin concentration to 10 nM shortened the time which required for the DNA damage induction to 5 minutes.

The micronucleus test, one of the most important genotoxicity tests was applied to confirm the induction of DNA damage by insulin, and cells incubated with 1 nM insulin for 4 hours exhibited a significant increase in micronucleus formation, while longer exposure time (6 days) reduced the insulin concentration required for the induction of chromatin damage to 0.5-1 nM, all these observations allow the conclusion that insulin can induce DNA damage if present at sufficient concentration .

Discussion

Tumor protein 53 (p53), can activate DNA repair proteins when DNA has sustained damage and can induce cell cycle arrest at the G₁/S regulation point upon DNA damage recognition. P53 becomes activated in response to different types of stress such as oxidative stress. This activation is marked by two major events. First, the half-life of the p53 protein is increased drastically, leading to a quick accumulation of p53 in stressed cells [142]. Second, a conformational change forces p53 to be activated as a transcription regulator in these cells [143-144]. In our study, p53 accumulation as an indicator of DNA damage and oxidative stress was investigated. Upon treatment of the cells with 10 nM insulin for different durations, p53 started to accumulate after 5 minutes incubation time with 10 nM insulin, and after stimulation of the cells with 0.5 nM insulin for 2 hours, p53 accumulation also observed.

Glucose and insulin are linked physiologically, and due to the presence of the possibility for glucose to interference in the insulin-mediated genotoxicity, different concentrations of glucose were applied to the cells. None of them showed an influence on our observations.

Insulin stimulates ROS production

During the last decade, it has become clearly evident that oxidative stress plays a key role in carcinogenesis, cancer progression, cancer therapy, and normal tissue damage that limits treatment efficacy during cancer therapy. We hypothesized that insulin can stimulate ROS production which then can cause DNA damage. To evaluate this hypothesis, oxidative stress and superoxide induction by insulin was examined in HT29 cells. ROS production is stimulated in the insulin-treated cells after 5 minutes treatment with 10 nM insulin and at 0.5 nM insulin when the exposure time extended to 30 minutes, in agreement with our findings, several authors showed that insulin stimulates ROS production in different tissues and other showed that ROS in physiological level is important in insulin signaling [104-106, 116, 145].

For evaluation of oxidative DNA-damage, a modified version of the comet assay using FPG enzyme was performed. This enzyme enables detection of the major purine oxidation product 8-oxoguanine as well as other altered purines, leading to increased comet formation if oxidative damage is present [4, 146], HT29 cells treated with FPG

Discussion

enzyme showed higher DNA damage in comparison to the untreated cells, confirming the contribution of oxidative DNA damage. The protective effect of tempol and apocynin against insulin induced DNA damage and formation of a superoxide specific product after oxidation of the dye DHE further confirms that the genotoxicity was derived mainly from oxidative stress and mainly superoxide-mediated.

Caco-2 as another models for colon cells and the primary rat colon cells which supporting the relevance for primary tissue as opposed to a more or less transformed cell line, also showed an induction of DNA damage upon treatment with insulin.

5.2 Signaling pathway of insulin genotoxicity in colon cells

Mechanistic pathway started from the insulin receptor

In the investigation of the mechanistic pathway for insulin genotoxicity, we started from the binding of insulin to its receptor or to the insulin-like growth factor1 receptor (IGF-1R); it is well known that insulin at high concentrations can bind to both receptors [134, 147]. Two factors were considered in our investigations,; the insulin concentration and the duration of exposure. In 2005, Li et al showed that insulin in concentrations of less than 5 nM binds selectively to the insulin receptor [147] which is in agreement with our findings where HT29 showed an activation of the insulin receptor at 0.5 nM and higher after 2 hours treatments. The half-life time of the insulin receptor is a few minutes and the binding process starts after 1 minute of exposure to insulin [148], followed by internalization of the receptor-insulin complex by the surrounding membrane forming an endosome. Inside the cell insulin is digested by proteases and the receptors are recycled. The insulin bound to the receptor increases with rising concentrations of free hormone with a non-linear relationship [149] which explains the non-linear response in the pIR level measurement [149]. Thus, active insulin outside the cells has the chance to bind frequently to the receptor. This explains why the genotoxicity and the ROS production were observed over a duration of several hours. Based on observation and the effect of the IR blocker (HNMPA(AM)₃), we can conclude that the insulin receptor is involved in the signaling mechanism of induction of DNA-damage by insulin.

Discussion

Insulin-like growth factor 1 receptor interferes in the insulin-mediated genotoxicity

Insulin concentrations higher than 5 nM enable insulin to bind to the IGF-1R receptor. This was observed to happen for duration of 4 hours after insulin addition as indicated by pIGF-1R level. The reduction in the genomic damage by using the IGF-1R blocker (PPP) confirmed contribution of the IGF-1 receptor in the signaling pathway. In 2010, Peak et al reported that activation of the IGF-1 receptor stimulates ROS production in colon cancer cells [150]. The link between the expression and activity of IGF-1 receptor and ROS was frequently discussed [151-152].

Activation of PI3 kinase and consequently AKT

Binding of insulin to both receptors can activate PI3K either directly by binding to the p85 regulatory subunit, or indirectly via IRS1. The PI3K inhibitor wortmannin reduced the genomic damage induced by insulin, highlighting PI3K as a key enzyme in the signaling towards genomic damage. Insulin activates PI3K, which in turn promotes the synthesis of D3 PPIs. AKT binds to the plasma membrane-associated D3 PPIs via its PH domain, and undergoes phosphorylation at Ser473 (by PDK2) and Thr308 (by PDK1). Activated AKT translocates from the plasma membrane to the cytosol or to the nucleus, where it phosphorylates a wide array of downstream effector proteins [153]. The observed reduction in PI3K/AKT level after longer times of exposure could be due to the activation of p53 which leads to activation of PTEN the deactivator for PI3K and AKT [154].

ROS production

At the step of AKT activation, different succeeding pathways could lead to ROS production. One of them is the direct activation of mitochondria by AKT. AKT was shown for the first time to be localized in mitochondria; upon stimulation of different cell types with insulin, insulin-like growth factor-1, or stress, translocation of AKT to the mitochondria occur within minutes of stimulation, causing increases of nearly eight- to 12-fold in mitochondrial AKT in its phosphorylated, active state [155]. Accordingly, we assumed that insulin activates AKT and enhances its translocation to the mitochondria

Discussion

which leads to stimulation of ROS production especially in the first few minutes of insulin treatment. Our assumption is in agreement with the findings of other studies [155-156]. In fact, the mitochondrial inhibitor rotenone which reduced the insulin mediated effects and the reduced induction of damage in the mitochondri-deprived rho0 cells support the contribution of the mitochondrial ROS in the signaling pathway. Rho0 cells can be established from many cell lines to study the contribution of mitochondria, and have been widely used as a successful model system [157].

On the other hand, insulin mediated ROS in cellular signaling have also been found to be formed by NADPH oxidase [159]. Several inhibitors of NADPH oxidases have been identified, although most of them so far have encountered difficulties for potential application in clinical practice. Apocynin, extracted from *Picrorhizakurroa*, prevents the formation of the active NADPH oxidase complex [160] and has been studied in a number of animal models of asthma, inflammation, and atherosclerosis [161]. However, apocynin is not specific for NADPH oxidases, but is rather a general flavoenzyme inhibitor or antioxidant [160, 162]. As described above, apocynin reduced the insulin induced effects. For a more specific inhibition of NADPH oxidase, 3-benzyl-7-(2-benzoxazolyl)thio-1,2,3-triazolo[4,5-d]pyrimidine (VAS2870) was employed [163-164], both inhibitors reduced the insulin induced DNA damage and both confirmed the involvement of NADPH oxidase enzyme in the signaling pathway. Overall, at least these two cellular sources (mitochondria and NADPH oxidase enzyme) contribute to the insulin induced elevated ROS levels.

In a more detailed specification, Nox1 was found to be the responsible isoform for the insulin-induced oxidative stress leading to oxidative DNA damage in colon cells, Nox1 can be activated by Rac1 which can be activated by AKT [59]. Another possibility which could be suggested in the present context is that the produced mitochondrial ROS leads to activation of PI3K followed by activation of AKT and Rac1 resulting in activation of Nox1; this suggestion would agree with findings of Lee et al [158].

Overall, I showed here for the first time that insulin induces genomic damage in mammalian colon cells through oxidative stress induction (fig. 94).

Discussion

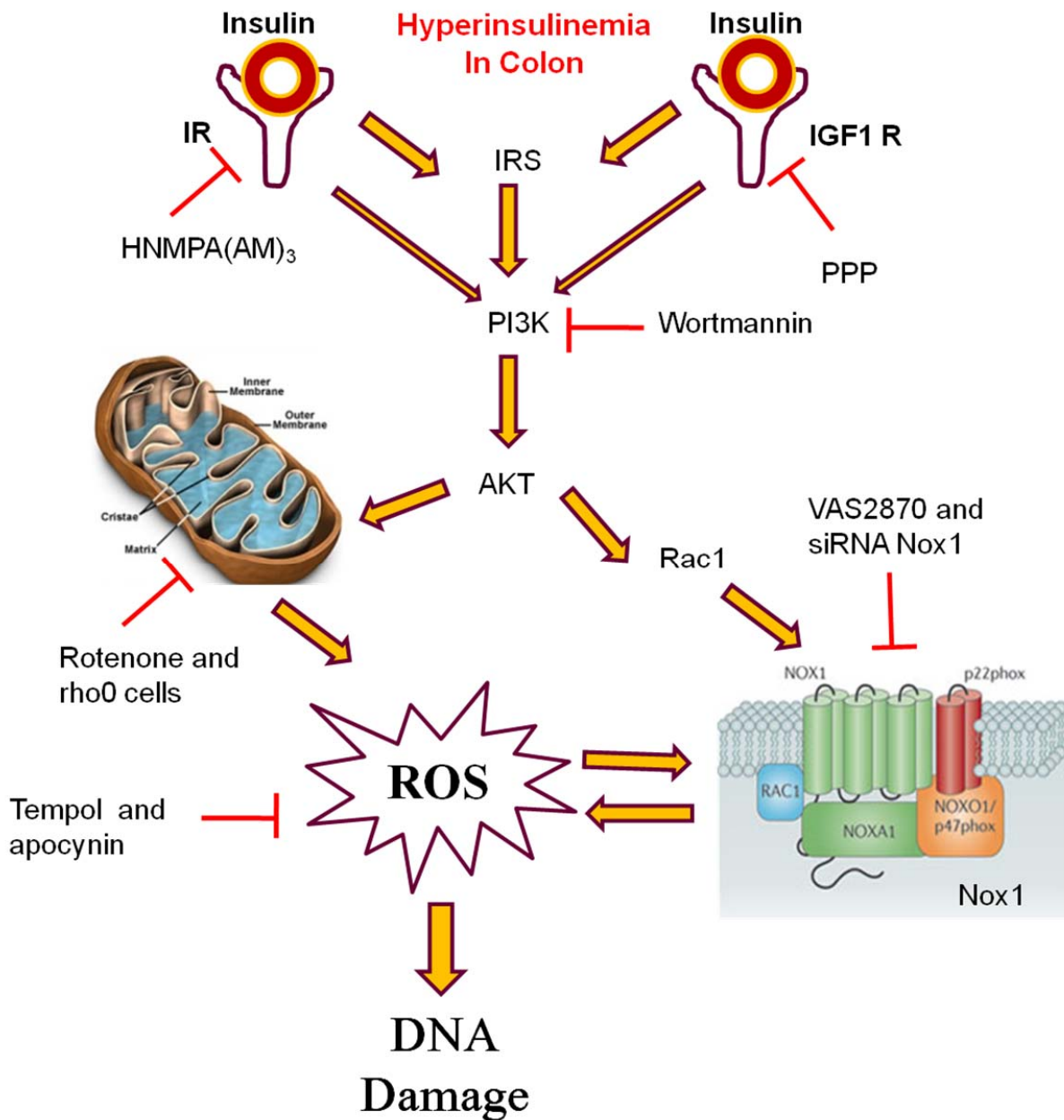


Figure 94: Model of signaling pathways in insulin-induced DNA damage in colon. Binding of insulin to the IR and IGF-1R receptors activates PI3K followed by phosphorylation of AKT, resulting in activation of mitochondria and Rac1 which lead to activation of the Nox1 isoform ending with production of reactive oxygen species which cause DNA damage.

IR = insulin receptor, IGF-1R = insulin-like growth factor 1 receptor, PI3K = Phosphatidylinositol 3-kinase and AKT = protein kinase B, ROS = reactive oxygen species.

Discussion

5.3 Insulin-mediated oxidative stress and DNA damage in mammalian kidney cells

A growing body of evidence found that having diabetes or signs of insulin resistance and hyperinsulinemia may lead to an increased risk of certain cancers. The connection is strongest among certain types of cancers, including kidney, pancreatic and colorectal [81, 89-90].

Insulin-induces DNA damage and oxidative stress in kidney cells

In the present study, insulin-induced genomic damage and oxidative stress were investigated in kidney cells in vitro and in vivo and we found a significant induction of damage with ≥ 5 nM insulin in LLC-PK1 and HK2 cells. The genomic damage did not depend on the presence of serum in the culture medium or the amount of glucose within the tested glucose range.

As mentioned before, the stimulation of ROS production can lead to deleterious effects on the cells and in agreement with this, superoxide radicals were produced by the tested cells in our investigation upon treatment with insulin. These radicals were scavenged by tempol, which acts mainly on superoxide anions [165]. The antioxidant flavoenzyme and mitochondrial inhibitor apocynin [162, 166] also reduced the ROS production. The damaging effects of ROS on DNA range from oxidized bases to single and double strand breaks [42]. Oxidized DNA bases as well as single or double strand breaks can result in gene or chromosomal mutations. In accordance with that, tempol and apocynin also prevented the genotoxicity of insulin in the comet assay and micronucleus frequency test, suggesting that the genotoxicity was superoxide-mediated.

5.4 Signaling pathway for insulin genotoxicity in kidney cells

Insulin at low concentrations (≤ 5 nM) is thought to react specifically with the insulin receptor [147]. Since we observed DNA-damage already at this concentration, it should be mediated by the insulin receptor. This idea was confirmed by different approaches, the measuring of pIR level in cells treated with insulin and the application of the insulin receptor antagonist HNMPA(AM)₃. Both approaches revealed that insulin genotoxicity

Discussion

starts with the activation of insulin receptor. However, this inhibitor may also interact with the IGF-1 receptor; since the two receptors are closely related tyrosine kinases [167-168].

Insulin at high concentrations may also bind to the IGF-1 receptor [169]. Therefore, we measured the pIGF-1R level after insulin treatment and also applied a blocker for the IGF-1 receptor, PPP, which has been found to react only with the IGF-1 receptor specifically [170-172]. pIGF-1R level was found to be elevated and blocking of that receptor also reduced the observed effects. At least in vitro and at higher concentrations, both receptors and their pathways seem to be involved in the DNA-damage induction.

In both signaling pathways, PI3K is the key enzyme. The ability of the PI3K inhibitor wortmannin to reduce the insulin mediated ROS production and genomic damage further demonstrated the involvement of these pathways. In addition, insulin mediated phosphorylation of AKT through PI3K was demonstrated and p53 accumulation indicated elevated DNA-damage.

PI3K was found to activate AKT which plays an important role in the mitochondrial ROS production. Mitochondria represent a cellular source of superoxide. Rotenone, a mitochondrial electron transport inhibitor, reduced the insulin mediated effects in LLC-PK1 cells and the Rho0 cells showed reduction in the DNA damage upon the treatment with insulin. Therefore, mitochondria may also be involved in the pathway for induction of genotoxicity by insulin.

One of the enzyme complexes known to produce superoxide are NADPH oxidases that are downstream of PI3K in the signaling pathway [115]. Again, the genotoxicity of insulin was reduced significantly by applying the NADPH inhibitor VAS2870.

In kidney cells, we found that Nox4 is the responsible NADPH isoform for ROS production upon insulin stimulation, the same observations were reported in other studies [59, 173]. It is noted that there is evidence showing that NADPH oxidase, although a ROS producer itself, can be activated in turn by ROS molecules. In vascular smooth muscle cells and fibroblasts, Li et al. have demonstrated that exogenous hydrogen peroxide acutely activated cellular superoxide production via NADPH oxidase

Discussion

[174]. Similar effects of hydrogen peroxide were also observed in isolated mouse pulmonary arteries [159, 175].

In this present study, it was assumed that the ROS production starts in the first few minutes by activation of the mitochondrial ROS production followed by activation of the NADPH oxidase isoform. A cross-talk between NADPH oxidase and mitochondria has been suggested [158]. The activation of both directions is resulting in DNA oxidization which was observed by the application of the FPG modification of the comet assay in HK2 cells.

Treatment of primary cells with insulin in vitro also resulted in the induction of genomic damage, supporting the relevance for primary tissue as opposed to a more or less transformed cell line.

5.5 Insulin-mediated oxidative stress and DNA damage in ZDF rat

It is not trivial to test the influence of insulin in vivo without affecting the blood glucose level, because these two are physiologically correlated. However, elevated glucose level may also induce oxidative stress. The best way to keep glucose constant while insulin is elevated is to apply a hyperinsulinemic-euglycemic clamp which is considered the "gold standard" method for assessing insulin action in vivo. The clamp procedure was performed with healthy, lean ZDF rats. With normal and equal blood glucose levels in all animals, the high insulin animals showed higher ROS production and p53 accumulation in the kidneys than the normal insulin animals after the clamp procedure. This clearly supports the ability of insulin to induce oxidative stress and genomic stress in vivo. The kidney of obese diabetic ZDF rats also exhibited a similar increase in ROS and p53. In these diabetic rats, the increase may be due to the elevated glucose as well as to the increased insulin levels. Interpretation is much more difficult and effects cannot be attributed to insulin alone, but the model nevertheless is useful to demonstrate the elevation of ROS and genomic damage in diabetes type II.

To evaluate the effect of treatment, the most common antidiabetic medication metformin was used to treat the ZDF placebo rat. Metformin is an insulin sensitizer to which the body reacts by lowering the insulin output and a decreased insulin level is reached, as

Discussion

well as a decreased blood sugar level. Many studies reported that metformin can reduce the cancer risk in diabetic and obese patients [134, 176-177], in the present study kidneys from ZDF rats (placebo and treated with metformin), a model for diabetes, obesity and hyperinsulinemia, were examined for oxidative stress and oxidized DNA expressed as 8-oxodG. Many indirect informations exist indicating that oxidation of DNA can play a causal role in the carcinogenic process [133]. Because of its propensity for attack by reactive oxygen species, products of guanine oxidation have been the most extensively studied, and the mutagenic potential of guanine oxidation products has been well characterized [178]. 8-hydroxy-2-deoxyguanosine (8-oxo-dG), is the most prevalent promutagenic oxidation product of guanine, which can give rise to G-to-T transversion mutations in key genes known to be involved in the development of cancer [179-180]. Evidence has recently been published documenting the accumulation of 8-oxo-dG in some tissues of knockout mice lacking 2 of the DNA glycosylases, a multifold increase in cancer rates in some of the tissues in which 8-oxo-dG accumulates; and a high frequency of occurrence, within those cancers, of the predicted G-to-T transversion mutations that activate an oncogene (K-ras) associated with cancer development in those tissues [181-182]. Collectively, these observations provide a strong basis for the hypothesis that the concentration of 8-oxo-dG in genomic DNA is a biomarker for cancer risk. The rationale underlying this hypothesis is that higher concentrations of this promutagenic lesion in cellular DNA favor higher rates of mutation and that higher rates of mutation over time increase the risk for cancer.

In the two rat groups (ZDF placebo and ZDF treated with metformin) an elevation in the oxidative stress, 8-oxodG as well as the kidney tissular insulin level was observed in comparison to the healthy lean group. A similar insulin increase in plasma levels was observed in this model without the euglycemic clamp by other groups [183]. In this model, metformin not only reduced kidney tissular insulin levels but also reduced oxidative stress and oxidative DNA-damages in comparison to ZDF obese rats treated with placebo. The male ZDF rat model mimics the complex phenotype of patients with type II diabetes, meaning that these rats also presented hyperglycemia. However, no literature data are available for comparison of our oxidative stress or genomic damage results in this model while data from diabetic patients are available which showed a

Discussion

significant increase in urine and plasma 8-oxodG level in comparison with the healthy individuals [184-186].

To sum up this part, this study showed for the first time that insulin induces genomic damage in kidney cells (fig. 95). The lowest tested and lowest active concentration in vitro was 5 nM in kidney cells. The concentration of insulin in the plasma of the rats under clamp reached 1.67 nM (high insulin group; up to 2.3 nM in individual animals). In vitro, the tested concentration was applied once, but in vivo the measured concentrations represent blood levels of circulating fresh insulin over some time. Therefore, an exact comparison between the concentrations of the in vitro and the in vivo situation cannot yet be made based on our experiments, but the order of magnitude in which the in vitro effects were observed can most likely be reached under some conditions of hyperinsulinemia.

Discussion

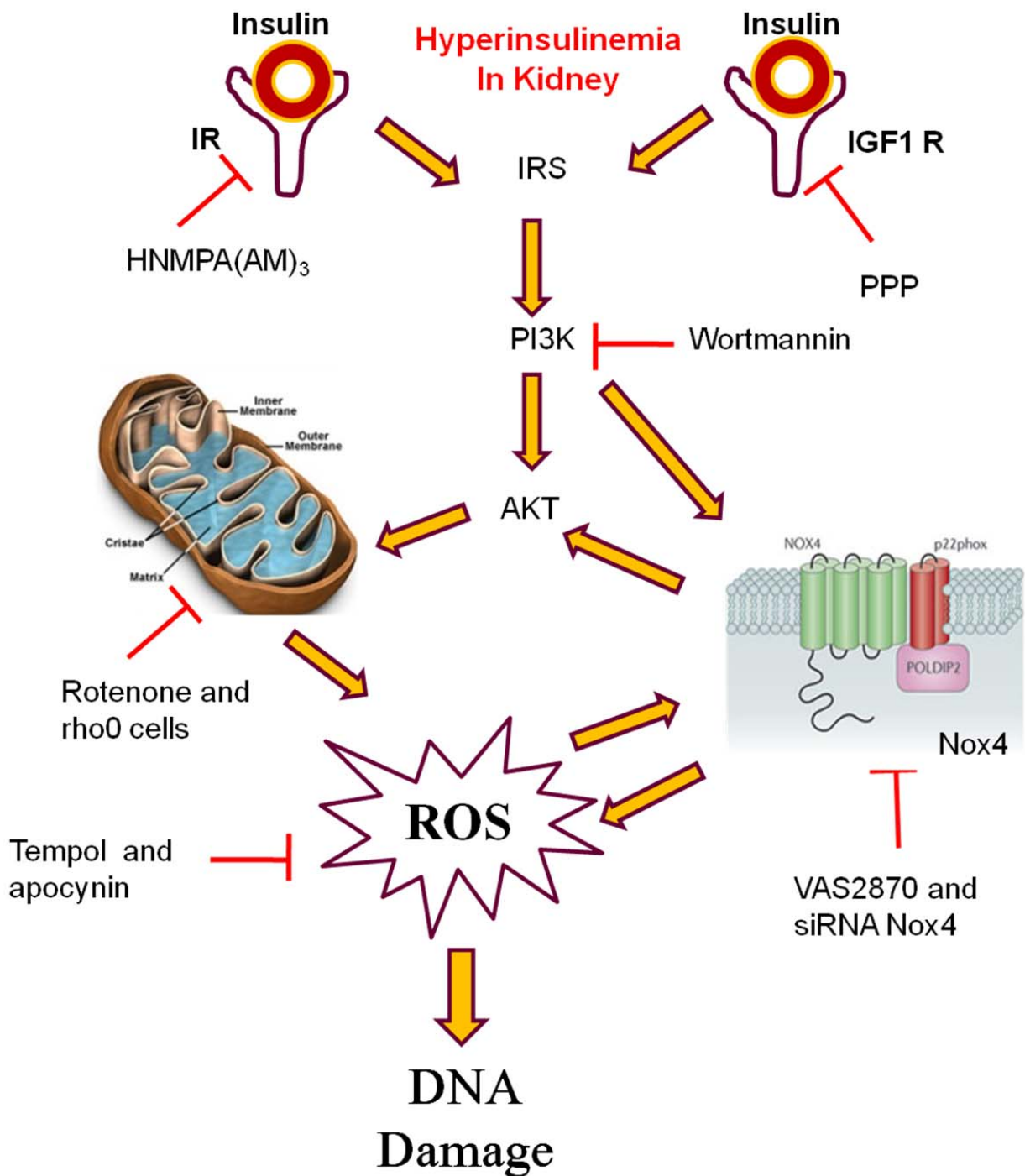


Figure 95: Model of signaling pathway in insulin-induced DNA damage in kidney cells. Binding of insulin to the IR and IGF-1R receptors activates PI3K which activates AKT and Nox4, AKT activation resulting in activation of mitochondria, the two pathways ending with production of reactive oxygen species which cause DNA damage.

IR = insulin receptor, IGF-1R = insulin-like growth factor 1 receptor, PI3K = Phosphatidylinositol 3-kinase and AKT = protein kinase B, ROS = reactive oxygen species.

Discussion

5.6 Insulin-induced DNA damage in HL60 , cultured peripheral lymphocyte and type II diabetic patients' lymphocytes

In the hemopoietic system, lymphocytes are the most common cells which are examined for the genomic damage. Many studies differentiated between healthy individuals and patients through examination of their peripheral lymphocytes, especially in cancer patients [31, 187-188],

In this study, the effect of insulin was investigated in HL60 human premyelocytic cells as well as in cultured human lymphocytes. The results showed that insulin can induce oxidative stress and genomic damage in the hemopoietic system cells. In this study as well as in other studies, high frequency of micronucleus formation in the peripheral lymphocytes of the obese as well as the diabetic patients who exhibit both hyperinsulinemia and hyperglycemia was observed [189-190]. To abolish the influence of glucose, peripheral lymphocytes isolated from healthy persons were treated with insulin in vitro and a DNA damage was observed under the treatment conditions which agrees with observations by Djelic [191]. In humans, a condition known as polycystic ovarian syndrome (PCOS) is associated with elevated insulin, but the affected individuals exhibit normal glucose levels. A higher genomic damage in the peripheral lymphocytes of such patients, detected as elevated micronucleus frequency and hydroxydeoxyguanosine level in plasma, was found [192-193], which further supports our findings.

Normal healthy human plasma insulin concentrations are in the order of 0.04 nM after overnight fasting and increase to less than about 0.2 nM after a meal. Pathophysiological levels can reach 1 nM and can stay above 0.2 nM for the majority of the daytime which is close to the active insulin concentrations determined in the present study. Whether the observed effects also occur in vivo and whether they actually initiate or promote tumor formation remains to be determined. However, if proof of that can be obtained, the experiments with inhibitors indicate chances for pharmacological intervention applying antioxidants or enzyme inhibitors. It will not be the aim to reduce ROS in any case or as much as possible because ROS have now been recognized as important signaling molecules and participants in immune defense, but a reduction to

Discussion

physiological levels instead of pathophysiological levels in the context of a disease associated with ROS overproduction might be beneficial.

Although the mechanisms of insulin mediated DNA damage still require further confirmation for the in vivo models or the human situation, I investigated for the first time that pathophysiological levels of insulin can cause oxidative stress and DNA damage which might render a factor in the initiation and /or promotion of malignancies.

Summary

6. Summary

Hyperinsulinemia, a condition with excessively high insulin blood levels, is related to an increased cancer incidence. Diabetes mellitus, metabolic syndrome, obesity and polycystic ovarian syndrome are the most common of several diseases accompanied by hyperinsulinemia. Since an elevated cancer risk especially for colon and kidney cancers, was reported for those patients, we investigated for the first time the induction of genomic damage by insulin mainly in HT29 (human colon cells), LLC-PK1 (pig kidney cells), HK2 (human kidney cells) and peripheral lymphocytes, and to confirm the genotoxicity of insulin in other cells from different tissues. To ascertain that the insulin effects were not only limited to permanent cell lines, rat primary colon, kidney, liver and fatty tissue cells were also studied. To connect the study and the findings to in vivo conditions, two in vivo models for hyperinsulinemia were used; Zucker diabetic fatty rats in a lean and diabetic state infused with different insulin concentrations and peripheral lymphocytes from type 2 diabetes mellitus patients.

First, the human colon adenocarcinoma cells (HT29) showed significant elevation of DNA damage using comet assay and micronucleus frequency analysis upon treatment with 5 nM insulin in standard protocols. Extension of the treatment to 6 days lowered the concentration needed to reach significance to 0.5-1 nM. Insulin enhanced the cellular ROS production as examined by the oxidation of the dyes 2',7'-dichlorodihydrofluorescein diacetate (H2DCF-DA) and dihydroethidium (DHE). The FPG modified comet assay and the reduction of damage by the radical scavenger tempol connected the insulin-mediated DNA damage to ROS production. To investigate the sources of ROS upon insulin stimulation, apocynin and VAS2870 as NADPH oxidase inhibitors and rotenone as mitochondrial inhibitor were applied in combination with insulin and all of them led to a reduction of the genomic damage.

Investigation of the signaling pathway started by evaluation of the binding of insulin to its receptor and to the IGF-1 receptor. The results showed the involvement of both receptors in the signaling mechanism. Following the activation of both receptors, PI3K activation occurs leading to phosphorylation of AKT which in turn activates two pathways for ROS production, the first related to mitochondria and the second through

Summary

activation of Rac1 , resulting in the activation of Nox1. Both pathways could be activated through AKT or through the mitochondrial ROS which in turn could activates Nox1.

Studying another human colon cancer cell line, Caco-2 and rat primary colon cells in vitro confirmed the effect of insulin on cellular chromatin. We conclude that pathophysiological levels of insulin can cause DNA damage in colon cells, which may contribute to the induction or progression of colon cancer.

Second, in kidney cells, insulin at a concentration of 5 nM caused a significant increase in DNA damage in vitro. This was associated with the formation of reactive oxygen species (ROS). In the presence of antioxidants, blockers of the insulin and IGF-1 receptors, and a phosphatidylinositol 3-kinases (PI3K) inhibitor, the insulin mediated DNA damage was reduced. Phosphorylation of AKT was increased and p53 accumulated. Inhibition of the mitochondrial and NADPH oxidase related ROS production reduced the insulin mediated damage. In primary rat cells insulin also induced genomic damage.

HK2 cells were used to investigate the mechanistic pathway in the kidney The signaling is identical to the one in the colon cells until the activation of the mitochondrial ROS production, because after the activation of PI3K activation of Nox4 occurs at the same time across talk between mitochondria and Nox4 activation has been suggested and might play a role in the observed effects.

In the in vivo model, kidneys from healthy, lean ZDF rats, which were infused with insulin to yield normal or high blood insulin levels, while keeping blood glucose levels constant, the amounts of ROS and p53 were elevated in the high insulin group compared to the control level group. ROS and p53 were also elevated in diabetic obese ZDF rats. The treatment of the diabetic rats with metformin reduced the DNA oxidation measured as 8-oxodG as well as the ROS production in that group.

HL60 the human premyelocytic cells and cultured lymphocytes as models for the hemopoietic system cells showed a significant induction for DNA damage upon treatment with insulin. The diabetic patients also exhibited an increase in the micronucleus formation over the healthy individuals.

In the present study, we showed for the first time that insulin induced oxidative stress resulting in genomic damage in different tissues, and that the source of the produced

Summary

ROS differs between the tissues. If the same mechanisms are active in patients, hyperinsulinemia might cause genomic damage through the induction of ROS contributing to the increased cancer risk, against which the use of antioxidants as well as mitochondrial and NADPH oxidase inhibitors might exert protective effects with cancer preventive potential under certain conditions.

Normal healthy human plasma insulin concentrations are in the order of 0.04 nM after overnight fasting and increase to less than about 0.2 nM after a meal. Pathophysiological levels can reach 1 nM and can stay above 0.2 nM for the majority of the daytime yielding conditions close to the insulin concentrations determined in the present study. Whether the observed effects also occur in vivo and whether they actually initiate or promote tumor formation remains to be determined. However, if proof of that can be obtained, our experiments with inhibitors indicate chances for pharmacological intervention applying antioxidants or enzyme inhibitors. It will not be the aim to reduce ROS in any case or as much as possible because ROS have now been recognized as important signaling molecules and participants in immune defense, but a reduction to physiological levels instead of pathophysiological levels in the context of a disease associated with ROS overproduction might be beneficial.

Zusammenfassung

7. Zusammenfassung

Hyperinsulinämie, ein Zustand mit sehr hohen Blutspiegeln an Insulin, ist mit einer erhöhten Krebsinzidenz verbunden. Diabetes mellitus, das metabolische Syndrom, Adipositas und das polyzystische Ovarialsyndrom sind die häufigsten Krankheiten, die mit Hyperinsulinämie einhergehen. Da ein erhöhtes Krebsrisiko insbesondere für Krebserkrankungen des Dickdarms und der Niere beobachtet wurde, untersuchten wir erstmals die Induktion von Genomschäden durch Insulin in HT29-Zellen (humane Dickdarmzellen), LLC-PK1-Zellen (Nierenzellen vom Schwein), HK2-Zellen (humane Nierenzellen) und peripheren humanen Lymphozyten. Um die Genotoxizität von Insulin zu bestätigen, wurden auch andere Zellen aus unterschiedlichen Geweben untersucht. Um sicherzustellen, dass die Effekte durch Insulin nicht auf permanente Zelllinien beschränkt sind, wurden außerdem primäre Rattenzellen aus Dickdarm, Niere, Leber und Fettgewebe untersucht. Um die Befunde auf die in-vivo-Situation übertragen zu können, kamen zwei Hyperinsulinämie-Modelle zum Einsatz: mit Insulin infundierte ZDF-Ratten (Zucker Diabetic Fatty Rats) und periphere Lymphozyten von Patienten mit Diabetes Typ 2.

Zuerst konnte in humanen Adenokarzinomzellen des Dickdarms (HT29) eine signifikante Erhöhung des DNA-Schadens in Standard-Protokollen des Comet Assays und des Mikrokerntests nach Behandlung mit 5 nM Insulin gezeigt werden. Bei Verlängerung der Behandlungszeit auf 6 Tage wurden signifikante Effekte bereits ab 0,5 nM beobachtet. Insulin erhöhte die zelluläre ROS-Produktion, die als Oxidation der Farbstoffe 2',7'-Dichlorodihydrofluoresceindiacetat (H₂DCF-DA) und Dihydroethidium (DHE) nachgewiesen wurde. Befunde aus dem FPG-modifizierten Comet Assay und das Ergebnis, dass der Radikalfänger Tempol die Zellen schützte stellen die Verbindung zwischen Insulin-verursachtem DNA-Schaden und ROS Produktion her. Um die ROS-Quelle nach Stimulation mit Insulin zu untersuchen, wurden Apocynin und VAS2870 als NADPH-Oxidase-Inhibitoren und Rotenon als Inhibitor der Mitochondrien mit Insulin kombiniert. Alle diese Stoffe reduzierten den Genomschaden.

Zur Charakterisierung der Signalwege wurde zunächst die Bindung von Insulin an seinen Rezeptor und an den IGF1-Rezeptor untersucht. Beide Rezeptoren sind an der Signaltransduktion beteiligt. Nach Aktivierung der Rezeptoren wird die PI3K aktiviert,

Zusammenfassung

dies führt zur Phosphorylierung von AKT. Dadurch werden zwei Wege zur ROS-Produktion aktiviert, der erste involviert die mitochondriale Atmungskette, der zweite agiert durch Rac1-Aktivierung. Letzteres resultiert in der Aktivierung der NADPH-Oxidase Isoform Nox1.

Der Effekt von Insulin auf zelluläres Chromatin konnte in einer weiteren humanen Dickdarmkrebs-Zelllinie und in primären Dickdarmzellen der Ratte *in vitro* bestätigt werden. Wir schlussfolgern aus diesen Ergebnissen, dass pathophysiologische Insulin-Blutspiegel DNA-Schäden im Dickdarm verursachen können. Dies könnte zur Induktion oder Progression von Dickdarmkrebs beitragen.

Weiterhin verursachte Insulin bei einer Konzentration von 5 nM einen signifikanten Anstieg von DNA-Schäden *in vitro*. Dies war verbunden mit der Bildung von reaktiven Sauerstoffspezies (ROS). Bei Anwesenheit von Antioxidantien, von Inhibitoren des Insulin-Rezeptors bzw. des IGF-1-Rezeptors und eines Phosphatidylinositol-3-Kinase (PI3K)-Inhibitors war der Insulin-vermittelte DNA-Schaden reduziert. Phosphorylierung von AKT war erhöht und das Protein P53 akkumulierte. Inhibierung der ROS-Produktion der Mitochondrien bzw. der NADPH-Oxidase reduzierte den Insulin-vermittelten Schaden. In primären Rattenzellen induzierte Insulin ebenfalls Genomschaden.

HK2-Zellen wurden zur Untersuchung der mechanistischen Signalwege in der Niere eingesetzt. Die Signalwege entsprechen denen der Dickdarmzellen bis zur Aktivierung der ROS-Produktion in den Mitochondrien. Als Folge der Aktivierung von PI3K wird Nox4 aktiviert. Eine Verbindung zwischen Mitochondrien und Nox4-Aktivierung wird vorgeschlagen.

Als *in-vivo*-Modell wurden gesunde ZDF-Ratten mit Insulin infundiert, um normale bzw. erhöhte Insulin-Blutspiegel bei konstanten Glukose-Blutspiegeln zu erreichen. In den Nieren war der Gehalt an ROS und an P53 in der Gruppe mit erhöhten Insulin-Blutspiegeln im Vergleich zur Kontrolle erhöht. ROS und P53 waren ebenfalls in den diabetischen und adipösen ZDF-Ratten erhöht. Die Behandlung der diabetischen Ratten mit Metformin reduzierte die DNA-Oxidation, die in Form von 8-oxodG bestimmt wurde, und die ROS-Produktion in dieser Gruppe.

Zusammenfassung

HL60-Zellen und kultivierte Lymphozyten als Modelle für das hämatopoetische System zeigten eine signifikante Induktion von DNA-Schäden nach Behandlung mit Insulin. Diabetes-Patienten zeigten eine erhöhte Mikrokern-Bildung im Vergleich zu gesunden Probanden.

In der vorliegenden Studie konnten wir erstmals zeigen, dass Insulin-induzierter oxidativer Stress zu Genomschaden führt, und dass in unterschiedlichen Geweben ROS aus verschiedenen Quellen stammten. Falls diese Mechanismen auch in Patienten auftreten, könnte Hyperinsulinämie durch ROS-Induktion zu Genomschaden führen und damit zu einem erhöhten Krebsrisiko beitragen. Unter bestimmten Bedingungen könnten Antioxidantien bzw. Inhibitoren der Mitochondrien oder der NADPH-Oxidase protektive Effekte ausüben.

References

References

1. Ames, B.N., J. McCann, and E. Yamasaki, *Methods for detecting carcinogens and mutagens with the Salmonella/mammalian-microsome mutagenicity test*. Mutat Res, 1975. **31**(6): p. 347-64.
2. Gatehouse, D., et al., *Recommendations for the performance of bacterial mutation assays*. Mutat Res, 1994. **312**(3): p. 217-33.
3. Oda, Y., et al., *Evaluation of the new system (umu-test) for the detection of environmental mutagens and carcinogens*. Mutat Res, 1985. **147**(5): p. 219-29.
4. Collins, A.R., *The comet assay for DNA damage and repair: principles, applications, and limitations*. Mol Biotechnol, 2004. **26**(3): p. 249-61.
5. Cook, P.R., I.A. Brazell, and E. Jost, *Characterization of nuclear structures containing superhelical DNA*. J Cell Sci, 1976. **22**(2): p. 303-24.
6. Ostling, O. and K.J. Johanson, *Microelectrophoretic study of radiation-induced DNA damages in individual mammalian cells*. Biochem Biophys Res Commun, 1984. **123**(1): p. 291-8.
7. Koppen, G. and K.J. Angelis, *Repair of X-ray induced DNA damage measured by the comet assay in roots of Vicia faba*. Environ Mol Mutagen, 1998. **32**(3): p. 281-5.
8. Singh, N.P., et al., *A simple technique for quantitation of low levels of DNA damage in individual cells*. Exp Cell Res, 1988. **175**(1): p. 184-91.
9. Olive, P.L., J.P. Banath, and R.E. Durand, *Heterogeneity in radiation-induced DNA damage and repair in tumor and normal cells measured using the "comet" assay*. Radiat Res, 1990. **122**(1): p. 86-94.
10. Collins, A.R., et al., *The comet assay: what can it really tell us?* Mutat Res, 1997. **375**(2): p. 183-93.
11. Collins, A.R. and M. Dusinska, *Oxidation of cellular DNA measured with the comet assay*. Methods Mol Biol, 2002. **186**: p. 147-59.
12. Olive, P.L., D. Wlodek, and J.P. Banath, *DNA double-strand breaks measured in individual cells subjected to gel electrophoresis*. Cancer Res, 1991. **51**(17): p. 4671-6.
13. Collins, A.R., S.J. Duthie, and V.L. Dobson, *Direct enzymic detection of endogenous oxidative base damage in human lymphocyte DNA*. Carcinogenesis, 1993. **14**(9): p. 1733-5.
14. Collins, A.R., et al., *UV-sensitive rodent mutant cell lines of complementation groups 6 and 8 differ phenotypically from their human counterparts*. Environ Mol Mutagen, 1997. **29**(2): p. 152-60.
15. Collins, A.R., M. Dusinska, and A. Horska, *Detection of alkylation damage in human lymphocyte DNA with the comet assay*. Acta Biochim Pol, 2001. **48**(3): p. 611-4.
16. McGlynn, A.P., et al., *The bromodeoxyuridine comet assay: detection of maturation of recently replicated DNA in individual cells*. Cancer Res, 1999. **59**(23): p. 5912-6.
17. Gedik, C.M., S.W. Ewen, and A.R. Collins, *Single-cell gel electrophoresis applied to the analysis of UV-C damage and its repair in human cells*. Int J Radiat Biol, 1992. **62**(3): p. 313-20.
18. Santos, S.J., N.P. Singh, and A.T. Natarajan, *Fluorescence in situ hybridization with comets*. Exp Cell Res, 1997. **232**(2): p. 407-11.
19. Fenech, M., *The in vitro micronucleus technique*. Mutat Res, 2000. **455**(1-2): p. 81-95.
20. Keen-Kim, D., F. Nooraie, and P.N. Rao, *Cytogenetic biomarkers for human cancer*. Front Biosci, 2008. **13**: p. 5928-49.
21. Stratton, M.R., P.J. Campbell, and P.A. Futreal, *The cancer genome*. Nature, 2009. **458**(7239): p. 719-24.

References

22. Loeb, L.A., J.H. Bielas, and R.A. Beckman, *Cancers exhibit a mutator phenotype: clinical implications*. *Cancer Res*, 2008. **68**(10): p. 3551-7; discussion 3557.
23. Norppa, H., et al., *Chromosomal aberrations and SCEs as biomarkers of cancer risk*. *Mutat Res*, 2006. **600**(1-2): p. 37-45.
24. Fenech, M., et al., *Molecular mechanisms of micronucleus, nucleoplasmic bridge and nuclear bud formation in mammalian and human cells*. *Mutagenesis*, 2011. **26**(1): p. 125-32.
25. Cloos, J., et al., *Mutagen sensitivity as a biomarker for second primary tumors after head and neck squamous cell carcinoma*. *Cancer Epidemiol Biomarkers Prev*, 2000. **9**(7): p. 713-7.
26. Cloos, J., et al., *Mutagen sensitivity: enhanced risk assessment of squamous cell carcinoma*. *Eur J Cancer B Oral Oncol*, 1996. **32B**(6): p. 367-72.
27. Wu, X., J. Gu, and M.R. Spitz, *Mutagen sensitivity: a genetic predisposition factor for cancer*. *Cancer Res*, 2007. **67**(8): p. 3493-5.
28. Wu, X., et al., *Interplay between mutagen sensitivity and epidemiological factors in modulating lung cancer risk*. *Int J Cancer*, 2007. **120**(12): p. 2687-95.
29. Wu, X., et al., *Mutagen sensitivity has high heritability: evidence from a twin study*. *Cancer Res*, 2006. **66**(12): p. 5993-6.
30. Iarmarcovai, G., et al., *Micronuclei frequency in peripheral blood lymphocytes of cancer patients: a meta-analysis*. *Mutat Res*, 2008. **659**(3): p. 274-83.
31. Bonassi, S., et al., *Micronuclei frequency in peripheral blood lymphocytes and cancer risk: evidence from human studies*. *Mutagenesis*, 2011. **26**(1): p. 93-100.
32. Halliwell, B., *Reactive species and antioxidants. Redox biology is a fundamental theme of aerobic life*. *Plant Physiol*, 2006. **141**(2): p. 312-22.
33. Symons, M.C., *Radicals generated by bone cutting and fracture*. *Free Radic Biol Med*, 1996. **20**(6): p. 831-5.
34. Sonntag, C.V., ed. *The Chemical Basis of Radiation Biology*. ed. T. Francis. 1987: London.
35. Freeman, B.A. and J.D. Crapo, *Biology of disease: free radicals and tissue injury*. *Lab Invest*, 1982. **47**(5): p. 412-26.
36. Cross, C.E., et al., *Oxygen radicals and human disease*. *Ann Intern Med*, 1987. **107**(4): p. 526-45.
37. Halliwell, B., J.M. Gutteridge, and C.E. Cross, *Free radicals, antioxidants, and human disease: where are we now?* *J Lab Clin Med*, 1992. **119**(6): p. 598-620.
38. Finkel, T., *Oxygen radicals and signaling*. *Curr Opin Cell Biol*, 1998. **10**(2): p. 248-53.
39. Rhee, S.G., *Redox signaling: hydrogen peroxide as intracellular messenger*. *Exp Mol Med*, 1999. **31**(2): p. 53-9.
40. Christman, M.F., et al., *Positive control of a regulon for defenses against oxidative stress and some heat-shock proteins in *Salmonella typhimurium**. *Cell*, 1985. **41**(3): p. 753-62.
41. Storz, G., L.A. Tartaglia, and B.N. Ames, *Transcriptional regulator of oxidative stress-inducible genes: direct activation by oxidation*. *Science*, 1990. **248**(4952): p. 189-94.
42. Loft, S. and H.E. Poulsen, *Cancer risk and oxidative DNA damage in man*. *Journal of Molecular Medicine-Jmm*, 1996. **74**(6): p. 297-312.
43. Kryston, T.B., et al., *Role of oxidative stress and DNA damage in human carcinogenesis*. *Mutat Res*, 2011. **711**(1-2): p. 193-201.
44. Han, D., E. Williams, and E. Cadenas, *Mitochondrial respiratory chain-dependent generation of superoxide anion and its release into the intermembrane space*. *Biochem J*, 2001. **353**(Pt 2): p. 411-6.
45. Kim, J.A., et al., *NADPH oxidase inhibitors: a patent review*. *Expert Opin Ther Pat*, 2011. **21**(8): p. 1147-58.

References

46. Drummond, G.R., et al., *Combating oxidative stress in vascular disease: NADPH oxidases as therapeutic targets*. Nat Rev Drug Discov, 2011. **10**(6): p. 453-71.
47. Lassegue, B. and R.E. Clempus, *Vascular NAD(P)H oxidases: specific features, expression, and regulation*. Am J Physiol Regul Integr Comp Physiol, 2003. **285**(2): p. R277-97.
48. Opitz, N., et al., *The 'A's and 'O's of NADPH oxidase regulation: a commentary on "Subcellular localization and function of alternatively spliced Noxo1 isoforms"*. Free Radic Biol Med, 2007. **42**(2): p. 175-9.
49. Brandes, R.P. and J. Kreuzer, *Vascular NADPH oxidases: molecular mechanisms of activation*. Cardiovasc Res, 2005. **65**(1): p. 16-27.
50. Bedard, K. and K.H. Krause, *The NOX family of ROS-generating NADPH oxidases: physiology and pathophysiology*. Physiol Rev, 2007. **87**(1): p. 245-313.
51. Lambeth, J.D., T. Kawahara, and B. Diebold, *Regulation of Nox and Duox enzymatic activity and expression*. Free Radic Biol Med, 2007. **43**(3): p. 319-31.
52. McNally, J.S., et al., *Role of xanthine oxidoreductase and NAD(P)H oxidase in endothelial superoxide production in response to oscillatory shear stress*. Am J Physiol Heart Circ Physiol, 2003. **285**(6): p. H2290-7.
53. Krause, K.H., *Tissue distribution and putative physiological function of NOX family NADPH oxidases*. Jpn J Infect Dis, 2004. **57**(5): p. S28-9.
54. McCord, J.M. and I. Fridovich, *The reduction of cytochrome c by milk xanthine oxidase*. J Biol Chem, 1968. **243**(21): p. 5753-60.
55. Jones, D.P., *Redox potential of GSH/GSSG couple: assay and biological significance*. Methods Enzymol, 2002. **348**: p. 93-112.
56. Berliner, L.J., et al., *Unique in vivo applications of spin traps*. Free Radic Biol Med, 2001. **30**(5): p. 489-99.
57. Utsumi, H. and K. Yamada, *In vivo electron spin resonance-computed tomography/nitroxyl probe technique for non-invasive analysis of oxidative injuries*. Arch Biochem Biophys, 2003. **416**(1): p. 1-8.
58. Halliwell, B. and M. Whiteman, *Measuring reactive species and oxidative damage in vivo and in cell culture: how should you do it and what do the results mean?* Br J Pharmacol, 2004. **142**(2): p. 231-55.
59. Geiszt, M., *NADPH oxidases: new kids on the block*. Cardiovasc Res, 2006. **71**(2): p. 289-99.
60. Zhao, H., et al., *Superoxide reacts with hydroethidine but forms a fluorescent product that is distinctly different from ethidium: potential implications in intracellular fluorescence detection of superoxide*. Free Radic Biol Med, 2003. **34**(11): p. 1359-68.
61. Robinson, K.M., et al., *Selective fluorescent imaging of superoxide in vivo using ethidium-based probes*. Proc Natl Acad Sci U S A, 2006. **103**(41): p. 15038-43.
62. Schmid, U., et al., *Angiotensin II induces DNA damage in the kidney*. Cancer Res, 2008. **68**(22): p. 9239-46.
63. Queisser, N., et al., *Aldosterone induces oxidative stress, oxidative DNA damage and NF-kappaB-activation in kidney tubule cells*. Mol Carcinog, 2011. **50**(2): p. 123-35.
64. Joosten, H.F., et al., *Genotoxicity of hormonal steroids*. Toxicol Lett, 2004. **151**(1): p. 113-34.
65. Liehr, J.G., *Genotoxicity of the steroidal oestrogens oestrone and oestradiol: possible mechanism of uterine and mammary cancer development*. Hum Reprod Update, 2001. **7**(3): p. 273-81.
66. Chen, S., et al., *The capture of phosphoproteins by 14-3-3 proteins mediates actions of insulin*. Trends Endocrinol Metab, 2011. **22**(11): p. 429-36.
67. Bell, G.I., et al., *Sequence of the human insulin gene*. Nature, 1980. **284**(5751): p. 26-32.

References

68. Hutton, J.C., *Insulin secretory granule biogenesis and the proinsulin-processing endopeptidases*. Diabetologia, 1994. **37 Suppl 2**: p. S48-56.
69. Shulman, G.I., *Cellular mechanisms of insulin resistance*. J Clin Invest, 2000. **106**(2): p. 171-6.
70. Pessin, J.E. and A.R. Saltiel, *Signaling pathways in insulin action: molecular targets of insulin resistance*. J Clin Invest, 2000. **106**(2): p. 165-9.
71. Previs, S.F., et al., *Contrasting effects of IRS-1 versus IRS-2 gene disruption on carbohydrate and lipid metabolism in vivo*. J Biol Chem, 2000. **275**(50): p. 38990-4.
72. Samuel, V.T., K.F. Petersen, and G.I. Shulman, *Lipid-induced insulin resistance: unravelling the mechanism*. Lancet, 2010. **375**(9733): p. 2267-77.
73. Kido, Y., J. Nakae, and D. Accili, *Clinical review 125: The insulin receptor and its cellular targets*. J Clin Endocrinol Metab, 2001. **86**(3): p. 972-9.
74. Kohn, A.D., et al., *Expression of a constitutively active Akt Ser/Thr kinase in 3T3-L1 adipocytes stimulates glucose uptake and glucose transporter 4 translocation*. J Biol Chem, 1996. **271**(49): p. 31372-8.
75. Kohn, A.D., et al., *Construction and characterization of a conditionally active version of the serine/threonine kinase Akt*. J Biol Chem, 1998. **273**(19): p. 11937-43.
76. Bandyopadhyay, G., et al., *Activation of protein kinase C (alpha, beta, and zeta) by insulin in 3T3/L1 cells. Transfection studies suggest a role for PKC-zeta in glucose transport*. J Biol Chem, 1997. **272**(4): p. 2551-8.
77. Kotani, K., et al., *Requirement of atypical protein kinase lambda for insulin stimulation of glucose uptake but not for Akt activation in 3T3-L1 adipocytes*. Mol Cell Biol, 1998. **18**(12): p. 6971-82.
78. Kitamura, T., et al., *Requirement for activation of the serine-threonine kinase Akt (protein kinase B) in insulin stimulation of protein synthesis but not of glucose transport*. Mol Cell Biol, 1998. **18**(7): p. 3708-17.
79. Ribon, V. and A.R. Saltiel, *Insulin stimulates tyrosine phosphorylation of the proto-oncogene product of c-Cbl in 3T3-L1 adipocytes*. Biochem J, 1997. **324 (Pt 3)**: p. 839-45.
80. Ribon, V., et al., *Thiazolidinediones and insulin resistance: peroxisome proliferator-activated receptor gamma activation stimulates expression of the CAP gene*. Proc Natl Acad Sci U S A, 1998. **95**(25): p. 14751-6.
81. Vigneri, P., et al., *Diabetes and cancer*. Endocr Relat Cancer, 2009. **16**(4): p. 1103-23.
82. Ferrannini, E. and C. Cobelli, *The kinetics of insulin in man. II. Role of the liver*. Diabetes Metab Rev, 1987. **3**(2): p. 365-97.
83. Nestler, J.E., *Role of hyperinsulinemia in the pathogenesis of the polycystic ovary syndrome, and its clinical implications*. Semin Reprod Endocrinol, 1997. **15**(2): p. 111-22.
84. Rhee, E.J., et al., *Hyperinsulinemia and the development of nonalcoholic Fatty liver disease in nondiabetic adults*. Am J Med, 2011. **124**(1): p. 69-76.
85. Zamami, Y., et al., *Hyperinsulinemia induces hypertension associated with neurogenic vascular dysfunction resulting from abnormal perivascular innervations in rat mesenteric resistance arteries*. Hypertens Res, 2011.
86. Arthur, L.S., et al., *Hyperinsulinemia in polycystic ovary disease*. J Reprod Med, 1999. **44**(9): p. 783-7.
87. Calle, E.E. and R. Kaaks, *Overweight, obesity and cancer: epidemiological evidence and proposed mechanisms*. Nat Rev Cancer, 2004. **4**(8): p. 579-91.
88. Neale, R.E., et al., *Does type 2 diabetes influence the risk of oesophageal adenocarcinoma?* Br J Cancer, 2009. **100**(5): p. 795-8.

References

89. Giovannucci, E., *The Role of Insulin Resistance and Hyperinsulinemia in Cancer Causation* Current Medicinal Chemistry - Immunology, Endocrine & Metabolic Agents, 2005. **5**: p. 53-60.
90. Bianchini, F., R. Kaaks, and H. Vainio, *Overweight, obesity, and cancer risk*. Lancet Oncol, 2002. **3**(9): p. 565-74.
91. Giovannucci, E., *Insulin and colon cancer*. Cancer Causes Control, 1995. **6**(2): p. 164-79.
92. Giovannucci, E., *Metabolic syndrome, hyperinsulinemia, and colon cancer: a review*. Am J Clin Nutr, 2007. **86**(3): p. s836-42.
93. Kroenke, C.H., et al., *Depressive symptoms and prospective incidence of colorectal cancer in women*. Am J Epidemiol, 2005. **162**(9): p. 839-48.
94. Glade, M.J., *Food, nutrition, and the prevention of cancer: a global perspective*. American Institute for Cancer Research/World Cancer Research Fund, American Institute for Cancer Research, 1997. Nutrition, 1999. **15**(6): p. 523-6.
95. Smith, U. and E.A. Gale, *Does diabetes therapy influence the risk of cancer?* Diabetologia, 2009. **52**(9): p. 1699-708.
96. Hundal, R.S. and S.E. Inzucchi, *Metformin: new understandings, new uses*. Drugs, 2003. **63**(18): p. 1879-94.
97. Tan, S., et al., *Metformin improves polycystic ovary syndrome symptoms irrespective of pre-treatment insulin resistance*. Eur J Endocrinol, 2007. **157**(5): p. 669-76.
98. Libby, G., et al., *New users of metformin are at low risk of incident cancer: a cohort study among people with type 2 diabetes*. Diabetes Care, 2009. **32**(9): p. 1620-5.
99. Monami, M., et al., *Sulphonylureas and cancer: a case-control study*. Acta Diabetol, 2009. **46**(4): p. 279-84.
100. Landman, G.W., et al., *Metformin associated with lower cancer mortality in type 2 diabetes: ZODIAC-16*. Diabetes Care, 2010. **33**(2): p. 322-6.
101. Zhang, Z.J., et al., *Reduced risk of colorectal cancer with metformin therapy in patients with type 2 diabetes: a meta-analysis*. Diabetes Care, 2011. **34**(10): p. 2323-8.
102. Renehan, A.G., et al., *Insulin-like growth factor (IGF)-I, IGF binding protein-3, and cancer risk: systematic review and meta-regression analysis*. Lancet, 2004. **363**(9418): p. 1346-53.
103. Pollak, M., *Insulin and insulin-like growth factor signalling in neoplasia*. Nat Rev Cancer, 2008. **8**(12): p. 915-28.
104. Krieger-Brauer, H.I., P.K. Medda, and H. Kather, *Insulin-induced activation of NADPH-dependent H₂O₂ generation in human adipocyte plasma membranes is mediated by Galphai2*. J Biol Chem, 1997. **272**(15): p. 10135-43.
105. Mahadev, K., et al., *Hydrogen peroxide generated during cellular insulin stimulation is integral to activation of the distal insulin signaling cascade in 3T3-L1 adipocytes*. J Biol Chem, 2001. **276**(52): p. 48662-9.
106. Mahadev, K., et al., *Insulin-stimulated hydrogen peroxide reversibly inhibits protein-tyrosine phosphatase 1b in vivo and enhances the early insulin action cascade*. J Biol Chem, 2001. **276**(24): p. 21938-42.
107. Nisimoto, Y., et al., *Activation of NADPH oxidase 1 in tumour colon epithelial cells*. Biochem J, 2008. **415**(1): p. 57-65.
108. Mei, S., et al., *Prolonged exposure to insulin induces mitochondrion-derived oxidative stress through increasing mitochondrial cholesterol content in hepatocytes*. Endocrinology, 2012. **153**(5): p. 2120-9.
109. Aggeli, I.K., et al., *Insulin-induced oxidative stress up-regulates heme oxygenase-1 via diverse signaling cascades in the C2 skeletal myoblast cell line*. Endocrinology, 2011. **152**(4): p. 1274-83.

References

110. Bae, Y.S., et al., *Epidermal growth factor (EGF)-induced generation of hydrogen peroxide. Role in EGF receptor-mediated tyrosine phosphorylation.* J Biol Chem, 1997. **272**(1): p. 217-21.
111. Bae, Y.S., et al., *Platelet-derived growth factor-induced H₂O₂ production requires the activation of phosphatidylinositol 3-kinase.* J Biol Chem, 2000. **275**(14): p. 10527-31.
112. Junn, E., et al., *Requirement of hydrogen peroxide generation in TGF-beta 1 signal transduction in human lung fibroblast cells: involvement of hydrogen peroxide and Ca²⁺ in TGF-beta 1-induced IL-6 expression.* J Immunol, 2000. **165**(4): p. 2190-7.
113. Meng, T.C., T. Fukada, and N.K. Tonks, *Reversible oxidation and inactivation of protein tyrosine phosphatases in vivo.* Mol Cell, 2002. **9**(2): p. 387-99.
114. Rhee, S.G., et al., *Hydrogen peroxide: a key messenger that modulates protein phosphorylation through cysteine oxidation.* Sci STKE, 2000. **2000**(53): p. pe1.
115. Espinosa, A., et al., *NADPH oxidase and hydrogen peroxide mediate insulin-induced calcium increase in skeletal muscle cells.* J Biol Chem, 2009. **284**(4): p. 2568-75.
116. San Jose, G., et al., *Insulin-induced NADPH oxidase activation promotes proliferation and matrix metalloproteinase activation in monocytes/macrophages.* Free Radic Biol Med, 2009. **46**(8): p. 1058-67.
117. Kwintkiewicz, J., et al., *Insulin and oxidative stress modulate proliferation of rat ovarian theca-interstitial cells through diverse signal transduction pathways.* Biol Reprod, 2006. **74**(6): p. 1034-40.
118. McCall, M.R. and B. Frei, *Can antioxidant vitamins materially reduce oxidative damage in humans?* Free Radical Biology and Medicine, 1999. **26**(7-8): p. 1034-1053.
119. Piao, W., et al., *Insulin-like growth factor-I receptor blockade by a specific tyrosine kinase inhibitor for human gastrointestinal carcinomas.* Mol Cancer Ther, 2008. **7**(6): p. 1483-93.
120. Gallagher, E.J. and D. LeRoith, *Diabetes, cancer, and metformin: connections of metabolism and cell proliferation.* Ann N Y Acad Sci, 2011. **1243**: p. 54-68.
121. Qian, W. and B. Van Houten, *Alterations in bioenergetics due to changes in mitochondrial DNA copy number.* Methods, 2010. **51**(4): p. 452-7.
122. Tice, R.R., et al., *Single cell gel/comet assay: guidelines for in vitro and in vivo genetic toxicology testing.* Environ Mol Mutagen, 2000. **35**(3): p. 206-21.
123. Simizu, S., et al., *Involvement of hydrogen peroxide production in erbstatin-induced apoptosis in human small cell lung carcinoma cells.* Cancer Res, 1996. **56**(21): p. 4978-82.
124. Shihabi, Z.K. and M. Friedberg, *Insulin stacking for capillary electrophoresis.* J Chromatogr A, 1998. **807**(1): p. 129-33.
125. Oli, R.G., et al., *No increased chromosomal damage in L-DOPA-treated patients with Parkinson's disease: a pilot study.* J Neural Transm, 2010. **117**(6): p. 737-46.
126. Chao, M.R., C.C. Yen, and C.W. Hu, *Prevention of artifactual oxidation in determination of cellular 8-oxo-7,8-dihydro-2'-deoxyguanosine by isotope-dilution LC-MS/MS with automated solid-phase extraction.* Free Radic Biol Med, 2008. **44**(3): p. 464-73.
127. Brink, A., et al., *Simultaneous determination of O6-methyl-2'-deoxyguanosine, 8-oxo-7,8-dihydro-2'-deoxyguanosine, and 1,N6-etheno-2'-deoxyadenosine in DNA using on-line sample preparation by HPLC column switching coupled to ESI-MS/MS.* J Chromatogr B Analyt Technol Biomed Life Sci, 2006. **830**(2): p. 255-61.
128. Cavalieri, E., et al., *Estrogens as endogenous genotoxic agents--DNA adducts and mutations.* J Natl Cancer Inst Monogr, 2000(27): p. 75-93.
129. Babior, B.M., J.D. Lambeth, and W. Nauseef, *The neutrophil NADPH oxidase.* Arch Biochem Biophys, 2002. **397**(2): p. 342-4.
130. Boyd, D.B., *Insulin and cancer.* Integr Cancer Ther, 2003. **2**(4): p. 315-29.

References

131. Hsu, I.R., et al., *Metabolic syndrome, hyperinsulinemia, and cancer*. Am J Clin Nutr, 2007. **86**(3): p. s867-71.
132. Belfiore, A. and R. Malaguarnera, *Insulin receptor and cancer*. Endocr Relat Cancer, 2011. **18**(4): p. R125-47.
133. Gallagher, E.J. and D. LeRoith, *Minireview: IGF, Insulin, and Cancer*. Endocrinology, 2011. **152**(7): p. 2546-51.
134. Braun, S., K. Bitton-Worms, and D. LeRoith, *The link between the metabolic syndrome and cancer*. Int J Biol Sci, 2011. **7**(7): p. 1003-15.
135. Malaguarnera, R. and A. Belfiore, *The insulin receptor: a new target for cancer therapy*. Front Endocrinol (Lausanne), 2011. **2**: p. 93.
136. Heuson, J.C. and N. Legros, *Influence of insulin deprivation on growth of the 7,12-dimethylbenz(a)anthracene-induced mammary carcinoma in rats subjected to alloxan diabetes and food restriction*. Cancer Res, 1972. **32**(2): p. 226-32.
137. Heuson, J.C., N. Legros, and R. Heimann, *Influence of insulin administration on growth of the 7,12-dimethylbenz(a)anthracene-induced mammary carcinoma in intact, oophorectomized, and hypophysectomized rats*. Cancer Res, 1972. **32**(2): p. 233-8.
138. Tran, T.T., A. Medline, and W.R. Bruce, *Insulin promotion of colon tumors in rats*. Cancer Epidemiol Biomarkers Prev, 1996. **5**(12): p. 1013-5.
139. Ma, J., et al., *A prospective study of plasma C-peptide and colorectal cancer risk in men*. J Natl Cancer Inst, 2004. **96**(7): p. 546-53.
140. Larsson, S.C., N. Orsini, and A. Wolk, *Diabetes mellitus and risk of colorectal cancer: a meta-analysis*. J Natl Cancer Inst, 2005. **97**(22): p. 1679-87.
141. Yang, Y.X., S. Hennessy, and J.D. Lewis, *Insulin therapy and colorectal cancer risk among type 2 diabetes mellitus patients*. Gastroenterology, 2004. **127**(4): p. 1044-50.
142. Oren, M., W. Maltzman, and A.J. Levine, *Post-translational regulation of the 54K cellular tumor antigen in normal and transformed cells*. Mol Cell Biol, 1981. **1**(2): p. 101-10.
143. Han, E.S., et al., *The in vivo gene expression signature of oxidative stress*. Physiol Genomics, 2008. **34**(1): p. 112-26.
144. Hock, A.K., et al., *Regulation of p53 stability and function by the deubiquitinating enzyme USP42*. EMBO J, 2011. **30**(24): p. 4921-30.
145. Goldstein, B.J., et al., *Role of insulin-induced reactive oxygen species in the insulin signaling pathway*. Antioxid Redox Signal, 2005. **7**(7-8): p. 1021-31.
146. Gedik, C.M., et al., *Oxidative stress in humans: validation of biomarkers of DNA damage*. Carcinogenesis, 2002. **23**(9): p. 1441-6.
147. Li, G., et al., *Insulin at physiological concentrations selectively activates insulin but not insulin-like growth factor I (IGF-I) or insulin/IGF-I hybrid receptors in endothelial cells*. Endocrinology, 2005. **146**(11): p. 4690-6.
148. Haring, H.U., et al., *Phosphorylation and dephosphorylation of the insulin receptor: evidence against an intrinsic phosphatase activity*. Biochemistry, 1984. **23**(14): p. 3298-306.
149. Seshiah, V. and C.V. Harinarayan, *Insulin kinetics*. INT. J. DIAB. DEV. COUNTRIES, 1998. **18**: p. 19-22.
150. Paek, A.R., et al., *IGF-1 induces expression of zinc-finger protein 143 in colon cancer cells through phosphatidylinositide 3-kinase and reactive oxygen species*. Exp Mol Med, 2010. **42**(10): p. 696-702.
151. Kavurma, M.M., et al., *Oxidative stress regulates IGF1R expression in vascular smooth-muscle cells via p53 and HDAC recruitment*. Biochem J, 2007. **407**(1): p. 79-87.
152. Papaconstantinou, J., *Insulin/IGF-1 and ROS signaling pathway cross-talk in aging and longevity determination*. Mol Cell Endocrinol, 2009. **299**(1): p. 89-100.
153. Du, K. and P.N. Tschlis, *Regulation of the Akt kinase by interacting proteins*. Oncogene, 2005. **24**(50): p. 7401-9.

References

154. Levine, A.J., et al., *Coordination and communication between the p53 and IGF-1-AKT-TOR signal transduction pathways*. Genes Dev, 2006. **20**(3): p. 267-75.
155. Yang, J.Y., et al., *Insulin stimulates Akt translocation to mitochondria: implications on dysregulation of mitochondrial oxidative phosphorylation in diabetic myocardium*. J Mol Cell Cardiol, 2009. **46**(6): p. 919-26.
156. Bijur, G.N. and R.S. Jope, *Rapid accumulation of Akt in mitochondria following phosphatidylinositol 3-kinase activation*. J Neurochem, 2003. **87**(6): p. 1427-35.
157. Chandel, N.S. and P.T. Schumacker, *Cells depleted of mitochondrial DNA (rho0) yield insight into physiological mechanisms*. FEBS Lett, 1999. **454**(3): p. 173-6.
158. Lee, S.B., et al., *Link between mitochondria and NADPH oxidase 1 isozyme for the sustained production of reactive oxygen species and cell death*. J Biol Chem, 2006. **281**(47): p. 36228-35.
159. Jiang, F., Y. Zhang, and G.J. Dusting, *NADPH oxidase-mediated redox signaling: roles in cellular stress response, stress tolerance, and tissue repair*. Pharmacol Rev, 2011. **63**(1): p. 218-42.
160. Stolk, J., et al., *Characteristics of the inhibition of NADPH oxidase activation in neutrophils by apocynin, a methoxy-substituted catechol*. Am J Respir Cell Mol Biol, 1994. **11**(1): p. 95-102.
161. Cai, H., K.K. Griendling, and D.G. Harrison, *The vascular NAD(P)H oxidases as therapeutic targets in cardiovascular diseases*. Trends Pharmacol Sci, 2003. **24**(9): p. 471-8.
162. Heumuller, S., et al., *Apocynin is not an inhibitor of vascular NADPH oxidases but an antioxidant*. Hypertension, 2008. **51**(2): p. 211-7.
163. Milosevic, N., et al., *Redox stimulation of cardiomyogenesis versus inhibition of vasculogenesis upon treatment of mouse embryonic stem cells with thalidomide*. Antioxid Redox Signal, 2010. **13**(12): p. 1813-27.
164. Sauer, H., et al., *Activation of AMP-kinase by AICAR induces apoptosis of DU-145 prostate activation of c-Jun N-terminal kinase*. Int J Oncol, 2012. **40**(2): p. 501-8.
165. Wilcox, C.S. and A. Pearlman, *Chemistry and antihypertensive effects of tempol and other nitroxides*. Pharmacol Rev, 2008. **60**(4): p. 418-69.
166. Garcia-Cazarin, M.L., et al., *The alpha1D-adrenergic receptor induces vascular smooth muscle apoptosis via a p53-dependent mechanism*. Mol Pharmacol, 2008. **74**(4): p. 1000-7.
167. Saperstein, R., et al., *Design of a selective insulin receptor tyrosine kinase inhibitor and its effect on glucose uptake and metabolism in intact cells*. Biochemistry, 1989. **28**(13): p. 5694-701.
168. Diaz, L.E., et al., *IGF-II regulates metastatic properties of choriocarcinoma cells through the activation of the insulin receptor*. Mol Hum Reprod, 2007. **13**(8): p. 567-76.
169. Varewijck, A.J. and J.A. Janssen, *Insulin and its analogues and their affinities for the IGF1 receptor*. Endocr Relat Cancer, 2012. **19**(5): p. F63-75.
170. Riedemann, J. and V.M. Macaulay, *IGF1R signalling and its inhibition*. Endocr Relat Cancer, 2006. **13 Suppl 1**: p. S33-43.
171. Girnita, A., et al., *Cyclolignans as inhibitors of the insulin-like growth factor-1 receptor and malignant cell growth*. Cancer Res, 2004. **64**(1): p. 236-42.
172. Doghman, M., M. Axelson, and E. Lalli, *Potent inhibitory effect of the cyclolignan picropodophyllin (PPP) on human adrenocortical carcinoma cells proliferation*. Am J Cancer Res, 2011. **1**(3): p. 356-361.
173. Mahadev, K., et al., *The NAD(P)H oxidase homolog Nox4 modulates insulin-stimulated generation of H2O2 and plays an integral role in insulin signal transduction*. Mol Cell Biol, 2004. **24**(5): p. 1844-54.

References

174. Li, W.G., et al., *H₂O₂-induced O₂ production by a non-phagocytic NAD(P)H oxidase causes oxidant injury*. J Biol Chem, 2001. **276**(31): p. 29251-6.
175. Rathore, R., et al., *Hypoxia activates NADPH oxidase to increase [ROS] and [Ca²⁺] through the mitochondrial ROS-PKCepsilon signaling axis in pulmonary artery smooth muscle cells*. Free Radic Biol Med, 2008. **45**(9): p. 1223-31.
176. Decensi, A., et al., *Metformin and cancer risk in diabetic patients: a systematic review and meta-analysis*. Cancer Prev Res (Phila), 2010. **3**(11): p. 1451-61.
177. Noto, H., et al., *Cancer risk in diabetic patients treated with metformin: a systematic review and meta-analysis*. PLoS One, 2012. **7**(3): p. e33411.
178. Cadet, J., et al., *Assessment of oxidative base damage to isolated and cellular DNA by HPLC-MS/MS measurement*. Free Radic Biol Med, 2002. **33**(4): p. 441-9.
179. Henderson, P.T., et al., *Oxidation of 7,8-dihydro-8-oxoguanine affords lesions that are potent sources of replication errors in vivo*. Biochemistry, 2002. **41**(3): p. 914-21.
180. Hsu, G.W., et al., *Error-prone replication of oxidatively damaged DNA by a high-fidelity DNA polymerase*. Nature, 2004. **431**(7005): p. 217-21.
181. Xie, Y., et al., *Deficiencies in mouse Myh and Ogg1 result in tumor predisposition and G to T mutations in codon 12 of the K-ras oncogene in lung tumors*. Cancer Res, 2004. **64**(9): p. 3096-102.
182. Russo, M.T., et al., *Accumulation of the oxidative base lesion 8-hydroxyguanine in DNA of tumor-prone mice defective in both the Myh and Ogg1 DNA glycosylases*. Cancer Res, 2004. **64**(13): p. 4411-4.
183. Pelzer, T., et al., *Pioglitazone reverses down-regulation of cardiac PPARgamma expression in Zucker diabetic fatty rats*. Biochem Biophys Res Commun, 2005. **329**(2): p. 726-32.
184. Hinokio, Y., et al., *Oxidative DNA damage in diabetes mellitus: its association with diabetic complications*. Diabetologia, 1999. **42**(8): p. 995-8.
185. Broedbaek, K., et al., *Urinary 8-oxo-7,8-dihydro-2'-deoxyguanosine as a biomarker in type 2 diabetes*. Free Radic Biol Med, 2011. **51**(8): p. 1473-9.
186. Al-Aubaidy, H.A. and H.F. Jelinek, *Oxidative DNA damage and obesity in type 2 diabetes mellitus*. Eur J Endocrinol, 2011. **164**(6): p. 899-904.
187. Palyvoda, O., et al., *DNA damage and repair in lymphocytes of normal individuals and cancer patients: studies by the comet assay and micronucleus tests*. Acta Biochim Pol, 2003. **50**(1): p. 181-90.
188. Bolognesi, C., et al., *High frequency of micronuclei in peripheral blood lymphocytes as index of susceptibility to pleural malignant mesothelioma*. Cancer Res, 2002. **62**(19): p. 5418-9.
189. Andreassi, M.G., et al., *The association of micronucleus frequency with obesity, diabetes and cardiovascular disease*. Mutagenesis, 2011. **26**(1): p. 77-83.
190. Martinez-Perez, L.M., et al., *Frequency of micronuclei in Mexicans with type 2 diabetes mellitus*. Prague Med Rep, 2007. **108**(3): p. 248-55.
191. Djelic, N., *Analysis of sister-chromatid exchanges and micronuclei in cultured human lymphocytes treated with insulin*. Folia Biol (Praha), 2001. **47**(1): p. 28-31.
192. Hamurcu, Z., et al., *Micronucleus frequency in lymphocytes and 8-hydroxydeoxyguanosine level in plasma of women with polycystic ovary syndrome*. Gynecol Endocrinol, 2010. **26**(8): p. 590-5.
193. Yesilada, E., et al., *Increased micronucleus frequencies in peripheral blood lymphocytes in women with polycystic ovary syndrome*. Eur J Endocrinol, 2006. **154**(4): p. 563-8.

Acknowledgment

8. Acknowledgment

First and foremost, I would like to thank my supervisor, **Prof. Dr. Helga Stopper**, who gave me the opportunity to work on this truly exciting research project. I wish to express my sincere thanks and gratitude to her for guidance, great support, encouragement, patience and discipline and rigor she taught me in my work. I consider myself extremely fortunate to have been able to complete my Ph.D. under her supervision.

My appreciation also goes out to my committee members, **Prof Dr. Klaus Brehm, Prof Dr. Ulric Holzgrabe and PD Dr. Robert Hock** who have always been very accessible and contributed to this work with their suggestions during the progress report meetings.

I'm very thankful to **Christin Thiel** and **Johanna Markert** for their excellent technical assistance and for great teamwork.

I would like to thank my medical PhD student (**Annekathrin Leyh**) for her contribution to my project

My thanks for **Dr Oli Gnana** and **Ezgi Eylül Bankoglu** for conducting mass spectroscopy measurements.

I am deeply thanking my colleagues and lab mates in Prof Stopper's working group for the wonderful working atmosphere and their support.

I am appreciating the help of **Dr Gholamreza Fazeli** in teaching me some techniques and providing me with knowledge.

Many thanks for **Dr Henning Hintzsche** for the German translation of the summery.

I am thankful to the **Egyptian Ministry of Higher Education** and **DAAD** for the financial support during my study in Germany.

Acknowledgment

I am thankful to **GSLs** for following upon my Ph.D. and providing me with helpful courses and workshops.

Finally, I am in debt to my **parents**, my husband (**Dr Usama Ramadan Abdelmohsen**) and my children (**Miram, Dareen and Anas**) as well as my brothers and sister for their endless and unconditional love, support and encouragement which enabled me to conquer all the difficulties in the long run of finishing my Ph.D. thesis.

Curriculum Vitae

Curriculum Vitae

Name: Eman Maher Othman Sholkamy

Date of birth: 01.09.1980

Place of birth: Minia, Egypt

Nationality: Egyptian

Status: Married

Education

10.2008 – present: Ph.D. thesis (In vitro and In vivo Analysis of Insulin-induced Oxidative stress and DNA damage) in Toxicology at the Institute of Pharmacology and Toxicology, University of Wuerzburg, Germany

09-2002 – 06-2006: M.Sc. of Pharmaceutical Sciences, Minia University, Egypt (Chemometrics-Assisted Spectrophotometric Determination of certain Antibiotic Mixtures)

06-2002: Bachelor of Pharmaceutical Sciences, Minia University, Egypt.
General grade: Excellent with distinction honor.

1997-2002: Faculty of pharmacy, Minia University, Egypt

09/1986-05/1997: Primary, Preparatory and Secondary Schools, Minia, Egypt

Academic career:

2002-2006: Demonstrator in Analytical Chemistry department, faculty of Pharmacy, Minia University, Egypt

2006- present: Assistant lecturer in Analytical Chemistry department, faculty of Pharmacy, Minia University, Egypt

Publications

- I. Abd El-Maboud, H. Salem and **Eman Maher Othman**. Spectrophotometric Determination of Binary Mixtures of Prednisolone with some Antibiotics. *Thai. J. Pharm. Sci.*, (30), 2006, pp.63-81.

Curriculum Vitae

- I. Abd El-Maboud, H. Salem and **Eman Maher Othman**. Chemometric-assisted Spectrophotometric Determination of certain β -lactam Antibiotics Combinations. *Thai. J.Pharm. Sci.* (31), 2007, 1-24.
- Usama Ramadan Abdelmohsen, Matthias Szesny, **Eman Maher Othman**, Tanja Schirmeister, Stephanie Grond, Helga Stopper and Ute Hentschel. Antioxidant and Anti-Protease Activities of Diazepinomicin from the Sponge-Associated Micromonospora Strain RV115. *Mar. Drugs* 2012, 10 (10), 2208-2221.
- **Eman Maher Othman**, Michael C. Kreissl, Franz R. Kaiser, Arias-Loza Paula-Anahi, Helga Stopper. Insulin mediated oxidative stress and DNA damage in LLC-PK1 pig kidney cell line, female rat primary kidney cells and male ZDF rat kidneys in vivo. *Endocrinology*,(154) 2013,p1434-1443.
- **Eman Maher Othman**, Annkathrin Leyh, Helga Stopper. Insulin mediated DNA damage in mammalian colon cells and human lymphocytes in-vitro. *Mutation research*, 2013.

Conferences attended and abstracts

- Assuit university eighth International Pharmaceutical Sciences Conference, Assuit Egypt March 2012.(poster and oral presentation)
Abstract: HPLC-Tandom mass spectrometry based analysis of potential oxaliplatin contamination during HIPEC.
Oral presentation: Hyperinsulinemia Induced genomic damage and increases cancer risk
- DGPT conference, March 2012, Dresden, Germany (Poster)
Abstract:Induction of oxidative stress and genomic damage by insulin.
- 7th GUM ³²P-postlabeling Workshop & UKEMS / Dutch EMS-sponsored Workshop on Biomarker of Exposure and Oxidative DNA damage. March 2011, Münster, Germany.(Poster)

Curriculum Vitae

Abstract: Hyperinsulinemia induced genomic damage and increased cancer risk.

- 26. Ernst Klenk Symposium in Molecular Medicine (NOX Family NADPH Oxidases as Therapeutic Targets) November 2010, Cologne, Germany (Poster)

Abstract: NADPH oxidase stress may contribute to insulin induced genomic damage.

- The 4th, 5th a 6th International Students' Symposium, 2009, 2010, 2011, Wuerzburg, Germany (Posters)

Abstracts: (2009) Insulin-induced oxidative stress and DNA damage in mammalian cells.

(2010) Hormone induced genomic damage: Insulin.

(2011) Hyperinsulinemia induced genomic damage and increased cancer risk.

- The 7th International Students' Symposium, 2012, Wuerzburg, (Poster and oral presentation)

Abstract: Insulin mediated DNA damage in mammalian cells.

Oral presentation: Genotoxicity of insulin in vitro.

Travel grant awards

GUM travel grant 2011

GSLs travel grant 2012

EEMS young scientist travel grant award 2012

Dedication

Dedication

This dissertation is dedicated to

Egypt

And

My Family

Affidavit

Affidavit

I hereby declare that my thesis entitled "**In Vitro and In Vivo Analysis of Insulin-Induced Oxidative Stress and DNA Damage**" is the result of my own work. I did not receive any help or support from commercial consultants or others. All sources and/or materials applied are listed and specified in the thesis. Furthermore, I verify that this thesis has not been submitted as part of another examination process, neither in identical nor in similar form.

Wuerzburg,

Eman Maher Othman Sholkamy